MONTHLY NOTICES

OF THE

ROYAL ASTRONOMICAL SOCIETY

Vol. 116 No. 5 1956

Published and Sold by the
ROYAL ASTRONOMICAL SOCIETY
BURLINGTON HOUSE
LONDON, W.1

Price Thirteen Shillings and Sixpence

ROYAL ASTRONOMICAL SOCIETY

Founded 1820

OCCASIONAL NOTES

of the

ROYAL ASTRONOMICAL SOCIETY

No. 19 of Volume 3 consists of a single article:

Close Binary Stars. By OTTO STRUVE and SU SHU HUANG

Now available: price 4s. 6d.; in U.S.A. $0.80.

MEMOIRS

of the

ROYAL ASTRONOMICAL SOCIETY

Volume LXVII, published during 1954/55, consists of four parts. These are on sale individually at the following prices:

Part I. **Photographic and photovisual magnitudes of 7^m–10^m stars in the $+15°$ Selected Areas.** By A. BEER, R. O. REDMAN and G. G. YATES.
Price £1 0s. 0d.; in U.S.A. $3.20

Part II. **Radial velocities of southern B stars determined at the Radcliffe Observatory (Paper I).** By M. W. FEAST, A. D. THACKERAY and A. J. WESSELINK.
Price £1 2s. 0d.; in U.S.A. $3.50.

Part III. **The Cambridge radio telescope.** By M. RYLE and A. HEWISH. **A survey of radio sources between declinations $-38°$ and $+83°$.** By J. R. SHAKESHAFT, M. RYLE, J. E. BALDWIN, B. ELSMORE and J. H. THOMSON.
Price £1 8s. 0d.; in U.S.A. $4.30.

Part IV. **A survey of southern H II regions.** By COLIN S. GUM.
Price £1 12s. 0d.; in U.S.A. $4.90.

Orders for the above should be addressed to:

THE ASSISTANT SECRETARY,
Royal Astronomical Society, Burlington House, London, W.1

MONTHLY NOTICES

OF THE

ROYAL ASTRONOMICAL SOCIETY

Vol. 116 No. 5

ADDITIONAL MEETING OF 1956 JULY 10

in the Physics Lecture Theatre of the University of Bristol

Professor Sir Harold Jeffreys, President, in the Chair

The President announced the death of Walter Sydney Adams, an Associate of the Society, and paid a brief tribute to his memory, the Fellows standing.

The President announced that this Additional Meeting was the eighth to take place outside the rooms of the Society in London. He expressed the thanks of the Society to the Vice-Chancellor and Senate of the University, at whose invitation the meeting was being held at Bristol, and to Professor M. H. L. Pryce for the use of the Physics Lecture Theatre. The thanks of the Society were also extended to the Warden and staff of Wills Hall, where accommodation had been provided for Fellows and guests participating in the various activities arranged in connection with the visit, and to Dr W. J. Bates, who had undertaken much of the work involved in the local organization of the meetings and associated activities.

One hundred and thirty-four presents were announced as having been received since the last meeting, including :—

J. de Sacrobosco : *Fr. Ivnctini commentaria in sphaeram Ioannis de Sacrobosco accuratissima (in duo priora capita)* (presented by Sir Eric Miller);

P. A. Moore : *The Planet Venus* (presented by the publishers);

Benjamin Gompertz : *A manuscript mathematical notebook and analysis and notation applicable to the value of life contingencies, with the author's manuscript notes* (presented by Mrs W. M. Archibald); and

P. W. Merrill : *Lines of the chemical elements in astronomical spectra* (presented by the Carnegie Institution of Washington).

Dr J. Öpik then spoke on changes that had recently taken place in the ADH organization; papers were read by Dr D. E. Blackwell, Mr B. Elsmore and Mr J. E. Geake; and an account was given by Professor H. Bondi of two papers by Mr C. B. Haselgrove and Mr F. Hoyle jointly.

Other meetings and activities in connection with the Society's visit to Bristol, included a symposium on *Schmidt Optics*, held in the morning of July 9, and, on the evening of the same day, a Public Lecture, entitled *The Isaac Newton*

Telescope Proposals, by the Astronomer Royal. Trips to places of interest included a number of excursions to points of scenic and archaeological interest in Somerset; a visit, kindly arranged by Mr Jack Miller, to the H. H. Wills Tobacco Factory at Bedminster; and an inspection of the work in progress at the University Physics Laboratory. On Tuesday evening, July 10, Fellows were the guests of the Lord Mayor and Council of the City at a reception in the Council House, and the programme came to an end with a dinner later in the evening at Wills Hall.

MEETING OF 1956 OCTOBER 12

Professor Sir Harold Jeffreys, President, in the Chair

The President announced the death of Gregory Shajn, an Associate of the Society, in whose memory the Fellows stood for a few moments in silence.

The election by the Council of the following Fellows was duly confirmed :—

Colin H. Barrow, 87 Park Hill Road, Bexley, Kent (proposed by L. A. Brown);

John Robert Brace, 1228 Pacific Highway, Pymble, N.S.W., Australia (proposed by J. H. Finch);

John Avery Crawford, University of California, Berkeley 4, Cal., U.S.A. (proposed by L. D. Henyey);

Richard Rayman Doell, University of Toronto, Canada (proposed by J. A. Jacobs);

Richard Mead Goody, Imperial College, London, S.W.7 (proposed by R. O. Redman);

Thomas Heath Hellings, 2 Poultney Road, Radford, Coventry (proposed by H. G. Miles);

John Heywood, Norwood Technical College, Knight's Hill, London, S.W. 27 (proposed by W. H. Marshall);

Geradus Franciscus Wilhelmus Mulders, c/o U.S. Office of Naval Research, Keysign House, 429 Oxford Street, W.1 (proposed by C. W. Allen);

Francis R. Openshaw, 5 Jointon Road, Folkestone, Kent (proposed by H. L. Hitchins);

Robert Paul Randall, 239 Minehead Court, Alexandra Avenue, South Harrow, Middlesex (proposed by A. Armitage);

Samuel Shenton, 22 London Road, Dover (proposed by H. Bondi);

Nevil Harvey Silverton, 238 Lidgett Lane, Leeds 17, Yorkshire (proposed by T. G. Cowling); and

Piyal Weerasinghe, 319 Peradeniya Road, Kandy, Ceylon (proposed by S. S. Ayer).

THE MOON'S OBSERVED LATITUDE FROM OCCULTATIONS 1932–1953

C. A. Murray

(Communicated by the Astronomer Royal)

(Received 1956 May 17)

Summary

The effects on the Moon's latitude from occultations, when compared with Brown's *Tables*, of (i) the change of ellipticity of the Earth, from Brown's value (1/294) to the International value (1/297), (ii) the known error of the FK3 equinox, (iii) the error in Brown's *Tables*, discovered by Woolard, are derived, and are shown to be fully confirmed by the occultation lunation solutions from 1932–1953.

After removing these terms, the observations are analysed in two series, 1932–1942 and 1943–1953, for periods corresponding to the Moon's mean anomaly and argument of latitude.

The existence of a term in the latitude with the period of the mean anomaly has been well established by other investigators, and has been attributed to the systematic effect of limb irregularities, varying with the libration in longitude; there is no dynamical foundation for such a term. The solutions for the two series confirm the character of the term, but the coefficient derived from the first series is only 75 per cent of that derived from the second. The phase of the term is very close to that of the libration in longitude, and it is suggested that it may arise through a real ellipticity of the lunar surface.

The solutions for the two series for the period of the argument of latitude are nearly identical and may be interpreted as corrections to the inclination and longitude of the node.

---

1. *Introduction.*—It is well known that the Moon's observed latitude, as deduced from lunation solutions of occultations, shows large systematic fluctuations with periods of the order of a year; that more than one such period is present is evident from inspection of the results (**1**). It is generally accepted that these periods are produced by a beat effect, arising from the fact that the mean epoch of the observed occultations occurs at nearly the same age of the Moon in each lunation; errors with true periods of the nodical, tropical and anomalistic months will thus appear as errors with periods of 11·74, 12·37 and 13·94 lunations respectively. It will be assumed throughout this paper that any observed period is due entirely to an error with the corresponding shorter period.

We investigate first certain known causes which give rise to terms in the Moon's observed latitude as deduced from occultations and compared with Brown's *Tables*. The sign throughout is of that which would appear in the residuals O–C, whether as tabular or observational corrections.

In the usual notation let

L = mean longitude of the Moon,
L' = mean longitude of the Sun,
ϖ = mean longitude of the Moon's perigee,
Ω = mean longitude of the Moon's node,
$D = L - L'$ = mean elongation of the Moon from the Sun,
$l = L - \varpi$ = mean anomaly of the Moon,
$F = L - \Omega$ = mean argument of latitude,
2γ = coefficient of sin F in latitude.

To a first approximation, a correction to 2γ is the same as a correction to the inclination of the Moon's orbit to the ecliptic.

We assume that the mean epoch of the occultations, within each lunation, occurs at the instant 5·5 days before full moon, i.e. when $D = 113°$.

2. *Figure of the Earth.*—The ellipticity of the Earth adopted by Brown in constructing his *Tables* was 1/294 (**2**); that given by modern geodetic and gravity data is 1/297 (**3**). This latter value is that of the International Spheroid which is used for computing geocentric coordinates of observers for the reduction of lunar observations. This inconsistency in the adopted system of astronomical constants has been pointed out in a previous paper (**4**). Assuming that the true value is 1/297, we can compute the corrections required by the Moon's tabular ecliptic coordinates.

The departure of the Earth's gravitational field from spherical symmetry introduces the following corrections to the elements of the Moon's orbit, (**5**), (**6**):

Ellipticity	1/297	1/294
	"	"
δL	+ 7·112 sin $\delta\delta$	+ 7·261 sin $\delta\delta$
$\delta\varpi$	− 2·034 sin $\delta\delta$	− 2·076 sin $\delta\delta$
$\delta\,\delta\delta$	+93·98 sin $\delta\delta$	+95·96 sin $\delta\delta$
$\delta\gamma$	− 4·229 cos $\delta\delta$	− 4·318 cos $\delta\delta$

If Δ_1 denotes the correction to a tabular quantity required in changing the ellipticity from 1/294 to 1/297, the only significant changes in the ecliptic coordinates are

$$\left.\begin{aligned}\Delta_1\lambda &= \Delta_1 L + 0{\cdot}1098\,(\Delta_1 L - \Delta_1\varpi)\cos l\\ \Delta_1\beta &= 2\Delta_1\gamma \sin F + 0{\cdot}0895\,(\Delta_1 L - \Delta_1\Omega)\cos F\end{aligned}\right\} \qquad (1)$$

or, with the values given above,

$$\left.\begin{aligned}\Delta_1\lambda &= -0''{\cdot}149\sin\Omega - 0''{\cdot}010\sin(l+\Omega) + 0''{\cdot}010\sin(l-\Omega)\\ \Delta_1\beta &= +0''{\cdot}171\sin(F+\Omega) + 0''{\cdot}007\sin(F-\Omega).\end{aligned}\right\} \qquad (2)$$

For the purpose of the present investigation, only the component of $\Delta_1\lambda$ perpendicular to the plane of the orbit will be required. The second and third terms in $\Delta_1\lambda$ are accordingly negligible.

3. *Equinox of the FK3.*—The star positions used in the reduction of occultations are taken from the Zodiacal Catalogue (Z.C.) (**7**) whose system is that of the FK3. Modern meridian observations have shown that the equinox of the FK3 requires a correction. A positive equinox correction E means that the tabular right ascensions of the stars are too small by E. It follows that the observed right ascension of the Moon when referred to the stars is also too small by E.

A small change in the right ascension, $\Delta_2\alpha$, say, may be converted into ecliptic coordinates by the transformation

$$\left.\begin{aligned}\Delta_2\lambda &= 15\Delta_2\alpha\cos\epsilon\,(1-\tan\beta\tan\epsilon\sin\lambda)\\ \Delta_2\beta &= -15\Delta_2\alpha\sin\epsilon\cos\lambda\end{aligned}\right\} \tag{3}$$

where ϵ is the obliquity of the ecliptic. It is sufficient in the present case to neglect the second term in $\Delta_2\lambda$ and to substitute $F+\Omega\,(=L)$ for λ in $\Delta_2\beta$.

As in a previous paper (**4**, p. 95) we adopt $E=-\Delta_2\alpha=+0^{s}\cdot022$, from the latest Washington meridian observations, whence

$$\left.\begin{aligned}\Delta_2\lambda &= -0''\cdot303\\ \Delta_2\beta &= +0''\cdot131\ \cos\ (F+\Omega).\end{aligned}\right\} \tag{4}$$

4. *Error in Brown's Tables.*—The investigations of Woolard (**8**) established that, in order to correct an error in Brown's *Tables*, the tabular ecliptic latitude must be increased by

$$\Delta_3\beta = +0''\cdot26\cos(\Omega-10^{\circ})\cos(2D-F+270^{\circ}). \tag{5}$$

Putting $D=113^{\circ}$ we obtain,

$$\begin{aligned}\Delta_3\beta = {}&+0''\cdot073\sin(F+\Omega)-0''\cdot108\cos(F+\Omega)+0''\cdot105\sin(F-\Omega)\\ &-0''\cdot076\cos(F-\Omega).\end{aligned} \tag{6}$$

5. *Combination of corrections.*—Combining (2), (4) and (6), and neglecting the small terms in $\Delta_1\lambda$, we obtain

$$\left.\begin{aligned}\Delta\lambda &= \Delta_1\lambda+\Delta_2\lambda = -0''\cdot303-0''\cdot149\sin\Omega\\ \Delta\beta &= \Delta_1\beta+\Delta_2\beta+\Delta_3\beta\\ &= +0''\cdot244\sin(F+\Omega)+0''\cdot023\cos(F+\Omega)+0''\cdot112\sin(F-\Omega)\\ &\qquad -0''\cdot076\cos(F-\Omega).\end{aligned}\right\} \tag{7}$$

The occultations give corrections to the orbital latitude, B. It is readily seen that, with sufficient accuracy,

$$\Delta B = \Delta\beta - 2\gamma\cos F\,.\,\Delta\lambda, \tag{8}$$

whence from (7)

$$\begin{aligned}\Delta B = {}&+0''\cdot03\cos F+0''\cdot25\sin(F+\Omega)+0''\cdot02\cos(F+\Omega)\\ &+0''\cdot11\sin(F-\Omega)-0''\cdot08\cos(F-\Omega)\end{aligned} \tag{9}$$

is what should appear in the lunation solutions, O–C, on account of the causes here considered.

6. *Observational material.*—The observations discussed are the lunation solutions for orbital latitude δB_l. Those from 1932–1942 have been taken from Table I of a paper by Brouwer and Watts (**9**). The solutions from 1932–40 have been reduced to the system of the Z.C. by the application of the corrections listed in column "*d*" of the Table. For 1941 and 1942 the solutions have been taken unchanged. The solutions from 1943–1953 have been taken from the annual discussions published by McBain (**10**).

Since 1941 all star places used in the occultation reductions have been taken from the Z.C. The whole series has thus been reduced to the same system of star places.

Only dark limb disappearances have been included in the adopted lunation solutions.

7. *Analysis.*—The original purpose of this investigation was to test the occultations for the $F \pm \Omega$ terms in (9). The results for these terms were very satisfactory, as will be seen below; it was then decided to carry out the analysis for the arguments l and F.

On the assumption that each lunation solution refers to the epoch when $D = 113^\circ$, the required arguments are given by the following expressions

$$\left.\begin{aligned} F+\Omega &= 48^\circ\cdot80 + 29^\circ\cdot107\,(n-112) \\ F-\Omega &= 50^\circ\cdot00 + 32^\circ\cdot234\,(n-112) \\ l &= 210^\circ\cdot58 + 25^\circ\cdot815\,(n-112) \\ F &= 49^\circ\cdot40 + 30^\circ\cdot670\,(n-112) \end{aligned}\right\} \qquad (10)$$

where n is the lunation number in Brown's series. (Lunation 112 began on 1932 Jan. 7, and is the first lunation used in the present discussion.)

The observations, δB_l, were grouped in 30° ranges of each argument, centred on 0°, 30°, etc., and the twelve mean values, $\overline{\delta B}$, for each 30° range were solved by harmonic analysis for a first harmonic only. Each lunation solution was given unit weight, and the small difference in weighting, due to the fact that the number of lunation solutions in each $\overline{\delta B}$ was not quite the same, has been neglected.

The values of $\overline{\delta B}$ for the arguments $F \pm \Omega$ are given in Table I.

TABLE I

Arg.	$F+\delta\delta$	$F-\delta\delta$	Arg.	$F+\delta\delta$	$F-\delta\delta$
°	″	″	°	″	″
0	−0·60	−0·78	180	−0·74	−0·47
30	− ·48	− ·69	210	− ·78	− ·62
60	− ·39	− ·61	240	− ·86	− ·82
90	− ·47	− ·50	270	− ·93	− ·78
120	− ·28	− ·58	300	− ·78	− ·76
150	−0·55	−0·36	330	−0·72	−0·65

The first harmonics deduced from these are

$$+0''\cdot26\sin(F+\Omega) + 0''\cdot04\cos(F+\Omega) + 0''\cdot12\sin(F-\Omega) - 0''\cdot10\cos(F-\Omega). \qquad (11)$$

The agreement between (11) and the corresponding terms in (9) is all that could be desired. The expected corrections to take account of the change of ellipticity, the error of the FK3 equinox and the error in Brown's *Tables*, are satisfactorily confirmed.

A term in $\sin(F+\Omega)$ could also arise from an error in the obliquity of the ecliptic; the agreement between (9) and (11) suggests that any such error must be very small.

The error in Brown's *Tables* has been corrected in the *Improved Lunar Ephemeris* (**11**). The ellipticity used in that work is, however, still 1/294; the inconsistency referred to above is thus perpetuated. If, as is generally accepted, the true value of the ellipticity is 1/297, observations of the Moon's longitude referred to the new ephemeris, as well as those referred to Brown's *Tables*, will contain an erroneous term $-0''\cdot15 \sin\Omega$. This term, having a period of 18·6 years, will not be eliminated from annual means, and will thus affect the derived E.T.–U.T. difference.

Before analysis for the arguments l and F, the observations were corrected for the terms in (9) with arguments $F \pm \Omega$. The whole series was then divided into two parts, each of 136 lunations. Series I extends from lunations 112 to 247, and Series II from lunations 248 to 383.

The values of $\overline{\delta B}$ for arguments l for each series are given in Table II.

TABLE II

Arg.	l(I)	l(II)	Arg.	l(I)	l(II)
°	"	"	°	"	"
0	−0·31	−0·66	180	−0·56	−0·75
30	−0·83	−0·93	210	−0·50	−0·61
60	−1·00	−1·02	240	−0·22	−0·30
90	−1·21	−0·95	270	−0·52	−0·11
120	−0·90	−1·09	300	−0·40	−0·08
150	−0·95	−0·90	330	−0·50	−0·22

The harmonic analyses of these give

$$\begin{aligned} &\text{Series I} && -0''\cdot36 \sin l + 0''\cdot04 \cos l \\ &\text{Series II} && -0''\cdot47 \sin l + 0''\cdot09 \cos l \\ &\text{mean} && -0''\cdot42 \sin l + 0''\cdot06 \cos l = -0''\cdot42 \sin (l - 8^\circ). \end{aligned} \qquad (12)$$

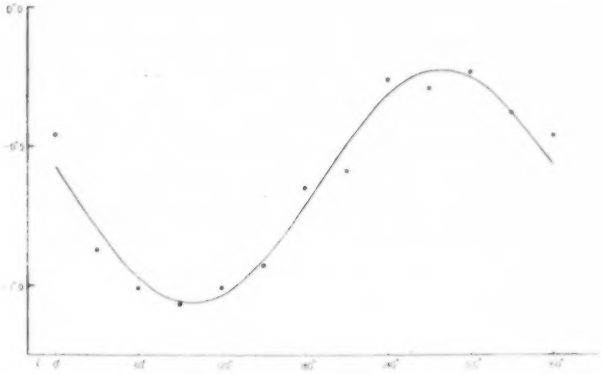

FIG. 1.—*Moon's latitude. Analysis for argument l.*

.... $\delta\beta$ *for argument l.*

—— $-0''\cdot64 - 0''\cdot42 \sin (l - 8^\circ)$.

The values of $\overline{\delta B}$ for argument l, Series I and II combined, are plotted in Fig. 1 together with the term $-0''\cdot64 - 0''\cdot42 \sin (l - 8^\circ)$.

Before analysis for argument F, the observations were corrected for (12).

Table III gives the values of $\overline{\delta B}$ for the two series for argument F.

TABLE III

Arg.	F(I)	F(II)	Arg.	F(I)	F(II)
°	"	"	°	"	"
0	−0·48	−0·51	180	−0·71	−0·65
30	−0·85	−0·68	210	−0·74	−0·50
60	−0·76	−1·02	240	−0·62	−0·54
90	−1·08	−0·81	270	−0·29	−0·48
120	−0·81	−0·84	300	−0·33	−0·20
150	−0·59	−0·90	330	−0·46	−0·40

The harmonic analyses of these give

$$\begin{aligned} &\text{Series I} && -0''\cdot24 \sin F + 0''\cdot07 \cos F \\ &\text{Series II} && -0''\cdot27 \sin F + 0''\cdot08 \cos F \\ &\text{mean} && -0''\cdot26 \sin F + 0''\cdot08 \cos F. \end{aligned} \tag{13}$$

The mean latitudes are, from Table III,

$$\begin{aligned} &\text{Series I} && -0''\cdot64 \\ &\text{Series II} && -0''\cdot63 \\ &\text{mean} && -0''\cdot64. \end{aligned} \tag{14}$$

8. *Discussion.*—The existence of a term with argument l in the latitude was first pointed out by Brown (**12**). Watts (**13**) has shown that about half of it could be explained by systematic irregularities of the limb varying with the libration in longitude. The main terms in the libration in longitude are

$$l' = +0^\circ\cdot66 \sin 2D + 6^\circ\cdot29 \sin l - 1^\circ\cdot27 \sin (l - 2D) \tag{15}$$

or with $D = 113^\circ$,

$$l' = -0^\circ\cdot5 + 7^\circ\cdot2 \sin (l - 7^\circ). \tag{16}$$

The observed term (12) is thus almost exactly in phase with the libration in longitude. Fig. 1 shows that the agreement between the twelve values of $\overline{\delta B}$ corresponding to this argument and a pure sine term is very striking. If the term were due to the fortuitous distribution of features round the limb, we should not expect such a smooth variation with the libration. The observations suggest that the term may be due to the overall figure of the Moon; an apparent ellipticity of the limb, varying with the libration, due to an ellipsoidal figure of the Moon such as that discussed by Hopmann (**14**), could account for the term.

Before discussion of (13), the first term of (9) must be removed. The terms which require interpretation are thus

$$-0''\cdot26 \sin F + 0''\cdot05 \cos F. \tag{17}$$

Formally we may identify (17) with

$$2\Delta\gamma \sin F - \Delta\Omega \cos F \tag{18}$$

where $2\Delta\gamma$ and $\Delta\Omega$ are corrections to the inclination and node. Thus

$$2\Delta\gamma = -0''\cdot26; \quad \Delta\Omega = -0''\cdot6. \tag{19}$$

The correction to the node is acceptably small and is in the same sense as that derived by Spencer Jones in his revision of Newcomb's occultations (**15**). There is, however, some difficulty in ascribing the coefficient of sin F in (17) to a correction to the inclination. The value of this constant used by Brown was derived from the Greenwich meridian observations, and that derived by Spencer Jones from occultations was in almost exact agreement with it. The mean epoch of both series was about 1875, so that the occultations and meridian observations during the last century both yield a value which does not represent the modern occultations. A possible cause of this discrepancy is that the modern occultations are confined to dark limb disappearances, whereas about 30 per cent of the occultations included by Newcomb and Spencer Jones were reappearances. It is very probable that, if limb corrections are not applied, the values of the inclination obtained from the two limbs will differ, as the principal term in the libration in latitude varies with sin F.

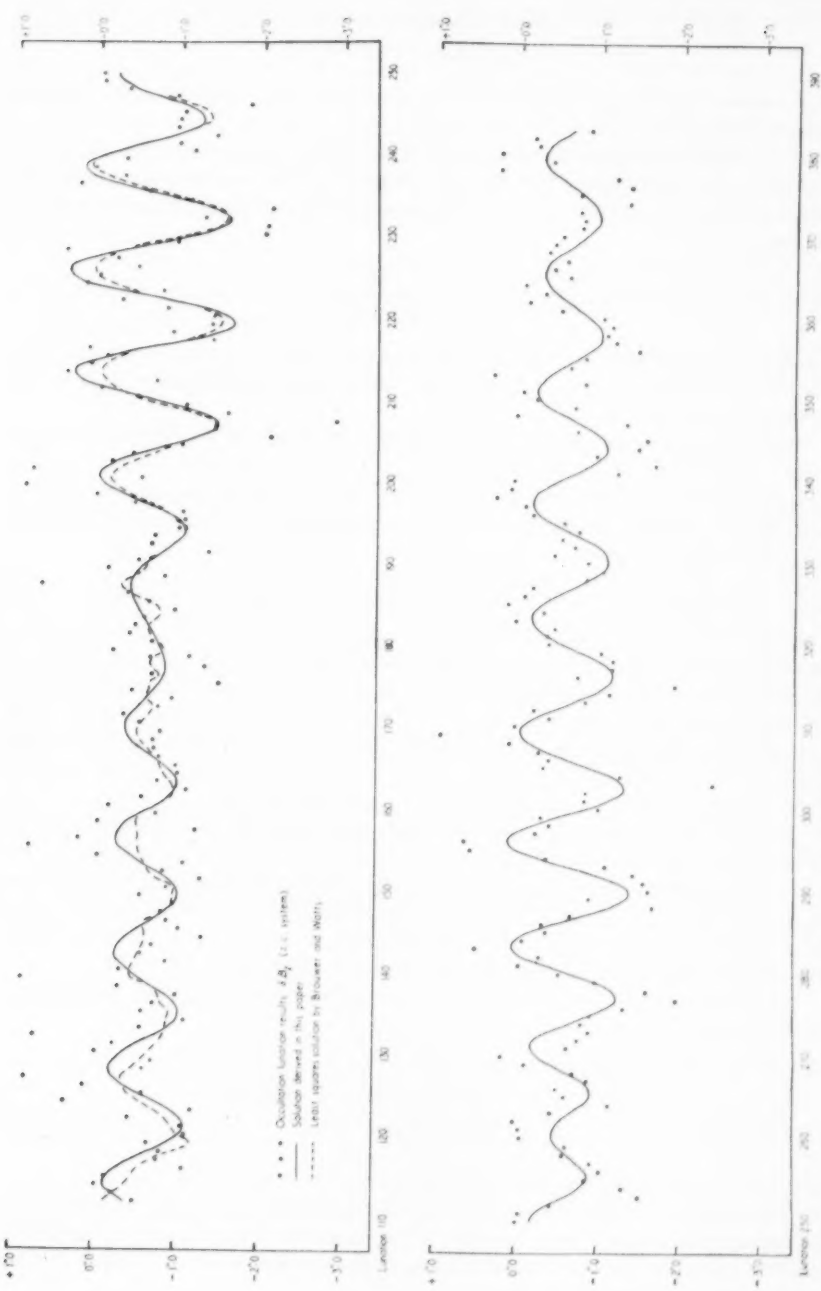

FIG. 2.—*Moon's latitude. Comparison of solutions with the occultations.*

The values of the mean latitude from Newcomb's occultations are given by Spencer Jones as

$$\left.\begin{array}{l}\text{disappearances } -0''\cdot61\\ \text{reappearances } -0''\cdot28.\end{array}\right\} \qquad (20)$$

That derived in the present discussion (14) agrees well with the corresponding phase in (20).

9. *Comparison with the observations.*—The full line curve in Fig. 2 is the sum of (9), (12), (14) and (17). The plotted points are the lunation solutions, δB_l, reduced to the system of the Z.C. The mean residuals from the smooth curve for one point are

Series I	$0''\cdot37$
Series II	$0''\cdot31$.

The larger value for the first period is due probably to fewer observations and more uneven distribution within each lunation, rather than intrinsic inferiority of the individual observations.

Series I is co-terminous with that analysed by Brouwer and Watts (loc. cit.). They solved for the three arguments $F+\Omega$, F, and l by least squares, weighting each δB_l according to its probable error, and applying limb corrections deduced from Watts' statistical discussion of Hayn's charts (**13**). Their solution for the $F+\Omega$ and F terms was

$$+0''\cdot35\sin(F+\Omega)+0''\cdot03\cos(F+\Omega)-0''\cdot20\sin F+0''\cdot22\cos F.$$

The difference between the coefficients of $\sin(F+\Omega)$ and $\cos F$, and the corresponding values derived in this paper, while due partly to the differences of weighting, must chiefly be due to the relatively short extent in time of Series I. During this period, Ω regressed from 0° to 148°; $\sin\Omega$, therefore, had the same sign for most of the period. The separation of $F+\Omega$ from F was thus not perfect. The unsuspected term in $F-\Omega$, introduced by the error in Brown's *Tables*, complicated the separation of these terms still further.

In order to compare the representation of the original observations, reduced to the system of the Z.C., by the two solutions over their common range, the curve of Brouwer and Watts was obtained by subtracting their residuals v_B from δB_l+"d" (loc. cit.; Table I). This curve is the broken curve in Fig. 2. The agreement between the two curves indicates that no serious error has been introduced by the simplified analysis adopted in this investigation.

10. *Conclusions.*—The results of this investigation show that the observations of the Moon's latitude confirm

(i) the known error in Brown's *Tables*,

(ii) the generally adopted value of the Earth's ellipticity,

(iii) the known error of the FK3 equinox,

and that these account completely for the terms with arguments $F\pm\Omega$.

The analyses for the two series are similar for argument l, and nearly identical for argument F and the mean latitude. The existence of these terms is confirmed, but their interpretation is doubtful owing to the possible systematic effect of limb irregularities, or figure of the Moon.

A good deal of the scatter of the points from the curve in Fig. 2 is most likely due to the simplifying assumptions that the lunation solutions can be treated as individual observations, equally spaced in time. It seems to be highly desirable that a rigorous analysis of individual occultations should be carried out when the Washington limb survey is completed. When Brown's *Tables* become obsolete in 1960, they will have been in use for 37 years, or almost two revolutions of the node. For half this period the places of the occulted stars have been taken from the same star catalogue. The occultations during this period form the most homogeneous series of lunar observations of comparable duration ever obtained. A discussion of these could be expected to yield valuable information on the adopted lunar constants.

My thanks are due to Dr R. d'E. Atkinson for many discussions on the subject of this paper, and to Mrs F. M. McBain Sadler for communicating the occultation results for 1953 in advance of publication.

Royal Greenwich Observatory,
Herstmonceux Castle,
Sussex:
1956 *May* 11.

References

(1) e. g., App. to *Green. Obs.*, 1939, p. 54.
(2) E. W. Brown, *Tables of the Motion of the Moon.* I, p. 28.
(3) H. Jeffreys, *M.N. Geophys. Suppl.*, **5,** 219, 1948.
(4) R. d'E. Atkinson and C. A. Murray, *M.N.*, **115,** 60, 1955.
(5) E. W. Brown, *M.N.*, **74,** 395, 1914.
(6) E. W. Brown, *Tables of the Motion of the Moon.* I, pp. 27–28.
(7) *Astr. Papers of A.E.*, X, part 2, 1940.
(8) E. W. Woolard, *A.J.*, **57,** 38, 1951.
(9) D. Brouwer and C. B. Watts, *A. J.*, **52,** 169, 1946.
(10) 1943 *A. J.*, **53,** 163, 1948; 1948 *A. J.*, **57,** 55, 1951.
1944–5 *A. J.*, **55,** 7, 1949; 1949–50 *A. J.*, **58,** 205, 1953.
1946 *A. J.*, **55,** 47, 1950; 1951–52 *A. J.*, **60,** 315, 1955.
1947 *A. J.*, **55,** 247, 1951; 1953– in preparation.
(11) *Improved Lunar Ephemeris*, Washington, 1955.
(12) E. W. Brown, *M.N.*, **93,** 603, 1933.
(13) C. B. Watts, *A. J.*, **48,** 170, 1939.
(14) J. Hopmann, *Sitz. Ost. Akad. Wiss.*, IIa, 161, 1952.
(15) H. Spencer Jones, *Cape Annals*, XIII, part 3, 1932.

MEAN DAILY AREAS AND HELIOGRAPHIC LATITUDES OF SUNSPOTS IN THE YEAR 1955

Royal Greenwich Observatory

(Communicated by the Astronomer Royal)

(Received 1956 September 20)

The following results are in continuation of those for the years 1953 and 1954 in *M.N.*, **115**, 577, 1955. They are derived from the measurement at Herstmonceux of photographs taken at the Royal Greenwich Observatory, at the Royal Observatory, Cape of Good Hope, and at the Kodaikanal Observatory, India. Plates for two missing days were supplied by the Superintendent, Mount Wilson Observatory, California, U.S.A., and the Director, Fraunhofer Institut, Freiburg, Western Germany.

TABLE I

No. of rotation	Rotation commenced U.T.	Days photographed	Mean daily areas: Projected* Umbrae	Projected* Whole spots	Projected* Faculae	Corrected for foreshortening† Umbrae	Corrected for foreshortening† Whole spots	Corrected for foreshortening† Faculae
	1954–5							
1355	Dec. 21·63	27	118	694	281	91	537	304
1356	Jan. 17·96	28	60	340	408	51	290	478
1357	Feb. 14·30	26	36	197	364	27	156	416
1358	Mar. 13·63	28	13	69	263	9	52	296
1359	Apr. 9·93	27	23	118	414	19	104	480
1360	May 7·18	28	72	402	486	51	284	561
1361	June 3·39	27	107	661	587	84	536	709
1362	June 30·59	27	53	300	749	41	227	847
1363	July 27·80	27	139	788	723	100	572	819
1364	Aug. 24·03	27	130	681	875	101	538	996
1365	Sept. 20·28	28	94	472	1070	78	385	1270
1366	Oct. 17·57	27	355	2007	910	281	1612	1104
1367	Nov. 13·87	27	318	1905	1121	234	1405	1271
1368	Dec. 11·18	28	193	1139	1350	142	846	1594

* Expressed in millionths of the Sun's disk
† Expressed in millionths of the Sun's hemisphere

TABLE II

Year	No. of days: Photographed	No. of days: Without spots	Mean daily areas: Projected* Umbrae	Projected* Whole spots	Projected* Faculae	Corrected for foreshortening† Umbrae	Corrected for foreshortening† Whole spots	Corrected for foreshortening† Faculae
1954	365	237	9	49	117	6	35	138
1955	365	45	125	715	684	96	553	794

* Expressed in millionths of the Sun's disk
† Expressed in millionths of the Sun's hemisphere

Table I gives the mean daily areas of umbrae, whole spots and faculae for each synodic rotation of the Sun in the year 1955. The numbers of the rotations are in continuation of Carrington's series. The annual means for the year appear in Table II, which also includes similar figures for the minimum year 1954.

Table III gives for each rotation in 1955 the mean daily area of the whole spots (corrected for foreshortening) and mean heliographic latitude of the spotted areas separately for the northern and southern hemispheres of the Sun. The mean heliographic latitude of the entire spotted area and the mean distance of all spots from the equator are also tabulated.

TABLE III

No. of rotation	Rotation commenced U.T.	Spots north of the equator: Mean daily area	Spots north of the equator: Mean heliographic latitude	Spots south of the equator: Mean daily area	Spots south of the equator: Mean heliographic latitude	Mean latitude of entire spotted area	Mean distance from equator of all spots
	1954–5		°		°	°	°
1355	Dec. 21·63	455	29·97	82	23·76	+21·79	29·03
1356	Jan. 17·96	169	29·83	122	22·73	+ 7·78	26·85
1357	Feb. 14·30	95	20·02	61	21·81	+ 3·63	20·72
1358	Mar. 13·63	44	23·80	8	24·96	+16·18	23·99
1359	Apr. 9·93	62	29·78	43	31·36	+ 4·78	30·43
1360	May 7·18	221	26·14	63	25·64	+14·59	26·03
1361	June 3·39	69	29·11	467	23·52	−16·71	24·24
1362	June 30·59	124	29·22	103	29·88	+ 2·38	29·52
1363	July 27·80	260	18·69	312	22·07	− 3·53	20·53
1364	Aug. 24·03	398	27·73	139	22·75	+14·66	26·44
1365	Sept. 20·28	319	23·16	66	22·13	+15·35	22·98
1366	Oct. 17·57	829	24·75	782	24·17	+ 1·01	24·47
1367	Nov. 13·87	882	24·51	523	15·06	+ 9·79	20·99
1368	Dec. 11·18	490	24·00	357	23·32	+ 4·06	23·71

TABLE IV

Year	Days photographed	Spots north of the equator: Mean daily area	Spots north of the equator: Mean heliographic latitude	Spots south of the equator: Mean daily area	Spots south of the equator: Mean heliographic latitude	Mean latitude of entire spotted area	Mean distance from equator of all spots
			°		°	°	°
1954	366	12	28·84	23	17·20	−1·55	21·16
1954	365 Old Cycle	1	9·25	12	8·24	−7·17	8·30
	365 New Cycle	11	30·27	11	27·60	+1·86	28·96
1955	365	325	25·39	228	22·35	+5·71	24·14

Corresponding annual mean values of all these quantities for 1954 and 1955 are given in Table IV.

Tables II and IV are in continuation of those in *Monthly Notices* for the years *1874* to *1888*, **49,** 381, 1889: *1889* to *1902*, **63,** 465, 1903: *1901* to *1914*,

76, 402, 1916: *1913* to *1924*, **85,** 1007, 1925: *1923* to *1933*, **94,** 870, 1934: *1933* to *1945*, **110,** 501, 1950: and *1944* to *1954*, **115,** 577, 1955.

The chief features of the record for 1955 are as follows:—

(1) The rise in sunspot activity was the steepest since the Greenwich records began in 1874. The mean area for the second six months was more than double that of the first half-year.

(2) The largest spot group crossed the Sun's central meridian on November 14·9, its mean latitude being 24°·0 N., and mean area 1026 millionths of the hemisphere. In addition to this group there were six others with mean areas exceeding 500 millionths.

(3) On 45 days no sunspots were seen and on 21 days faculae were also absent; for 1954 the figures were 237 and 180 respectively.

(4) The ratio of mean corrected areas of faculae/sunspots was 1·44, and that of mean corrected areas of umbrae/whole spots 0·174.

(5) As in 1954, the northern hemisphere was more spotted than the southern.

The number and distribution, northern and southern hemispheres, of spot groups of

(*a*) two days' duration or longer

(*b*) one day's duration

were as follows:—

	(*a*)	(*b*)
Northern spots	96	24
Southern spots	65	16
Total	161	40

(6) The following table gives the mean daily areas of sunspots and faculae, corrected for foreshortening and expressed in millionths of the Sun's hemisphere, for each calendar month.

Month, 1955	Spots	Faculae
January	541	400
February	287	520
March	37	311
April	80	443
May	302	519
June	490	716
July	216	831
August	574	769
September	437	1126
October	921	1163
November	1665	1273
December	1077	1445

Royal Greenwich Observatory,
Herstmonceux Castle, Sussex:
1956 *September* 19.

MOTIONS IN THE SUN AT THE PHOTOSPHERIC LEVEL
VII. Vertical Distribution of the Equatorial Velocity Field

A. B. Hart

(Communicated by the Director, University Observatory, Oxford)

(Received 1956 August 21)

Summary

In an attempt to determine the vertical distribution of the velocity field from its centre-limb variation, 274 line-of-sight velocities obtained in an earlier paper (from Fe line Doppler displacements) are analysed. They are divided into 3 groups, whose successive positions are separated by 11°·0 of heliographic longitude, and a relation is sought between the velocity dispersion displayed by a group and its position on the disk. No definitive result is obtained.

A positive result is, however, derived from a comparison of velocity measurements on strong (the two Na D) lines and on weak (one Ni and one Ti) lines having, respectively, average Rowland intensities 25 and 2·5. The Doppler shifts are found from microphotometer tracings at 40 positions on each of 4 of the spectra earlier used for the Fe line measurements. At each of the 40 positions the four measurements are combined, thereby reducing the error in the velocity at any point to $\pm 0{\cdot}05(8) \pm 0{\cdot}03(7)$ km sec^{-1} for the Ni–Ti sequence and to $\pm 0{\cdot}06(0) \pm 0{\cdot}03(8)$ km sec^{-1} for the Na sequence.

After correction for effects of measurement error, the mean velocity amplitude is $\pm 0{\cdot}16(2)$ km sec^{-1} for the Ni–Ti sequence, compared with $\pm 0{\cdot}12(0)$ km sec^{-1} for the Na. A statistical discussion shows that the velocity sequences are similar, but that the difference in mean amplitude is significant. From a simple model of line formation and taking account of redistribution of light by the apparatus function of the spectroscope, the weak and strong line velocities are shown to refer to approximate optical depths 0·42 and 0·32, respectively, as measured in the continuum. The amplitude of the velocity field, therefore, diminishes extremely rapidly with increasing height in the photosphere.

Introduction.—The presence of a velocity field in the equatorial region of the solar photosphere has been demonstrated in a previous paper (**7**). It was shown there that the field takes the form of irregular deviations from the mean rotational velocity, having line-of-sight components of up to $\pm 0{\cdot}5$ km sec^{-1} and extending over distances of the order of 10^4 km. That this velocity distribution retains its identity for a considerable period of time was shown by the marked stability observed over a period of an hour. However, before the motion can be completely specified and the physical mechanism producing it identified, several more facts need to be known. Of these, the distribution of the field with depth in the photosphere will clearly be of paramount importance; it forms the subject of the investigation described in the present paper.

There are two ways in which the variation of velocity with depth can be determined. The centre-limb variation of the velocity field is one and a comparison of the velocities found from weak and from strong lines is the other. In the first section the former method is considered; the two subsequent sections contain a discussion of the second method.

Papers in the series "Motions in the Sun at the Photospheric Level" will be referred to in the text by their serial numbers.

1. *The centre-limb variation of the velocity field.*—The material for an analysis of the variation of the velocity field across the solar disk is contained in Paper VI* (7). It consists of velocity measurements in the equatorial region, made at the beginning and end of an hour's interval, along an arc of solar surface extending inwards from the limb over 34°·5 of longitude. These velocity values, E_1 and E_2 respectively, are given in VI, Tables IV (i) and (ii) in the form of residuals from the mean rotational velocity; each of the two sequences contains 140 velocities. Corresponding entries in the tables refer to measurements made at the same disk positions in the two cases (VI, Section 2.3), but owing to the solar rotation the tabulated heliographic longitudes differ by approximately 0°·5.

The procedure is first to divide the velocity residuals into groups and then to see if there is any relation between the velocity dispersion displayed by a group and its position on the disk. It was shown in VI, Section 4.1, that the average linear extent of a velocity "oscillation" in the field is $2{\cdot}6 \times 10^4$ km, which is equivalent to 2°·1 of longitude. In order that the mean velocity dispersion should be well determined, each group must contain several oscillations. Accordingly, the measurements were divided into three groups each covering 11°·0 of longitude (and containing between them 274 of the measured velocities). Position on the disk is defined by the value of $(\theta+\theta_1)$, θ and θ_1 being the angles subtended by the sub-terrestrial point and the mid-point of the range at the centre of the Sun and at the observer, respectively. Table I below gives the values of $\cos(\theta+\theta_1)$ for the three ranges. The column headed L shows the relevant longitude values for entry into VI Tables IV (i) and (ii), and D is the root-mean-square velocity deviation calculated from the n corresponding velocity values. It is useful to have some indication of the limits between which D may be expected to lie, if the n velocities are regarded as a sample from a hypothetical infinite population of velocity measurements for the group. This is provided by the standard error, $D/[2(n-1)]^{1/2}$ (Paper IV (6), Section 4.1), of D, given in the last column of Table I.

If the emergent light from the Sun can be considered to originate at a fixed distance $\bar{l}$ in the line-of-sight, below the surface (**10a**), then the radial depth of

TABLE I

L	$\cos(\theta+\theta_1)$	D km sec^{-1}	n	$D/[2(n-1)]^{1/2}$ km sec^{-1}
(i) 224°·5–235°·3 (ii) 224°·0–234°·8	0·355	±0·13(1)	62	±0·01(2)
(i) 235°·6–246°·3 (ii) 235°·1–245°·8	0·527	0·18(9)	92	0·01(4)
(i) 246°·6–257°·4 (ii) 246°·0–256°·8	0·676	0·15(5)	120	0·01(0)

* References to sections, tables etc. in Paper VI, "Large-Scale Motions in the Equatorial Region", are preceded by VI.

observation is $\bar{\iota}\cos(\theta+\theta_1)$. Thus the variation of the velocity dispersion with $\cos(\theta+\theta_1)$ gives the variation with depth in the atmosphere. The values of $\cos(\theta+\theta_1)$ and D given in Table I are plotted in Fig. 1, the vertical line through each point showing the estimated standard error of D. No regular change of dispersion with height is clearly revealed. A solution for a linear variation, $D=m\cos(\theta+\theta_1)+k$, was therefore made by the method of least squares; in so doing, equal weight was given to the three regions. Values of

$$m=+0{\cdot}07(7)\pm0{\cdot}16(0)\text{ km sec}^{-1} \quad \text{and} \quad k=0{\cdot}11(8)\pm0{\cdot}08(6)\text{ km sec}^{-1}$$

were obtained, and the resulting line is shown in Fig. 1. However, the relative sizes of m and its error show that the solution is, unfortunately, entirely formal.

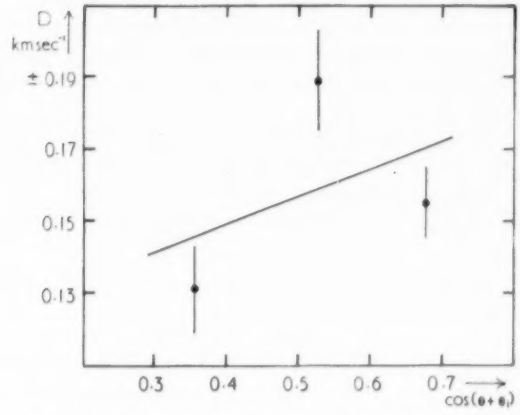

FIG. 1.—*Variation of velocity dispersion with depth in the solar photosphere. Abscissae are proportional to the depth in the photosphere. Ordinates are values of the velocity dispersion.*

Thus no information concerning the distribution of the velocity field with height can be derived from the existing data. The reason for this is clear. Owing to the large linear extent of a velocity oscillation, each region contains only a small number of complete oscillations. The values of the velocity dispersions are therefore very much more uncertain than would appear from the number of measured velocity residuals in each group. Observations at a number of well separated epochs are necessary if the centre-limb variation of the field is to be used to determine its distribution with depth. Moreover, if line-of-sight velocities are used in the analysis, the centre-limb variation due to a change in velocity with height must be distinguished from that due to any anisotropy of the field.

2. *Velocity measurements on weak and strong lines*

2.1. *Plan of investigation.*—With the failure of the centre-limb variation of the field to give its vertical distribution, the possibility of a comparison between weak and strong line velocities was considered. The first investigation of this kind was made by W. S. Adams (**1**), who in 1906 measured the velocities displayed by the Hα line of hydrogen and λ 4227 of Ca and compared them with measurements made on lines of Rowland intensity 1 and 2 in the wave-length region 4195–4295 A. As, however, the measures were differential cross-wire ones made on two juxtaposed lines, the shifts found for the wide strong lines were liable to a considerable subjective error.

The velocities obtained in Paper VI and analysed in Section 1 above, were found from measurements on six Fe lines of Rowland intensity 2–6 in the wave-length region 5900 A. Consequently, the same (two) plates provide ideal material for the new investigation, if the velocities exhibited by the Na D lines, Rowland intensities 20 and 30, are also measured. As there are only two solar lines from which to obtain the new velocities, the determination of their Doppler shifts with sufficient accuracy presents some difficulty. The width of the lines excludes the possibility of micrometer measurements; to make microphotometer tracings at low magnification and then to measure these seemed the best procedure. Even so, it is unlikely that the accuracy will equal that of the Fe line measurements. Hence it was decided to limit the measurement to a region where the previous results had shown that the largest velocity deviations were likely to occur. Inspection of VI, Fig. 4, shows that the region between heliographic longitudes 225°·9 and 238°·3 on the second of the two plates is the most suitable; the velocity values appear in VI, Table IV(ii).

The selected plate, obtained at Oxford on 1953 May 5, carries four spectra 15·5 mm in height extending inwards from the East equatorial limb on a solar image 85 mm in diameter; the four spectra were exposed within a few minutes of each other (VI, Section 1). Each of the spectra was measured at exactly the same disk positions (VI, Section 3.2) and it is the mean of the four velocities at each disk position which appears in VI Table IV(ii) and is shown graphically in VI, Fig. 4.

TABLE II

Terrestrial lines		Solar lines			
Wave-length A	Row. int.	Wave-length A	Row. int.	Element	Vel. factor km sec^{-1} (TU)$^{-1}$
5885·977	5	5889·973	30	Na(D_2)	93·89
5887·222	5	5892·883	4	Ni	94·02
5891·661	4	5895·940	20	Na(D_1)	94·16
5898·169	4	5899·304	1	Ti	94·30
5901·468	6				

In the wave-length range covered by the water-vapour lines needed to provide a reliable standard of zero velocity (**16**) for the new measurements, one Ni and one Ti line also occur. The intensities of these lines are closely comparable with those of the Fe lines previously measured (VI, Table II), so that a comparison of the velocities derived from the two sets of lines will provide a most stringent test of the reliability of the new results, since only one water-vapour line is common to both series of measurements. The wave-lengths recommended by the International Astronomical Union (**2, 5**) and the Rowland intensities (**20**) for the four solar and five water-vapour lines are given in Table II.

2.2. *Photometry.*—Photometry of the spectra was performed with the Oxford Moll-type microphotometer (**14**). Light from a constant-voltage lamp is focused on a slit, whose height and width can be varied and which is in turn focused on the plate being measured. The plate is driven across the beam at a uniform rate and the transmitted light falls on a Moll quick vacuum thermocouple. This is

connected to a Moll microgalvanometer, the deflection of which is recorded, by a spot of light, on a piece of bromide paper moving in a direction perpendicular to the excursion of the light spot. Simultaneously with the registration of the plate transmission, a coordinate system is recorded on the paper. The horizontal lines of the grid are impressed continuously throughout the recording. A series of teeth, engaging with a contact-maker at equal fractions of a revolution of the screw driving the plate carriage, actuate the device providing the vertical lines.

Measurements of line positions made earlier by Miss Adam, from microphotometer tracings, had shown large discrepancies between tracings made with the plate travelling in opposite directions past the analysing light beam. This forward–reverse discordance presumably arises from the inability of the galvanometer to respond sufficiently quickly to sharp changes in light intensity incident on the thermocouple. If this is so, the effect will be much reduced if the maximum light intensity, corresponding to clear film transmission of the plate, is reduced. Filters were therefore placed between the lamp-house and the slit to give, with the slit height used, a zero-clear film excursion of approximately 16 mm on the tracing, compared with the value of about 100 mm normally used. (Irrespective of whether the reduction in the maximum excursion has the desired effect, it makes measurement of the tracings simple (Section 2.3) and comparatively quick.)

The height of the microphotometer slit was adjusted to give a projected image of 0·1 mm on the plate, comparable with the diaphragm aperture of 0·13 mm used in the earlier measurements (VI, Section 2.3). The projected width of the slit exceeded that of the thermocouple, so that the effective width, 0·03 mm, of the latter determines the dimension of the analysing beam parallel to the direction in which the plate moves; 1 mm on the plate is equivalent to 1·5 A. A tracing-to-plate magnification of 6·89 (**14**) was used, and the plate was driven at a speed of approximately 3 mm min^{-1}. The wave-length range containing the lines to be measured (Table II) therefore occupies a length of some 80 mm on the tracing and takes about 4 minutes to record.

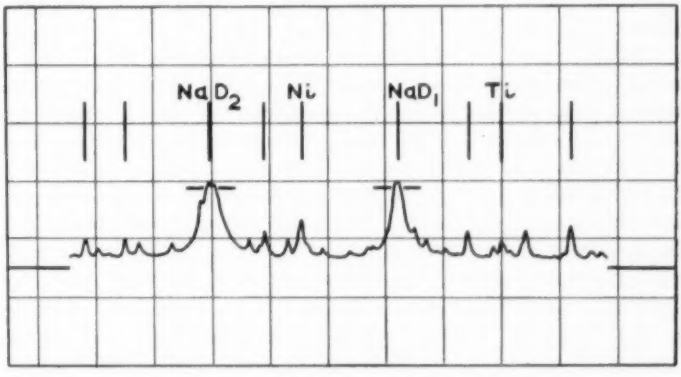

FIG. 2.—*Reproduction of a typical tracing.*

Scale: The side of one tracing unit measures 8·71 mm on the original.
Lines listed in Table II are marked. *The short horizontal lines indicate approximately the positions at which measurements were made on the D lines.*

Table IV (ii) in Paper VI shows that the earlier velocity measurements were made at 40 positions in the longitude range on the single plate selected for further investigation (Section 2.1). Tracings were made parallel to the dispersion, in the forward and reverse directions, at precisely the same positions as before, on each of the four spectra on the plate (making a total of 320). Between successive tracings on any spectrum, the plate was therefore moved by 0·1 mm perpendicular to the dispersion (VI, Section 2.3). Press Contrast developer was used to develop the tracings; they were fixed in the usual way. Fig. 2 is a reproduction of a typical tracing.

2.3. *Measurement.*—All measurements were made on a Hilger photo-measuring micrometer. The tracing was clipped between two sheets of plane glass, $\frac{1}{4}$ inch thick, and mounted on a small stage on top of the main stage of the machine. This subsidiary stage can be moved over the main stage in a direction perpendicular to the direction of run of the main measuring screw. Cross-wires oriented parallel and perpendicular to the direction of the main screw were carried in the eyepiece.

A tracing was first aligned with the horizontal grid lines parallel to the run of the measuring screw. For all lines except the D lines, the subsidiary stage was then moved until the tip of the line being measured fell on the horizontal cross-wire. The positions of the line tip and of the vertical grid lines on either side at this level were noted. The tips of the D lines are broad (Fig. 2) and, owing to the small number of developed silver grains in the core of the line, are frequently irregular. To measure the position of maximum intensity would introduce a very large accidental error into the measurements, probably masking the true velocity shifts altogether. Consequently, measurements were made on the sloping sides of the lines immediately below the tip (the approximate positions are marked in Fig. 2); the mean of the two measurements was used for the corresponding line position in the reductions. Measurement of the neighbouring grid lines was made at the same level as that of the lines. The recorded value of every measurement was the mean of three settings. This reduces the accidental error of the D line measurements, which are difficult to make, and ensures that the positions of the grid lines, upon which the whole process of finding the line shifts depends, are known as precisely as possible.

2.4. *Reduction to velocities.*—During the processing of the tracings the paper is distorted, as shown by the variation in the distance between successive grid lines which were impressed during the recording at equal fractions of a revolution of the screw. An analysis of the measured lengths of 360 tracing units (T.U.) gave a mean value 8·708 mm; a displacement of 0·001 units corresponds to $(8{\cdot}708 \times 10^{-3}/6{\cdot}89)$ mm, i.e. to 1·3 microns, on the plate. The root-mean-square deviation of a single grid interval from the mean, as calculated from Peters' formula, is $\pm 0{\cdot}041$ mm, equivalent to $\pm 0{\cdot}005$ T.U. Since the microphotometer has been in frequent use for the past twenty years, it was feared that the two teeth operating the grid line mechanism (Section 2.2) might have worn unequally, causing the distances between alternate grid lines to vary systematically. Investigation of the 360 values for this effect gave $8{\cdot}707 \pm 0{\cdot}003$ mm and $8{\cdot}708 \pm 0{\cdot}003$ mm for the average alternate distances. The difference between the two values lies within their uncertainty and is therefore not significant.

The following method was used to reduce the tracings. The measured position of any line was converted to its fractional position between two grid

lines, which were numbered consecutively. In this way the line positions are expressed on a uniform scale, since the grid lines mark equal fractions of a revolution of an accurate screw. It is these reduced values which are used in all subsequent calculations.

The velocity corresponding to a given line position can be found most simply, and also independently of any asymmetry in the horizontal apparatus function of the spectroscope (**3, 15**), by reference to some standard spectrum, usually of the centre of the Sun. In this case, however, the mean position of the measured lines was found for each of the four separate spectra and the spectrum's own mean used as the standard in each case. Conversion of line shifts to velocities then follows the method described in VI Section 2.3; the relevant velocity factors are given in Table II.

At each point on each spectrum (160 positions in all), the mean velocity from the Ni line and the Ti line (Table II) was then calculated, and similarly the mean Na velocities. All four spectra were exposed within such a short time of each other (VI, Table I) that the measurements made at exactly the same 40 disk positions on each spectrum (Section 2.2) have also been made at the same positions on the solar surface. A mean velocity for each of the 40 positions can therefore be calculated. These values are given in Table III for the Ni and Ti lines and for the Na lines in the columns headed V(Ni + Ti) and V(Na) respectively. h is the distance on the solar image from the limb to the point at which the velocity has been found; it is measured along the E–W chord of the image defined by the spectroscope slit (VI, Section 1).

TABLE III

h mm	V(Fe) km sec^{-1}	V(Ni + Ti) km sec^{-1}	V(Na) km sec^{-1}	h mm	V(Fe) km sec^{-1}	V(Ni + Ti) km sec^{-1}	V(Na) km sec^{-1}
2·04	+0·18	+0·12	+0·02	4·04	+0·11	+0·11	+0·04
2·14	+ ·09	+ ·09	+ ·10	4·14	— ·01	+ ·03	+ ·06
2·24	+ ·04	+ ·06	— ·02	4·24	— ·05	— ·12	+ ·01
2·34	— ·01	·00	— ·22	4·34	+ ·02	+ ·21	+ ·08
2·44	— ·12	— ·18	— ·15	4·44	+ ·08	·00	— ·14
2·54	— ·27	— ·12	+ ·02	4·54	— ·01	+ ·01	— ·13
2·64	— ·16	— ·16	— ·02	4·64	— ·08	— ·07	— ·10
2·74	— ·10	— ·01	·00	4·74	+ ·08	+ ·10	+ ·10
2·84	+ ·15	+ ·15	+ ·05	4·84	+ ·28	+ ·34	+ ·24
2·94	+ ·15	+ ·10	+ ·09	4·94	+ ·38	+ ·38	+ ·26
3·04	+ ·16	+ ·07	+ ·07	5·04	+ ·42	+ ·38	+ ·24
3·14	— ·03	+ ·08	·00	5·14	+ ·28	+ ·21	+ ·20
3·24	— ·20	— ·18	— ·13	5·24	·00	— ·02	— ·14
3·34	— ·33	— ·24	— ·06	5·34	— ·15	— ·17	— ·15
3·44	— ·15	— ·10	— ·07	5·44	— ·19	— ·29	— ·22
3·54	— ·04	— ·19	— ·20	5·55	— ·22	— ·26	— ·21
3·64	— ·10	— ·04	— ·13	5·64	— ·34	— ·36	— ·28
3·74	— ·02	+ ·01	— ·01	5·74	— ·22	— ·17	+ ·03
3·84	+ ·10	+ ·04	+ ·12	5·84	·00	+ ·04	+ ·06
3·94	+0·20	+0·15	+0·09	5·94	+0·07	+0·04	+0·07
				$(\Sigma V^2/n)^{1/2}$	±0·177	±0·172	±0·131

Three of the four solar lines used for velocity determinations are essentially unblended, but the Na D_2 line has several water-vapour companions. One of the advantages of the use of the mean spectrum as standard is that the wave-length correction normally applied in stellar radial velocity work, to reduce the mean algebraic residual of a blended line to zero, has automatically been made.

Also given in Table III are the Fe line velocities, from Paper VI, for the corresponding disk positions. Like the new measurements, they are uncorrected for solar rotation and are expressed as residuals from the mean velocity for the 40 positions; they differ therefore from the entries between heliographic longitudes 225°·9 and 238°·3 in VI, Table IV(ii).

2.5. *Reliability of the velocities.*—In the analysis (Sections 3.1 and 3.2) of the weak-line and strong-line velocities the uncertainties in the measured velocities are needed. It is interesting first to see how far the method of photometry has been successful in removing the forward–reverse discordance (Section 2.2). The average F–R of the 160 Ni–Ti values is $+0{\cdot}00(4)$ km sec^{-1}, that of the Na values is $-0{\cdot}07(4)$ km sec^{-1}. Although the discrepancy has not been entirely removed in the case of the strong lines, the value is small, corresponding to a displacement on the plate of only 1 micron.

The method of assessing the uncertainties introduced into the velocities during measurement is fully explained in VI Section 2.4. Table IV gives the results of the calculations for the three groups of lines, Ni–Ti, Na and water-vapour, in the present instance. The column headed $\bar{s}$ contains the average of the 160 values of the root-mean-square error of a single line found from the deviations of the n individual lines in a group. In the column headed σ is the corresponding estimate of the error of a single line from a hypothetical infinity of measurements, the uncertainty of this estimate being $\sigma/[2(n-1)]^{1/2}$; the value, $\sigma(\mu)$, of the displacement on the plate to which σ corresponds is also given. The error to be attributed to the mean of n measurements is $\sigma_n = \sigma/\sqrt{n}$; $\sigma_n/[2(n-1)]^{1/2}$ is the uncertainty of this value.

TABLE IV

	$\bar{s}$ km sec^{-1}	n	σ km sec^{-1}	$\sigma/[2(n-1)]^{1/2}$ km sec^{-1}	σ_n km sec^{-1}	$\sigma_n/[2(n-1)]^{1/2}$ km sec^{-1}	$\sigma(\mu)$ microns
Ni-Ti	±0·11(3)	2	±0·14(2)	±0·10(0)	±0·10(0)	±0·07(1)	1·9
Na	0·11(8)	2	0·14(8)	0·10(5)	0·10(5)	0·07(4)	2·0
w-v	0·11(7)	5	0·12(4)	0·04(4)	0·05(6)	0·02(0)	1·7
Fe	±0·13(4)	6	±0·14(1)	±0·04(5)	±0·05(8)	±0·01(8)	1·9
w-v	0·16(0)	6	0·16(8)	0·05(3)	0·06(9)	0·02(2)	2·2

In the lower part of Table IV are given, for comparison, the values of $\bar{s}$, σ, etc. from Paper VI, found for measurements on the photographic plate itself (VI, Section 2.4). The values of $\bar{s}$ found in the present case are very uniform and somewhat smaller than the earlier ones. (This slightly greater consistency of measurement is, however, achieved at the expense of a factor of three and a half in the time taken for measurement.) The close agreement of the $\bar{s}$ values for the Na and Ni–Ti groups of lines shows how satisfactorily the positions of the strong D lines are found with the method of measurement adopted. Moreover, the

general similarity in the values of σ obtained by the two entirely different methods of measurement (Sections 2.2 and 2.3 and VI, Section 2.1) strongly suggests that the limit of accuracy, set by irregularities in the silver grain distribution on the plate, is being reached.

By a simple extension of the analysis in Paper VI one obtains for the root-mean-square error, e, of a velocity in Table III, $\pm 0{\cdot}05(8) \pm 0{\cdot}03(7)$ km sec^{-1} and $\pm 0{\cdot}06(0) \pm 0{\cdot}03(8)$ km sec^{-1} for a Ni–Ti and a Na entry respectively. (Equal reliance is thus to be placed on the two velocity sequences.) On the other hand, the average root-mean-square deviation of the velocity at a point, as calculated from the dispersion in the four measured velocities (Section 2.4), is $\pm 0{\cdot}05(4)$ km sec^{-1} for the Ni–Ti sequence and $\pm 0{\cdot}06(1)$ km sec^{-1} for the Na sequence. Hence no greater velocity differences exist than can be ascribed to the errors of measurement and the tabulated mean values should represent more accurately than the individual measurements the velocities actually occurring on the solar surface (cf. VI, Section 3.2).

The smaller value of e, $\pm 0{\cdot}04(5) \pm 0{\cdot}01(4)$ km sec^{-1}, for a tabulated Fe velocity (VI, Section 4.1) mainly reflects the fact that only two solar lines contribute to a measured velocity in the present investigation, compared with six in the previous one (Table IV).

3. *Distribution of the velocity field with depth in the photosphere*

3.1. *Comparison of the Fe and Ni–Ti velocities.*—Fig. 3 shows the Ni–Ti, Na and Fe velocity sequences given in Table III; the dispersion in velocity (measured by the deviation $[\Sigma V^2/n]^{1/2}$, also given in Table III) is for the Ni–Ti sequence $\pm 0{\cdot}17(2)$ km sec^{-1}, and for the Na sequence $\pm 0{\cdot}13(1)$ km sec^{-1}. Now the weight to be accorded to differences in velocity dispersion displayed by the groups of weak (Ni–Ti) and strong (Na) lines depends largely on the extent to which the weak line velocities reproduce the values found in Paper VI from the measurement of Fe lines of comparable intensity (Section 2.1). The resemblance between the Fe and Ni–Ti velocity sequences in Fig. 3 is very marked and is reflected in the close agreement of the velocity dispersion, $\pm 0{\cdot}17(7)$ km sec^{-1}, of the Fe sequence with that of the Ni–Ti. Proof of the identity of the two sequences is, in fact, hardly necessary, but it will provide a standard for the interpretation of the strong-line velocities.

The coefficient of correlation r (**22a**) between the Fe and Ni–Ti sequences is $+0{\cdot}926$ and one wishes to know if this shows that the two sequences have the same "pattern" or whether the correlation could arise by random sampling from an uncorrelated population (correlation coefficient $\rho = 0$). For this purpose it is best to use Fisher's $z - \zeta$ test (**9b**); z and ζ are transformations of r and ρ. One finds that the probability of the observed correlation between the series arising by chance (1 in 10^{22}) is utterly negligible.

Having established the identity in pattern of the two sequences one must also show, in order to prove complete identity, that the patterns have the same scale. This necessitates a comparison of the velocity dispersions of the two sequences. The apparent velocity dispersion, $[\Sigma V^2/n]^{1/2}$, calculated from the entries in Table III, is larger than the true dispersion owing to the effects of errors of measurement. The best estimate of the true dispersion is given by (**22b**)

$$nd^2 = \Sigma V^2 - ne^2, \qquad (1)$$

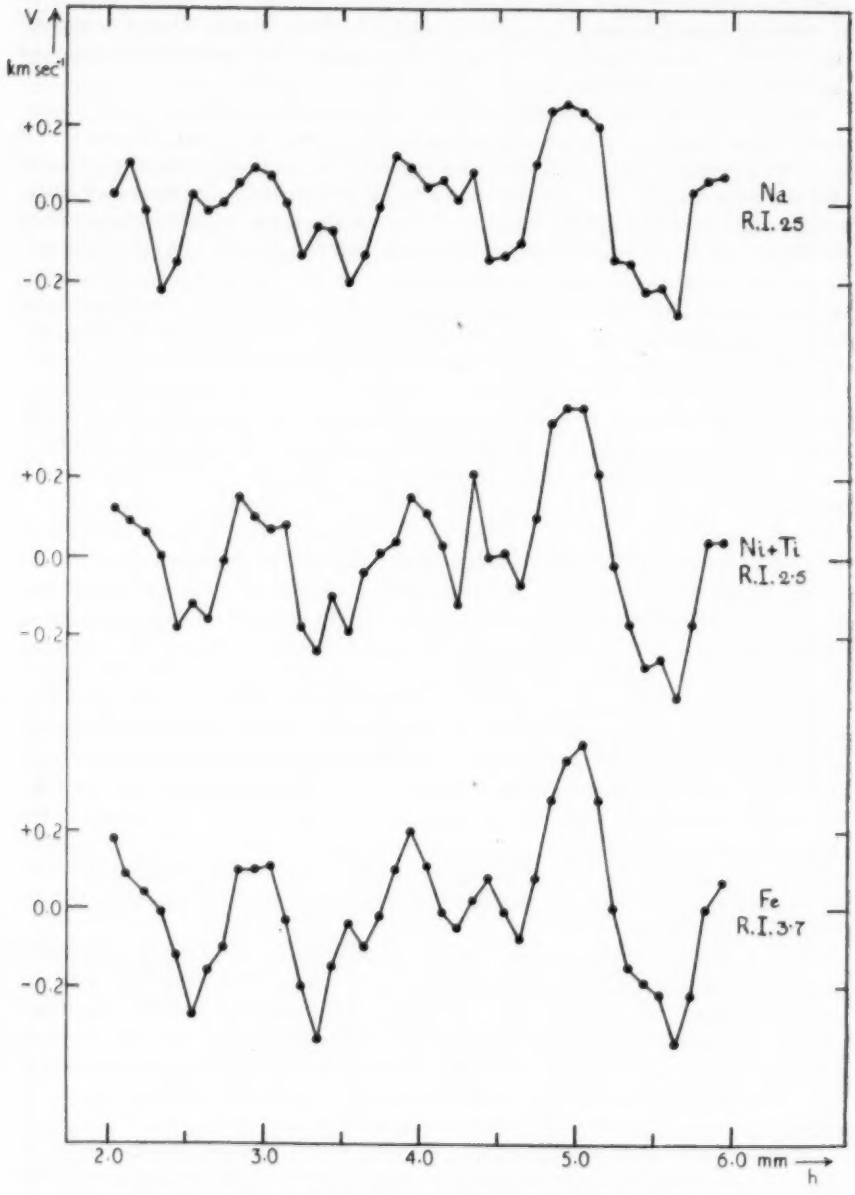

FIG. 3.—*Comparison of the velocities displayed by weak and by strong lines.*

Abscissae: *Distances from the limb along an E–W chord of the solar image.*
Ordinates: *Line-of-sight velocities.*
Upper curve: *Velocities obtained from two Na lines, average Rowland intensity 25.*
Middle curve: *Velocities obtained from one Ni and one Ti line, average Rowland intensity 2·5.*
Lower curve: *Velocities obtained from six Fe lines, average Rowland intensity 3·7.*

where e is the error in a tabulated velocity, given in Section 2.5. Values of $d_1 = \pm 0{\cdot}17(2)\,\mathrm{km\,sec^{-1}}$ and $d_2 = \pm 0{\cdot}16(2)\,\mathrm{km\,sec^{-1}}$ are obtained for the Fe and Ni–Ti sequences respectively.

The question is now, is this difference in dispersion significant or could the two dispersions have arisen by random sampling from the same parent population? It may be answered by calculating the quantity

$$P = (F-1)(n-2)^{1/2}/[4(1-r^2)F]^{1/2},$$

due to Pitman (**12**), where $F = d_1^2/d_2^2$ and r is the coefficient of correlation between the two sequences of n members. With the present values of d and r and $n = 40$ (Section 2.4), $P = 0{\cdot}933$. P is distributed like "Student's" t (**9a**) with $n-2$ degrees of freedom; for fairly large values of n the distribution is approximately normal with unit standard deviation about zero mean. The deviation of P from the mean of the distribution is thus less than the standard deviation, which is not significant; the two dispersions do come from the same parent population, as one expects.

The identity of the Fe and Ni–Ti sequences has thus been formally demonstrated in a satisfactory manner, and the results of the comparison of strong-line and weak-line velocities may be treated with considerable confidence.

3.2. *Comparison of the Fe and Na velocities.*—Following the procedure laid down in the last sub-section, the Na sequence of velocities will now be compared with the weak-line sequence. Since the velocities in the Fe series were derived from measurements on six solar lines, while those in the Ni–Ti series depend only on two (Section 2.1), the Fe sequence represents more nearly the true velocity variation of the weak lines. Consequently, the Fe sequence will be used as the standard for comparison.

The coefficient of correlation between the Fe and Na series is $+0{\cdot}745$. Again one wishes to know whether this is likely to be only a chance resemblance. Application of Fisher's $z-\zeta$ test shows that the probability of this happening is less than 1 in 10^8, which is negligible. Confirmation of the obvious similarity of the three velocity sequences shown by Fig. 3 is thus provided.

It has, however, already been pointed out (Section 3.1) that the amplitude of the Na velocity sequence, $\pm 0{\cdot}131\,\mathrm{km\,sec^{-1}}$ (Table III), is smaller than that of either of the weak-line sequences. Is the difference significant? The true dispersion, obtained from equation (1) by substitution of the relevant values, is $d_3 = \pm 0{\cdot}12(0)\,\mathrm{km\,sec^{-1}}$. Consequently, the value of Pitman's P for a comparison of the Fe and Na sequences is 3·384, and this is the multiple of the standard deviation by which P deviates from the mean of the nearly normal P-distribution. Hence the probability that the Na velocities arise from a parent population having the same dispersion as that of the Fe and Ni–Ti sequences is only 1 in 1400.

The conclusion to be drawn from the present investigation is, therefore, that the velocity field displayed by strong lines is similar to that shown by the weak lines, but that its amplitude is reduced. (This fact incidentally explains why the correlation coefficient found in this section is smaller than the one in Section 3.1: the proportionately greater effect of errors of measurement destroys more of the correlation.) The next problem is to find the vertical distribution of the field implied by the observed change in amplitude.

3·3. *Location of the observed velocity field.*—An expression for the mean optical depth τ_m of the radiation $I(0,\theta)$ emerging at an angle θ (Section 1) from the solar surface has been given by H. H. Plaskett (**13**). It is

$$\tau_m = \int_0^\infty \tau d\left\{ I(\tau,\theta) \exp\left[-\int_0^\tau (1+\eta_\lambda) \sec\theta \, d\tau' \right] \right\} \Bigg/ \int_0^\infty d\left\{ I(\tau,\theta) \exp\left[-\int_0^\tau (1+\eta_\lambda) \sec\theta \, d\tau' \right] \right\}, \quad (2)$$

where $I(\tau,\theta)$ is the intensity at optical depth τ in the continuum and η_λ is the ratio of the line absorption coefficient at wave-length λ to the coefficient of continuous absorption at the same wave-length; η_λ varies from a maximum in the centre of the line to zero in the continuum. Since velocities were deduced from displacements of the centres of intensity of the spectral lines (Section 2.3), a knowledge of the variation of $I(\tau,\theta)$ and η_λ for the centres of the lines would give the photospheric depths to which the measured velocities refer.

In the present case, as the data are not available, it is only possible to estimate the mean depths of formation of the emergent light for a representative weak line and for a representative strong line, using some simple model of line formation.

For an atmosphere in local thermodynamic equilibrium and stratified in plane parallel layers, the equation of transfer formulated by A. S. Eddington (**4**) gives

$$\int_0^\infty d\left\{ I(\tau,\theta) \exp\left[-\int_0^\tau (1+\eta_\lambda) \sec\theta \, d\tau' \right] \right\} = -\int_0^\infty \left\{ [(1+\epsilon\eta_\lambda)B(\tau) + (1-\epsilon)\eta_\lambda J] \sec\theta \exp\left[-\int_0^\tau (1+\eta_\lambda) \sec\theta \, d\tau' \right] \right\} d\tau, \quad (3)$$

where $B(\tau)$ is the Planckian source function, J is the average of $I(\tau,\theta)$ over the solid angle 4π and ϵ is the fraction of atoms de-excited by super-elastic collisions. (The equation implies that an absorbed photon is re-emitted without change in frequency.) With a linear approximation to the source function, $B(\tau) = B_0(1+\beta\tau)$, equation (3) is easily evaluated (**21**) if η_λ and ϵ are assumed independent of optical depth; the integral is in fact the emergent intensity $I(0,\theta)$. Limb darkening observations at λ 5900 A give $\beta \simeq 2{\cdot}0$ (**17**). The value of τ_m corresponding to given values of η_λ and ϵ can then be found from equation (2) (**13**).

Appropriate values of ϵ and η_λ must now be assigned. The simplest assumption is that for the strong lines $\epsilon = 0$ (pure coherent scattering) and that for the weak lines $\epsilon = 1$ (pure absorption). Simple asymptotic forms for η_λ in the line core and in the wings are (**18**)

$$\eta_\lambda = K \exp[-(\Delta\lambda/b)^2] \quad (4a)$$

and

$$\eta_\lambda = Kb\delta/\sqrt{\pi}(\Delta\lambda)^2, \quad (4b)$$

respectively; $\Delta\lambda$ is the wave-length difference from the line centre, b is a species of Doppler width and δ is a collisional constant. The value of K is chosen to give a line of the correct equivalent width at the centre of the disk, $\theta = 0$. For the weak lines, only the Doppler core (equation (4*a*)) is developed and $K = 10$, $b = 2{\cdot}63 \times 10^{-2}$ A (actually the Doppler half-width for an Fe atom at 6000 deg.) give a line of some 50 mA equivalent width at the centre of the disk, roughly corresponding to the values (**11**) relevant to the weak Ti, Fe and Ni lines which

have been measured. Measured equivalent widths of the Na D_1 and D_2 lines are 636 mA and 906 mA respectively (**18**). The D_1 line is represented approximately by values of $K = 5 \times 10^3$, $b = 4{\cdot}09 \times 10^{-2}$ A (the Doppler half-width for a Na atom at 6000 deg.) and $\delta = 6{\cdot}49 \times 10^{-4}$ A (corresponding to a collisional damping width some eleven times the natural damping width), giving a line of 650 mA equivalent width. With these data it is possible to find from equation (2) the optical depth of the emergent light not only at the centre of the lines, but also at any other point in the line profile. This depth decreases from the value 0·58 in the continuum to a minimum in the centre of the line, 0·04 for the model weak line and 0·0001 for the strong line.

The values of τ_m so found, however, take no account of the redistribution of light by the horizontal apparatus function of the spectroscope. Let $I(\lambda, 0, \theta)$ be the value of $I(0, \theta)$ found from equation (3) for wave-length λ and let $\tau_m(\lambda)$ be the value of τ_m calculated from equation (2) for the same wave-length. Then the effective optical depth $\tau_e(\lambda)$ at which light of apparent wave-length λ originates is given by

$$\tau_e(\lambda) = \int_0^\infty \tau_m(\lambda') I(\lambda', 0, \theta) A(\lambda - \lambda')\, d\lambda' \Big/ \int_0^\infty I(\lambda', 0, \theta) A(\lambda - \lambda')\, d\lambda', \qquad (5)$$

where A is the horizontal apparatus function of the spectroscope; it has been determined for the Oxford spectroscope in the region λ 5900 A by R. J. Bray (**3**).

The measurements of velocity described in Section 2 refer to a mean disk position $\theta = \cos^{-1} 0{\cdot}4$. Consequently, the values of τ_e for the centres (Section 2.3) of the two representative lines were found for this value of θ from equation (5), by numerical integration. For this purpose, the experimentally determined apparatus function was smoothed and made symmetrical; the model of line formation is too crude to justify a more detailed treatment. Values of $\tau_e = 0{\cdot}32$ and $\tau_e = 0{\cdot}42$ were obtained for the strong line and for the weak line, respectively.

While the treatment in the present sub-section is admittedly greatly oversimplified, it does enable some general conclusions to be drawn from the observational material. In the first place, it has been shown that the information obtained from measurements on strong lines refers to a higher level in the photosphere than that derived from weak-line measurements (**10b**). Reference to a table of physical conditions in the photosphere, constructed by H. H. Plaskett (**19**) from mean limb darkening observations, shows that the difference in geometrical depth is only some 25 km. As the velocities given by the D line measurements are significantly smaller than the weak-line velocities (Section 3.2), the field must diminish extremely rapidly with height in the photosphere or be limited to a layer below a certain depth. It is also perhaps of interest that the effective level of the observed velocity field lies above the granulation zone, the top of which occurs approximately at optical depth unity (**19**). However, some 50 per cent of the light comes of course from layers below τ_e, so that the observations indicate at least the persistence of the field to very much deeper layers and possibly a considerable increase in velocity at these greater depths.

Acknowledgments.—I am deeply indebted to Professor H. H. Plaskett for suggesting the problem investigated in the present paper and the observational technique used in its solution. Dr M. G. Adam suggested the procedure used in reducing the microphotometer tracings and the method of measuring the wide lines, for which I am most grateful. To Dr R. J. Bray I express my thanks

for providing the values of the smoothed apparatus function and for numerous discussions concerning line formation.

University Observatory,
Oxford:
1956 *July* 23.

References

(1) W. S. Adams, *Papers of the Mount Wilson Observatory*, **1**, Part 1, 1911.
(2) H. D. Babcock, *Trans. I.A.U.*, **3**, 93, 1928.
(3) R. J. Bray, *M.N.*, **114**, 540, 1954; *Comm. Univ. Obs., Oxford*, No. 45.
(4) A. S. Eddington, *M.N.*, **89**, 620, 1929.
(5) A. Fowler, *Trans. I.A.U.*, **4**, 60, 1932.
(6) A. B. Hart, *M.N.*, **114**, 17, 1954; *Comm. Univ. Obs., Oxford*, No. 43 (IV).
(7) A. B. Hart, *M.N.*, **116**, 38, 1956; *Comm. Univ. Obs., Oxford*, No. 54 (VI).
(8) J. Houtgast, *The Variations in the Profiles of Strong Fraunhofer Lines along a Radius of the Solar Disk* (Thesis), Utrecht, 1942.
(9a) M. G. Kendall, *The Advanced Theory of Statistics*, Vol. I, 4th edn., p. 239, Griffin, London, 1948.
(9b) M. G. Kendall, *ibid.*, p. 345.
(10a) E. A. Milne, *Thermodynamics of the Stars, Handbuch der Astrophysik*, Vol. III, 1st. edn., p. 145, Springer, Berlin, 1930.
(10b) E. A. Milne, *ibid.*, p. 157.
(11) G. F. W. Mulders, *Aequivalente Breedten van Fraunhofer-Lijnen in het Zonnespectrum* (Thesis), Utrecht, 1934.
(12) E. J. G. Pitman, *Biometrika*, **31**, 9, 1939.
(13) H. H. Plaskett, *M.N.*, **91**, 870, 1931.
(14) H. H. Plaskett, *M.N.*, **95**, 160, 1934; *Comm. Univ. Obs., Oxford*, No. 4.
(15) H. H. Plaskett, *M.N.*, **112**, 177, 1952; *Comm. Univ. Obs., Oxford*, No. 33.
(16) H. H. Plaskett, *M.N.*, **112**, 414, 1952; *Comm. Univ. Obs., Oxford*, No. 34.
(17) H. H. Plaskett, *M.N.*, **114**, 251, 1954; *Comm. Univ. Obs., Oxford*, No. 44.
(18) H. H. Plaskett, *M.N.*, **115**, 256, 1955; *Comm. Univ. Obs., Oxford*, No. 46.
(19) H. H. Plaskett, *Physical Conditions in the Solar Photosphere, Vistas in Astronomy*, Vol. I, p. 637, Pergamon Press, London and New York, 1955.
(20) C. E. St. John *et al.*, *Papers of the Mount Wilson Observatory*, **3**, 1928.
(21) R. v. d. R. Woolley and D. W. N. Stibbs, *The Outer Layers of a Star*, p. 134, Clarendon Press, Oxford, 1953.
(22a) G. U. Yule and M. G. Kendall, *An Introduction to the Theory of Statistics*, 14th edn., p. 232, Griffin, London, 1950.
(22b) G. U. Yule and M. G. Kendall, *ibid.*, p. 326.

STAR FORMATION IN MAGNETIC DUST CLOUDS

L. Mestel and L. Spitzer, Jr

(Received 1956 July 27)*

Summary

The paper deals with the problem of gravitational condensation in the presence of a magnetic field. It is shown that as long as the field is frozen into the contracting cloud the magnetic pressure sets a lower limit to the mass that can remain gravitationally bound: if the field is taken as 10^{-6} gauss in regions of density 10 H atoms/cm^3, this lower limit is $\simeq 5 \times 10^3 \odot$. However, if the bulk of the cloud is obscured from galactic starlight by dust grains, the plasma density within the cloud will decline rapidly, as ions and electrons attach themselves to the grains. When the plasma density is low enough the frictional coupling between plasma and neutral gas will be so small that the distorted magnetic field will be able to straighten itself, dragging the remains of the plasma with it, while the bulk of the cloud contracts across the field. With the magnetic energy so reduced to a small fraction of the gravitational energy, the cloud is able to break up into stars.

---

1. *Introduction.*—In recent years many workers have been led to postulate a strong large-scale magnetic field in the Galaxy. Interpretations of the observed polarization of starlight involve selective extinction by magnetically oriented, non-spherical dust grains (**1, 2**). Fermi proposed a magnetic mechanism for the acceleration of charged particles to cosmic-ray energies (**3**), while Chandrasekhar and Fermi explain the lateral equilibrium of a spiral arm as a balance between gravitation, turbulent pressure and magnetic pressure (**4**). The field is assumed to arise through large-scale galactic mass-motions causing a small initial field to grow until approximate equipartition of energy exists between the magnetic and kinetic fields (**5**).

The objections to the existence of such a field have been of two types: (i) doubts as to whether hydromagnetic turbulence will lead to equipartition of energy between any but the small-scale components of field and motion (**6, 7**), and (ii) concern at the difficulty of star formation in the presence of so much magnetic energy. It is with this second objection that this paper is concerned.

Some workers would argue that the evidence for a strong magnetic field is fairly impressive, whereas our knowledge of the process of star formation is not sufficiently precise to yield a strong argument for or against the field's existence. Others would regard a theory of star formation which successfully takes account of the field as removing one of the principal theoretical objections to the field. Whichever view one adopts, it is clear that the possible or probable existence of the field should not be ignored when discussing the origin of stars. In this paper the field is assumed, and the problem of star formation re-examined.

* Received in original form 1956 May 11.

2. *The mechanical effect of a magnetic field.*—For a non-magnetic mass in mechanical equilibrium, the virial theorem relates the thermal energy U, the gravitational energy Ω, and K, the kinetic energy of mass-motions (**8**)

$$2K + 3(\gamma - 1)U + \Omega = 0, \tag{1}$$

γ being the ratio of the two principal specific heats. If the left-hand side of (1) is not zero but positive, the mass expands; if negative, it contracts. As we are interested in the best possible conditions for condensation, and in contrasting the non-magnetic case with the magnetic, we shall assume that turbulent and rotational kinetic energy in the cloud are small, so that $K = 0$. We shall also put $\gamma = 5/3$, the value for a monatomic gas. Then for a mass M of radius R at temperature T the condition for contraction is approximately

$$\frac{GM^2}{R} > 3\mathfrak{R}MT, \tag{2}$$

$\mathfrak{R}$ and G being respectively the gas constant and the gravitational constant. Density variations in the cloud will introduce factors of order unity in (2). Alternatively, a mass M at temperature T must be of mean density

$$\rho > 3 \times 10^{-21} T^3 / \overline{M}^2 \tag{3}$$

($\overline{M} = M/\odot$) for contraction to ensue. Conversely, the mass of the smallest sphere able to hold itself together gravitationally decreases with decreasing temperature and increasing density.

At normal interstellar densities and temperatures, $\overline{M}$ from (3) is much above stellar order. For example, with $T = 100$ deg. K, ρ must be at least $3 \times 10^{-15}/\overline{M}^2$, so that for a solar mass to be gravitationally bound, the density must be some 10^8 times that in a normal H I cloud. It appears, then, that in order to build stars out of interstellar clouds the density must increase by contraction, without any great rise in temperature. The energetics of this problem have been discussed by Hoyle (**9**) for a cloud of atomic hydrogen; his results are summarized in Section 4, where similar ideas are applied to the case of a cool dust cloud.

Consider now a roughly spherical cloud with high magnetic energy, again neglecting turbulence and rotation. The equilibrium virial theorem now has the form (**8**)

$$2U + \mathfrak{M} + \Omega = 0, \tag{4}$$

where $\mathfrak{M}$ is the magnetic energy. If the average field within the cloud is H gauss, then

$$\mathfrak{M} \simeq \frac{4\pi}{3} R^3 \left(\frac{H^2}{8\pi}\right) = \tfrac{1}{6} H^2 R^3. \tag{5}$$

In a medium of high conductivity, the freezing of the lines of force into the matter leads to a rapid increase of field with decreasing radius*

$$HR^2 = H_0 R_0^2 \tag{6}$$

(suffixes referring to initial values), so that during contraction the magnetic energy increases at the same rate, $\propto 1/R$, as the negative gravitational energy. Thus a magnetic field acts so as to dilute gravity by a factor *independent* of the density (in contrast to the centrifugal field in a cloud conserving its angular

* The assumption that the galactic field is "large-scale" is implicit here; a "small-scale" field could very well straighten itself during contraction, leading to a much smaller increase of field with density.

momentum). The smallest mass able to withstand the magnetic pressure is given by (4) with $U=0$, i.e.

$$M=\frac{H^3}{(6G)^{3/2}}\left(\frac{3}{4\pi\rho}\right)^2. \tag{7}$$

As a conservative estimate for the actual galactic field, we take $H=10^{-6}$ gauss in regions where $\rho=1{\cdot}66\times10^{-23}$; the lower limit (7) is then $\simeq 5\times10^2\odot$. A cloud with non-vanishing thermal energy will need even more mass to withstand both magnetic and thermal pressure. As long as the field is frozen into the material, the cloud cannot break up into fragments of mass smaller than the limit (7).

It may be objected that the difficulties are exaggerated, in that increases of density without corresponding increases of field can arise through condensation along the lines of force. Thus consider the simplified model of a spiral arm adopted by Chandrasekhar and Fermi (**4**): a cylinder of gas and stars with lines of magnetic force parallel to the axis. Once condensation along the field has set in, it will proceed more rapidly than transverse contraction; only when the unstable portion of the cylinder has formed a rough spheroid, oblate to the direction of the field, will uniform contraction be possible, as only then will gravitation along the field be the same as the magnetically diluted force across the field. In this way a cloud of high density and low magnetic energy could be formed, and stars could condense without magnetic impedance.

However, it is very doubtful whether this could occur. Jeans' criterion for the gravitational contraction of a length L of the cylinder is

$$L>c\sqrt{\frac{\pi}{G\rho}}=\sqrt{\frac{\pi\mathfrak{R}T}{G\rho}}, \tag{8}$$

where c is the velocity of sound. (Condition (2) is essentially the three-dimensional analogue of (8) for an isotropic medium.) But the condition for the lateral equilibrium of a cylinder of mass M, radius R, and length L is (**8**):

$$2\mathfrak{R}MT+\frac{1}{4}\frac{(H^2R^4)}{R^2}L=\frac{GM^2}{L}, \tag{9}$$

and this yields as a condition on the density

$$\rho=\frac{M}{\pi R^2L}>\frac{2\mathfrak{R}T}{\pi GR^2}. \tag{10}$$

Comparing (8) and (10), we see that the length of cylinder that is just unstable against longitudinal contraction is of the same order as R. It is easy to see from (7) that in order to build up densities high enough to allow star formation without magnetic impedance, we need condensation of a length of cylinder several hundred times R, to a length of order R. If we take account of the decrease of R and the increase of H, due to the increase of density as the cylinder contracts, the length of cylinder required is even greater. It is quite implausible that a length so much in excess of the Jeans limit (8) should contract *as a whole* by such a large factor without breaking up into sub-cylinders of length comparable with (8).

It is clear, then, that a strong large-scale magnetic field will prevent star formation, as long as the field is frozen into the cloud. If a magnetic cloud is to break up into stars, some means must be found by which the matter may slip across the lines of force.

3. ***The coupling between matter and magnetic field.***—The matter in an ordinary H I cloud is largely neutral hydrogen, both atomic and molecular, with a small admixture of partially ionized heavier elements with their free electrons, and of dust grains. The essentials of the problem are preserved if we write n_H = number density of hydrogen atoms and molecules, n_e = number density of electrons, n_g = number density of dust grains, and n_i = number density of ions, $= n_e/Z$, where Z is the mean ionic charge. Also we write $\mathbf{F}_{ei}$ = mean force on an electron due to collisions with ions, $\mathbf{F}_{eH}$ = mean force on an electron due to collisions with H atoms and molecules, $\mathbf{F}_{iH}$ = mean force on an ion due to collisions with H atoms and molecules. In considering the momentum balance for the gas, we may ignore collisions with the grains.

Per unit volume, the condition of momentum balance for the electron gas is

$$-en_e\left(\mathbf{E}+\frac{\mathbf{v}_e\wedge\mathbf{H}}{c}\right)+n_e\mathbf{F}_{ei}+n_e\mathbf{F}_{eH}-\nabla p_e=0, \tag{11}$$

where $\mathbf{v}_e$ and p_e are respectively the mean drift and the partial pressure of the gas, $-e$ the electronic charge and $\mathbf{E}$ the electric field. Because of the small electronic mass, gravitation and inertia are neglected. For the ionic gas we have similarly

$$Zen_i\left(\mathbf{E}+\frac{\mathbf{v}_i\wedge\mathbf{H}}{c}\right)-n_e\mathbf{F}_{ei}+n_i\mathbf{F}_{iH}-\nabla p_i+n_im_i\nabla\phi=n_im_i\frac{d\mathbf{v}_i}{dt}, \tag{12}$$

where ϕ is the gravitational potential, m_i the ionic mass, and $d\mathbf{v}_i/dt$ a total time derivative. Remembering that the current density $\mathbf{j}$ is given by

$$\mathbf{j}=n_iZe\mathbf{v}_i-n_ee\mathbf{v}_e=n_ee(\mathbf{v}_i-\mathbf{v}_e), \tag{13}$$

we can deduce from (11) and (12) the equation to the motion of the plasma:

$$\frac{\mathbf{j}\wedge\mathbf{H}}{c}+(n_i\mathbf{F}_{iH}+n_e\mathbf{F}_{eH})-\nabla(p_i+p_e)+n_im_i\nabla\phi=n_im_i\frac{d\mathbf{v}_i}{dt}. \tag{14}$$

For the motion of the neutral gas, we have

$$-(n_i\mathbf{F}_{iH}+n_e\mathbf{F}_{eH})-\nabla p_H+n_Hm_H\nabla\phi=n_Hm_H\frac{d\mathbf{v}_H}{dt}. \tag{15}$$

These equations illustrate how the magnetic force acts directly on the plasma, and affects the neutral gas only indirectly through the friction between plasma and neutral gas.

In treating collisions between light and heavy particles, it is a good approximation to assume that on the average the heavy particle acquires all the momentum of relative drift of the light particle, which after a collision has a purely random relative motion. Thus $\mathbf{F}_{eH}$ is given by

$$n_H\sigma_{eH}(v_e)_Tm_e(\mathbf{v}_H-\mathbf{v}_e), \tag{16}$$

where σ_{eH} is the cross-section for e–H collisions and $(v_e)_T$ the electronic thermal velocity. Similarly, as in an H I region $m_H\ll m_i$, $\mathbf{F}_{iH}$ is of order

$$n_H\sigma_{iH}(v_H)_Tm_H(\mathbf{v}_H-\mathbf{v}_i). \tag{17}$$

Now in (14), both $\nabla(p_i+p_e)$ and $n_im_i\nabla\phi$ must be small compared with the magnetic force. By hypothesis we are dealing with a cloud in which the magnetic force is comparable with the *total* pressure gradient and gravitational force density.

But the plasma density in an H I region is always much smaller than the total density; hence the equation for the motion of the plasma reduces to

$$\frac{\mathbf{j}\wedge\mathbf{H}}{c}+n_H n_i\{\sigma_{iH}(v_H)_T m_H(\mathbf{v}_H-\mathbf{v}_i)+Z\sigma_{eH}(v_e)_T m_e(\mathbf{v}_H-\mathbf{v}_e)\}=n_i m_i\frac{d\mathbf{v}_i}{dt}. \qquad (18)$$

Thus as the cloud contracts, the tendency of the distorted magnetic field to straighten itself, represented by the force term $\mathbf{j}\wedge\mathbf{H}/c$, is countered only by the friction between plasma and neutral gas.

As an example, consider a cloud of mass $M=10^3\odot$, and with temperature $T=100$ deg. K; we suppose it initially to be in a state of mathematical equilibrium, so that by (4)

$$3\mathfrak{R}MT=\frac{GM^2}{R}-\tfrac{1}{6}\frac{(H^2R^4)}{R}. \qquad (19)$$

We again assume that the cloud has arisen through isotropic compression of a region of density $n_H=10$, and with $H=10^{-6}$, magnetic flux being conserved.* We then have

$$\left.\begin{aligned} R&=(5{\cdot}4\times10^{15})\overline{M}-(3\times10^{17})\overline{M}^{1/3}=2{\cdot}4\times10^{18}\\ n_H&=2\times10^4\\ \tau&=\text{time of free-fall}\simeq 1/\sqrt{G\rho}=2{\cdot}1\times10^{13}\\ H&=1{\cdot}5\times10^{-4}\\ U&=2{\cdot}5\times10^{46}\\ -\Omega&=10^{47}\\ \mathfrak{M}&=6\times10^{46}\end{aligned}\right\}. \qquad (20)$$

As the currents maintaining the distorted field $\mathbf{H}$ flow in a region of linear dimension R, the magnetic force $\mathbf{j}\wedge\mathbf{H}/c\simeq H^2/4\pi R=7{\cdot}5\times10^{-28}$. The components of $\mathbf{v}_H$ and $\mathbf{v}_e$ in the meridional planes defined by the direction of the field must be nearly identical; for any meridional e.m.f. set up is rapidly cancelled out by slight non-uniformities of rotation across the magnetic field (**10**). Thus taking $\sigma_{iH}\simeq10^{-16}$, and $(v_H)_T$ at 100 deg. K as $1{\cdot}6\times10^5$, we find that the friction balances the magnetic force if

$$|\mathbf{v}_H-\mathbf{v}_i|\simeq 1{\cdot}5\times10^3/n_i. \qquad (21)$$

If the cloud is falling freely under gravitation from its initial state of approximate equilibrium, $v_H\simeq R\sqrt{(G\rho)}\simeq10^5$, and the drift of the plasma relative to the neutral gas is small compared with the inward velocity of the neutral gas provided $n_i\gg1{\cdot}5\times10^{-2}$.

Current estimates of the proportion of metallic ions in H I clouds give one such ion for 10^4 hydrogen atoms or molecules. As in our cloud $n_H=2\times10^4$, we see that the normal proportion of plasma is too high by a factor 10^2 for any sensible drift to take place during the time of free-fall.

However, in normal H I clouds the ratio of plasma to neutral hydrogen is maintained by a balance between ionization by galactic starlight, and decay of the plasma through a variety of causes, in particular through attachment of ions and electrons to the dust grains. If, then, the cloud is dense enough for the

* The compression will not be strictly isotropic, because of the increasing importance of $\mathfrak{M}$ as compared with U with increasing density, but this approximation is of no consequence.

galactic starlight to be absorbed at the surface by the dust grains, the plasma may be expected to decay at the rate

$$\frac{dn_i}{dt} = -n_i n_g \sigma_g (v_i)_T. \tag{22}$$

Here σ_g is the area of cross-section of the grains, and it is assumed that a high proportion of the ions that hit a grain remain attached, or leave the grain as neutral atoms. Thus n_i decays exponentially with a time-constant $1/\sigma_g (v_i)_T n_g$. Because of their higher thermal velocity, the electrons will tend to adhere more rapidly still, but the rate of plasma decay must be determined by the slower rate of ion attachment: a negatively charged grain will repel further electrons and attract ions. Other mechanisms of plasma decay, such as radiative recombination, must be less efficient, in that they are proportional to n_i^2.

For σ_g we adopt $\pi(3 \times 10^{-5})^2$ and for n_g/n_H $2{\cdot}5 \times 10^{-13}$ (**11**). The mean atomic weight of the ions we take as 10, so that $(v_i)_T \simeq 5 \times 10^4$. The time-constant of decay is then approximately $1{\cdot}4 \times 10^{12}$ sec, which is shorter than the time of free-fall by a factor 10. Thus, under the most favourable conditions, the plasma density can reach such a low value that the magnetic field is able to move the plasma through the freely-falling neutral gas.

The forces acting on the plasma remain closely in balance: the magnetic field accelerates the plasma through the neutral gas until friction just balances the magnetic force. From (18), the time for this quasi-equilibrium to be reached is of the same order as the collision-time $1/n_H \sigma_{iH} (v_H)_T$ between ions and hydrogen atoms. In our cloud this time is about 10^6 seconds, which is far shorter than either the time of decay of the plasma, or the time taken by the plasma to move through the cloud. Hence in (12) and (18) we may ignore the inertia term as well as pressure and gravitation; the Joule term is also dropped, as it is well known to be negligible in the time available (**7**). The electric field is then given by

$$\mathbf{E} + \frac{\mathbf{v}_i \wedge \mathbf{H}}{c} + \frac{n_i \mathbf{F}_{iH}}{n_e e} = 0. \tag{23}$$

Substituting from (13) and (18), and remembering that $|n_e \mathbf{F}_{eH}|$ is small compared with $|n_i \mathbf{F}_{iH}|$, we have

$$\mathbf{E} + \frac{\mathbf{v}_e \wedge \mathbf{H}}{c} = 0. \tag{24}$$

When combined with the induction equation $c\nabla \wedge \mathbf{E} = -\dfrac{\partial \mathbf{H}}{\partial t}$, this shows that the magnetic field follows closely the outward motion of the electrons, and hence of the plasma as a whole. Thus the cloud magnetic field, which is just a distorted part of the local galactic field, straightens itself out as it forces the plasma through the lightly resisting neutral gas.

As the curvature of the field decreases, the drift of plasma and field through the cloud slows up. If the decay of the plasma proceeds steadily, the field will drag the remains of the plasma out until the field strength has reached the assumed galactic value of 10^{-6} gauss. On the other hand, if the extinction of the galactic starlight is incomplete, the plasma density will be stabilized at some value lower than the normal equilibrium level, and the outward drift of field and plasma will be halted when the field strength has reached a value somewhat higher than 10^{-6} gauss. However, the principal object will have been attained: an increase of density without a simultaneous increase of field strength at the rate given by (6).

The close balance between friction and magnetic force shows that hardly any of the magnetic energy released becomes kinetic energy of mass motion of the plasma. The energy equation of the problem follows by adding together the scalar products of (11) and (12) with $\mathbf{v}_e$ and $\mathbf{v}_i$ respectively:

$$\mathbf{j}\cdot\mathbf{E} = n_i m_i \frac{d}{dt}(\tfrac{1}{2}\mathbf{v}_i^2) + \{n_e\mathbf{F}_{ei}\cdot(\mathbf{v}_i-\mathbf{v}_e) + n_i\mathbf{F}_{iH}\cdot(\mathbf{v}_H-\mathbf{v}_i) + n_e\mathbf{F}_{eH}\cdot(\mathbf{v}_H-\mathbf{v}_e)\} - (n_i\mathbf{F}_{iH}+n_e\mathbf{F}_{eH})\cdot\mathbf{v}_H, \qquad (25)$$

again ignoring gravitation and gas pressure. The rate of working $\mathbf{j}\cdot\mathbf{E}$ of the electromagnetic forces measures the rate of decrease of the magnetic energy density; when $\mathbf{j}\cdot\mathbf{E}$ is integrated over all space it transforms with the help of Maxwell's equations to

$$-\frac{d}{dt}\left[\int (H^2/8\pi)\,d\tau\right]_{\text{all space}}.$$

The inertia term in (25) has already been shown to be negligible. The second term on the right is the dissipation of energy due to collisions between the different particles; the Joule term is again negligible, and the largest contribution comes from $n_i\mathbf{F}_{iH}\cdot(\mathbf{v}_H-\mathbf{v}_i)$. The last term gives the work done on the neutral gas in decelerating its gravitational collapse. Thus if $|\mathbf{v}_H-\mathbf{v}_i| \ll |\mathbf{v}_H|$, so that coupling between plasma and neutral gas is strong, the magnetic field energy increases at the expense of the gravitational energy maintaining the velocity $\mathbf{v}_H$; the friction terms serve to dissipate only a little of the (gravitational) energy that would become magnetic energy if the field were *strictly* bound into the neutral gas. In the critical case $\mathbf{v}_i = 0$, the magnetic energy remains stationary (apart from the effect of the small terms neglected); the gravitational energy that would have become magnetic energy in the frozen-in case is instead all dissipated. Finally, if $|\mathbf{v}_H-\mathbf{v}_i| \gg |\mathbf{v}_H|$ and the plasma and field move back through the cloud, part of the magnetic energy is used up in decelerating the cloud, but most of it goes into heat.*

4. *The subsequent evolution of the cloud.*—With the magnetic field within the cloud restored to the galactic level, and the bulk of the cloud contracting, the magnetic energy is soon a small fraction of the gravitational energy. We now summarize Hoyle's discussion (**10**) of the fragmentation of an isothermal cloud into stars.

During the initial contraction from a state of mechanical equilibrium, the gravitational energy released is almost all thermally dissipated by compression—very little goes into macroscopic kinetic energy. After the cloud radius has decreased by a factor of about 3, the reverse is true, and further contraction of the cloud as a whole would convert nearly all the extra gravitational energy released into kinetic energy of mass motion. However, once densities have been so much increased without any accompanying rise in temperature, the cloud is unstable against the formation of sub-condensations—i.e. Jeans' criterion (2) now applies to fragments of the cloud. Again, the initial condensation

* Independently of this work, Piddington (**12**) and Cowling (**13**) have recently pointed out the enormously increased dissipation of magnetic energy in a lightly ionized gas. We are indebted to Professor Cowling for showing us his manuscript before publication, and for a helpful correspondence. Our treatment differs from his somewhat, because in the case of most interest here the accelerations of neutral gas and plasma are not even approximately equal. However, as shown in the text, the mass-acceleration of the plasma remains small as the field straightens itself, so that the plasma acquires very little kinetic energy.

of the fragments dissipates nearly all the gravitational energy released. In Hoyle's semi-quantitative treatment a cloud that has shrunk from R_0 to $R_0/3$ will then break up into five approximately equal masses, each of radius $R_0/5$ and density $25\rho_0$. As long as the isothermal assumption is justified, the process is repeated for each fragment; it stops when the fragments become so opaque that in order to drive out the energy generated in free-fall, the temperature gradient becomes high enough to give hydrostatic support against gravity. The fragment then contracts as a whole in the Kelvin–Helmholtz time-scale, and no further break-up occurs.

In his paper Hoyle treated the case of a mass of atomic hydrogen condensing and fragmenting during the early life of the Galaxy, with no stellar radiation field, and no dust grains or molecules. The radiative properties of hydrogen keep the temperature at $\simeq 10^4$ deg. K, so that the isothermal condition is satisfied. We now apply similar ideas to a dust cloud containing molecules. The first problem is to estimate the temperature variation within the contracting cloud. The surface of the cloud is maintained at $\simeq 100$ deg. K by a balance between absorption of galactic radiation and radiation loss from the grains and molecules (**14**). During compression the gas is heated, but much of its energy is transferred to the grains by inelastic collisions. We first show that the cloud is optically thick in the thermal radiation from the grains and the molecular line emission. If $\lambda_{\max}$ is the wave-length of maximum intensity emitted by the grains, then, by Wien's displacement law, $\lambda_{\max} T_g = 0{\cdot}29$, T_g being the internal temperature of the grains. With the grain radius $b = 3 \times 10^{-5}$, the parameter $\alpha = 2\pi b/\lambda \ll 1$, and so the cross-sections for absorption plus scattering of radiation by the grains are (**11**)

$$A(\lambda) = \left\{ \begin{array}{l} \pi b^2(\alpha^4/3) \text{ approximately for dielectric grains} \\ \\ \pi b^2(2{\cdot}8\alpha) \text{ approximately for metallic grains} \end{array} \right\}. \tag{26}$$

We shall assume that a fair proportion of the grains are metallic, so that by (26) much the largest contribution to the cloud opacity comes from the metallic grains. The optical depth of the cloud in the grain radiation is of the order

$$R_0(\pi b^2) \times 2{\cdot}8 \left(\frac{2\pi b}{\lambda_{\max} T_g}\right) n_g T_g \left(\frac{R_0}{R}\right)^2 \simeq 6 \times 10^{-2} T_g \left(\frac{R_0}{R}\right)^2, \tag{27}$$

where R_0 is the initial cloud radius. Similarly, the line-emission from the H_2 molecules is of wave-length short enough to be absorbed by the grains before escaping (**15**). We therefore expect a Planck distribution of temperature T_g to be built up within the cloud, in a time of order

$$\frac{\text{Energy/cm}^3 \text{ of temperature radiation}}{\text{Rate of emission by grains/cm}^3} = \frac{\sigma T_g^4}{n_g c \int_0^\infty B_\lambda(T_g) A(\lambda)\, d\lambda}. \tag{28}$$

(The use of Kirchhoff's law in the denominator of (28) is justified, since $A(\lambda)$ for the metallic grains is largely true absorption rather than scattering.) This time is approximately

$$\frac{\sigma T_g^4}{n_g c (2{\cdot}8\pi b^2)(2\pi b/\lambda_{\max}) \sigma T_g^4} = \frac{1{\cdot}3 \times 10^9}{T_g} \left(\frac{R}{R_0}\right)^3 \tag{29}$$

which is far less than the time of free-fall. The compressional energy of the cloud will build up a temperature gradient sufficiently steep to drive out this energy. Most of the opacity arises from the grains, the molecular line absorption merely making kinks in the opacity function.

In order that the cloud should fragment, this temperature gradient must be small compared with that yielding hydrostatic equilibrium; in other words, the thermal energy must increase much more slowly than the negative gravitational energy. We shall assume that the cloud stays nearly isothermal, compute the compressional heating and the resultant temperature gradient, and so check up on the isothermal assumption. At gas temperature T, the rate of compressional heating during free-fall is

$$-p\frac{d}{dt}\left(\frac{M}{\rho}\right)=\Re MT\frac{\dot{\rho}}{\rho}\simeq 3\Re MT\sqrt{(G\rho)}=2{\cdot}4\times 10^{31}T\left(\frac{R}{R_0}\right)^{3/2} \tag{30}$$

on substituting from (20). When T and T_g differ, the rate of heating of the grains by inelastic collisions is given by Spitzer's formula (**15**), which for our problem gives

$$5\times 10^{31}\left(\frac{R_0}{R}\right)^3 T^{1/2}(T-T_g). \tag{31}$$

The rate of loss down a temperature gradient dT_g/dR is of order

$$4\pi R_0{}^2\left(\frac{4}{3}\frac{ac}{(n_g)_0(2{\cdot}8\pi b^2)}\frac{(\lambda_{\max}T_g)}{2\pi b}\right)\frac{T_g{}^3}{T_g}\left|\frac{dT_g}{dR}\right|\left(\frac{R}{R_0}\right)^5\simeq 8{\cdot}5\times 10^{53}T_g{}^2\left|\frac{dT_g}{dR}\right|\left(\frac{R}{R_0}\right)^5. \tag{32}$$

The equating of (30) and (31) determines the difference between T and T_g, while from equating (30) and (32) we find the excess of internal T over the surface value, necessary to drive out the compressional heat.

With $R=R_0$ and an assumed temperature $T_g=100$ deg. K, the same as the surface value, T is found to be $\simeq 105$ deg. K and $|dT_g/dR|\simeq 10^{-25}$ with $|dT/dR|$ of the same order. This is much smaller than $GM_0/\Re R_0{}^2\simeq 3\times 10^{-16}$, the temperature gradient required for hydrostatic equilibrium; this is also the case when R has reached $R_0/3$, when according to Hoyle the first fragmentation takes place. In fact, the opacity of the grains is so low that the fragmentation process stops only when the cloud has broken up into masses of order $\odot/2$. The mass, radius and density of the nth fragments are respectively M_0/k^n, R_0/k^n and $\rho_0 k^{2n}$ with $k\simeq 5$ (**9**); hence with the temperature gradient just equal to the hydrostatic value, the radiative flux through the fragments is

$$8{\cdot}5\times 10^{53}\left(\frac{GM_0}{\Re R_0}\right)^3\frac{1}{R_0}k^{-3n}\simeq 10^{44}k^{-3n} \tag{33}$$

(the difference between T and T_g is quite negligible). On the other hand, the rate of compressional heating during free-fall is

$$3\Re\left(\frac{M_0}{k^n}\right)T\sqrt{(G\rho_0)}k^n=2{\cdot}4\times 10^{31}\left(\frac{GM_0}{\Re R_0}\right). \tag{34}$$

Fragmentation ceases when (33) and (34) are approximately equal; they yield $k^n\simeq 2\times 10^3$, so that the proto-stars that contract to the main-sequence are $\simeq\odot/2$ in mass

However, the successive break-up of the cloud may very well be halted before such small masses are reached. We began by considering a cloud with a large

magnetic field but with negligible centrifugal force, and showed how the field may be eliminated. But rapid contraction of the cloud and its fragments, with conservation of angular momentum, must send up the centrifugal force. It needs only a moderate amount of angular momentum in the initial cloud for rotation to halt contraction perpendicular to the axis and lead to disk formation, long before the increase in opacity has stopped fragmentation. Thus the masses of the disks will be determined not by the equating of (33) and (34) but by the amount of vorticity in the cloud.

The evolution of such a disk will depend on the means for gradual redistribution of angular momentum. If the obscuration of galactic starlight is incomplete, coupling between magnetic field and matter may be restored, because of the much greater densities. The strong interaction between rotation and magnetic field is well known. Either the bulk of the angular momentum will be transferred to the Galaxy, so that the disk as a whole gradually contracts into a main sequence star, probably with high rotation; or the cloud will break up into two or more masses, with most of its angular momentum going into the orbital motion of the proto-stars. Further discussion is beyond the scope of this paper.

5. *The evolution of a cloud with a frozen-in magnetic field.*—In Section 3 it was shown that the minimum time of plasma decay, and hence of loss of magnetic energy, is shorter than the time of free-fall, but not by a very large factor. The magnetic field does not much increase the time of free-fall; hence if the mechanism of attachment of ions to the grains is somewhat less efficient than supposed, coupling between plasma and neutral gas will remain strong, and the collapsing cloud will drag the field with it. However, in contrast to the case of a cloud with low magnetic energy, even if the contraction is isothermal the cloud cannot break up into smaller masses—the magnetic energy sets a lower limit to the mass that can remain gravitationally bound. Thus the cloud as a whole continues to contract, with more and more gravitational energy being converted into macroscopic kinetic energy: after the first stages of contraction very little of the gravitational energy released is thermally dissipated, because of the impossibility of sub-condensations being formed.

It is clear, then, that if the magnetic field is to be lost from the cloud by the mechanism of this paper, something must prevent the cloud from collapsing so quickly. One tempting suggestion is turbulent pressure, maintained by the release of gravitational energy; if strong enough, it could regulate the time of contraction to its decay-time. However, it is doubtful if in fact the time of contraction will be increased in this way. Certainly, if *all* the gravitational energy released but not thermally dissipated were to become turbulent kinetic energy, the virial theorem shows that the pressure would halt the contraction at a radius $\simeq R_0/3$. But the time of decay of the turbulence is given by $L/\tilde{u}$, where L is the scale and $\tilde{u}$ the mean velocity of the motion containing most of the energy (**16**). At radius R, the energy that has been released by contraction is somewhat less than $\eta(GM^2/R)$, where η is the constant factor by which the magnetic field reduces gravity. Hence $\tilde{u} \simeq \sqrt{(\eta GM/R)} \simeq R\sqrt{(G\rho\eta)}$, and so the time of decay is of the same order as the time of free-fall $1/\sqrt{(\eta G\rho)}$.* In any case, the assumption that all the energy of the mean flow becomes turbulent

* The suggestion that the decay-time of the turbulence might not exceed the time of free-fall was made to one of us by Dr. F. D. Kahn.

is probably over-generous. Experiments with wind-tunnels indicate that only a few per cent goes into turbulence (**16**); the decay-time of the turbulence is then longer as $\tilde{u}$ is smaller, but the turbulent energy is then too small to exert an important pressure.

Thus we conclude that turbulence could be important only if nearly all the energy available becomes turbulent, and also if the presence of a strong magnetic field reduces considerably the rate at which energy cascades down to smaller and smaller eddy-sizes, to be dissipated by viscosity. Even so, we need to take account of the extra loss of energy through compressional heating and radiation; this sink will be important when the kinetic energy is comparable with the thermal energy.

If turbulence is negligible, there remain two other possible ways in which the cloud can lose its magnetic energy:

(i) The angular momentum present leads to disk formation, and the subsequent evolution of the disk is slow enough for the field and plasma to diffuse outwards, in spite of the increased densities. The objection to this is that the strong frozen-in magnetic field will probably remove angular momentum too rapidly; the time of travel of a hydromagnetic wave across the cloud is of the same order as the time of free-fall, and so it is not obvious that a rotating disk will form.

(ii) The cloud as a whole falls freely until the opacity becomes too high for the compressional heat generated during free-fall to be radiated away. The cloud then contracts in mechanical quasi-equilibrium, the rate of contraction being determined by the energy leak down the temperature gradient. Because of the high molecular opacity in the infra-red, this time of contraction may be very long, giving the magnetic field time to diffuse outwards. As the temperature in the cloud increases the molecules will ultimately dissociate, and the opacity decrease. With the magnetic energy now negligible, the cloud can fragment and evolve either according to Hoyle's picture, or through formation of rotating disks.

One of us (L. M.) wishes to record with thanks the generous financial aid of the Commonwealth Fund of New York, and the warm hospitality of the Princeton University Observatory.

Faculty of Mathematics,
Arts School,
Bene't Street,
Cambridge:
1956 *July* 26.

Princeton University Observatory,
Princeton, N.J.,
U.S.A.

Note added in proof.—One of us (L. S.) has pointed out that dissociative recombination of electrons with molecular ions has a high cross-section, and is a possible alternative to grain attachment as an efficient process of plasma decay in an obscured cloud.

References

(1) L. Spitzer Jr. and J. W. Tukey, *Ap. J.*, **114**, 187, 1951.
(2) L. Davis and J. L. Greenstein, *Ap. J.*, **114**, 206, 1951.
(3) E. Fermi, *Phys. Rev.*, **75**, 1169, 1949.
(4) S. Chandrasekhar and E. Fermi, *Ap. J.*, **118**, 113, 1953.
(5) L. Biermann and A. Schlüter, *Z. f. Naturforschung*, **5A**, 237, 1950.

(6) G. K. Batchelor, *Proc. Roy. Soc.* A, **201**, 405, 1950.
(7) T. G. Cowling, *Solar Electrodynamics*, in *The Sun*, G. P. Kuiper (Ed.), Chicago, 1953.
(8) S. Chandrasekhar and E. Fermi, *Ap. J.*, **118**, 116, 1953.
(9) F. Hoyle, *Ap. J.*, **118**, 513, 1953.
(10) L. Mestel, *M.N.*, **116**, 324, 1956.
(11) J. L. Greenstein, *Interstellar Matter*, in *Astrophysics*, J. A. Hynek (Ed.), McGraw-Hill, 1951.
(12) J. H. Piddington, *M.N.*, **114**, 651, 1954.
(13) T. G. Cowling, *M.N.*, **116**, 114, 1956.
(14) L. Spitzer Jr. and M. P. Savedoff, *Ap. J.*, **111**, 593, 1950.
(15) L. Spitzer Jr., *Ap. J.*, **109**, 337, 1949.
(16) G. K. Batchelor, *Homogeneous Turbulence*, Cambridge, 1953

A MATHEMATICAL DISCUSSION OF THE PROBLEM OF STELLAR EVOLUTION, WITH REFERENCE TO THE USE OF AN AUTOMATIC DIGITAL COMPUTER

C. B. Haselgrove and F. Hoyle

(Received 1956 May 10)

Summary

The partial differential equations describing the evolution of a star have been reduced to a form suitable for numerical integration by an electronic computer. The integration has been programmed for the electronic computer EDSAC I and the results will be discussed in later papers.

---

1. *Preliminary remarks.*—Investigations of stellar structure have hitherto been concerned with a determination of the density and temperature within a star of prescribed composition. The problem in such a case is governed by a set of non-linear ordinary differential equations.

This type of treatment cannot be used to investigate stellar evolution because in this problem the composition cannot be prescribed except in the initial stages before nuclear processes become important. Subsequent changes of composition, arising from the nuclear processes, must be worked out as a part of the problem. This alters the mathematical structure of the equations giving a set of non-linear partial differential equations in two variables, one variable being the time and the other describing distribution within the star. The distance from the centre of the star, for instance, may be taken as the latter variable, although this is not the only possibility.

This increased mathematical complexity would be extremely severe were it not that several simplifying approximations can be introduced without any sensible loss of accuracy. These will now be mentioned.

2. *Simplifying approximations.*—(i) The star possesses spherical symmetry. This is an approximation because stars do not possess spherical symmetry, for example because of rotation, or because magnetic fields make contributions to the pressure. It follows that magnetic and rotary effects are being neglected.

(ii) The equation of hydrostatic equilibrium is satisfied. That is to say, the dynamical equations of fluid motion reduce to the hydrostatic equation. This is an excellent approximation except in cases of violent oscillation or of explosion —as in supernovae.

(iii) There is negligible stirring of material in the interior of a star, except in regions that are convectively unstable where the material may be taken to be well mixed (Mestel, 1953).

(iv) In the following section the main variables of the problem are defined. Subsidiary variables have to be determined when the main variables are specified. Notable instances of subsidiary variables are the density, opacity, and the rate of energy generation. In all these examples the accurate determination of the subsidiary variables necessitates long and somewhat intricate calculations. With a digital computer of very large storage capacity and high speed, such calculations could undoubtedly be performed. But with a machine of moderate storage and

speed, approximations in the determination of the subsidiary variables have perforce to be accepted. This has been the case with all work performed at Cambridge with the aid of EDSAC I. The relevant approximations will be given later in this paper when the construction of the subsidiary variables comes to be considered.

3. *The main variables.*—The main variables in the problem are as follows:

t, the time,
M, the mass inside a spherical surface within the star,
R, the radius of this spherical surface,
Q, the energy flux across this surface,
P, the total pressure at radius R,
T, the temperature at radius R,
X, the fraction by mass at radius R of the stellar material consisting of the particular element undergoing nuclear transformation.

The following subsidiary variables, defined at radius R, are required:

ρ, the density,
K, the opacity,
U, the rate of thermonuclear energy generation per unit mass,
Γ, the adiabatic exponent Γ_2 of Chandrasekhar (1938),
ϵ, the potential energy per unit mass.

There are two independent variables, t, and a second variable, usually taken as R, but chosen in our work as M. The other variables, including X, are therefore considered as functions of M, t. It may be noted that the functional dependence of X on M, t is unaltered by an expansion or contraction of the material of the star. This condition is more difficult to take account of if R is chosen instead of M as the second independent variable.

A further point concerning X needs emphasis. It seems to be generally the case that for given M, t there is never more than one element that makes appreciable contribution to the energy generation by nuclear processes. Thus if hydrogen is present no other element makes appreciable contribution. If helium is present, but not hydrogen, no other element but helium makes appreciable contribution —and so on. This explains why in any particular sample of stellar material only one quantity X is needed to specify the concentration of the energy-producing element, whatever this may be.

As t changes, the dependence of X on M varies on account of the nuclear reactions. For a particular M, the value of X decreases with increasing t. Now X cannot decline below zero. A decline to zero implies that at the values of M, t in question the element subject to nuclear transformation becomes exhausted. But this exhaustion does not demand an entire cessation of nuclear activity, for as t continues to increase, nuclear reactions involving some other different element may subsequently become important. In such a case X cannot stay at zero value.

To deal with this possibility we introduce a parameter β that takes positive integral values. This parameter identifies the particular element subject to nuclear transformation. The statement $\beta = 1$ is taken to mean that the main element subject to transformation is hydrogen, while $\beta = 2$ is taken to mean that the main element under transformation is helium, and so on for other values of β and other elements. Accordingly for any M, t we not only have X, giving the concentration of nuclear fuel, but also β specifying the identity of the fuel.

Should X fall to zero, the value of β must be changed and X must be reset to take account of the concentration of a new fuel.

A simple example will make this clearer. Suppose we start with pure hydrogen. Then initially $X=1$, $\beta=1$. As t increases X decreases. Suppose X declines to zero, implying that all the hydrogen has been changed to helium. Then β is changed to 2 and X is reset to 1.

Not only is X a function of M, t, but β is in general a function of these variables. This means that β may have different values in different parts of a star.

Evidently the mathematical formula to be used for the generation of energy by nuclear reactions must be changed when β changes. In programming the calculation for a digital computer, β serves to indicate to the machine which of a number of routines is to be used for the calculation of the energy generation and also of other quantities, such as the mean molecular weight and the opacity.

4. *Procedure for determining ρ when T, P are specified.*—It will be noticed that the density ρ does not appear in our list of main variables. The density can be determined, however, when T, P are specified. The following procedure

(i) takes account of radiation pressure;

(ii) gives the correct ρ when the pressure due to the material arises overwhelmingly from either (*a*) the thermal motions within the material, or (*b*) non-relativistic degeneracy of the electrons, or (*c*) relativistic degeneracy of the electrons;

(iii) gives $\log_{10}\rho$ in the transition region between (*a*) and (*b*) to a better accuracy than $\pm 0{\cdot}01$; and

(iv) gives $\log_{10}\rho$ to a comparable accuracy in the transition region between (*b*) and (*c*).

Define
$$P' = P - \tfrac{1}{3}aT^4, \tag{1}$$
a being Stefan's constant. Define ρ_1, ρ_2, ρ_3 as follows:
$$\rho_1 = \frac{\mu P'}{\mathfrak{R}T} \tag{2}$$
where $\mathfrak{R}$ is the gas constant, and
$$\mu = \frac{4}{5X+3}, \quad \beta=1; \qquad \mu = \frac{4}{2+X}, \quad \beta=2; \qquad \mu \simeq 2, \quad \beta>2; \tag{3}$$
$$\rho_2 = \mu_e\left(\frac{P'}{K_1}\right)^{3/5}, \qquad \rho_3 = \mu_e\left(\frac{P'}{K_2}\right)^{3/4}, \tag{4}$$
where K_1, K_2 are the well-known constants for non-relativistic and relativistic degeneracy (Chandrasekhar, 1938), and
$$\mu_e = \frac{2}{1+X}, \quad \beta=1; \qquad \mu_e \simeq 2, \quad \beta>1. \tag{5}$$
The formulae adopted for μ in the case $\beta=1$, 2, and the formula for μ_e for $\beta=1$, are not exact, but give good approximations when, as seems always to be the case, the material is initially composed almost wholly of hydrogen and helium.

The required value of the density is then determined by
$$\rho = [\rho_1^{-2} + (\rho_2^{\,2} + \rho_3^{\,2})^{-1}]^{-1/2}. \tag{6}$$

Still more accurate procedures than this can no doubt be obtained at the expense of more complicated formulae and of a longer calculation. The present procedure was felt to be a suitable compromise between accuracy and storage requirements in the case of the machine at our disposal. The values in c.g.s. units

of the constants required in this routine are $\log_{10} a = \bar{1}5{\cdot}8779$, $\log_{10}\mathfrak{R} = 7{\cdot}9161$, $\log_{10} K_1 = 12{\cdot}996$, $\log_{10} K_2 = 15{\cdot}080$.

5. *General procedure for determining the evolution of a star when X is a slowly varying function of M.*—The composition of an evolving star at a time t is determined in part by the original composition and in part by the evolutionary stages that preceded t. For the moment, suppose that the composition at time t is known, together with the course of the evolution preceding t. Then the structure of the star at time t can be determined by the method that will be set out in detail in the next section. Suppose this is done. Then $X(M, t+\delta t)$, $\beta(M, t+\delta t)$ can be determined, δt being a small time increment. The crucial point in this determination is that the structure worked out for time t can be taken as a good approximation over the whole time increment, provided δt is small enough. Thus the energy generation by nuclear processes occurring in δt can be regarded as known and hence the change of X (and any change of β) can be computed.

Equipped now with $X(M, t+\delta t)$, $\beta(M, t+\delta t)$ we can work out the new structure for time $t+\delta t$. Then a further time step can be made, and so on. Accordingly the evolution can be followed provided $X(M, t)$, $\beta(M, t)$ are known at any one time. This indeed we are entitled to suppose, since clearly the composition of the star at the moment of its origin must be given.

It may be added that, although this step by step procedure can be made as accurate as one pleases by taking δt small enough, this is not the best numerical way of achieving a given degree of accuracy.

6. *Equations for determining the structure of a star at time t.*—In accordance with what has just been said $X(M, t)$, $\beta(M, t)$ will be regarded as known.

Differential equations

$$\frac{dR}{dM} = \frac{1}{4\pi R^2 \rho}, \tag{7}$$

$$\frac{dP}{dM} = -\frac{GM}{4\pi R^4}, \tag{8}$$

$$\frac{dQ}{dM} = U + \frac{\partial \epsilon}{\partial t}, \tag{9}$$

$$\frac{dT}{dM} = -\frac{3KQ}{64\pi^2 ac\rho T^3 R^4} \tag{10}$$

provided the value of $\dfrac{dT}{dM}$ given by (10) is

$$\geqslant \frac{\Gamma - 1}{\Gamma} \frac{T}{P} \frac{dP}{dM};$$

otherwise

$$\frac{dT}{dM} = \frac{\Gamma - 1}{\Gamma} \frac{T}{P} \frac{dP}{dM}. \tag{11}$$

Constants appearing in these equations

$\log_{10} G = 8{\cdot}8241$, $\log_{10} c = 10{\cdot}4768$, using c.g.s. units.

Subsidiary variables appearing in these equations

Routines have to be given for determining the subsidiary variables ρ, U, $\partial\epsilon/\partial t$, K, Γ when the main variables and $\beta(M, t)$ are given. Of these the case of ρ has already been discussed.

(i) *Procedure for obtaining* U.—The following formulae* are considered to give an adequate accuracy for cases $\beta = 1, 2$.

$$\beta = 1, \quad U = [-29{\cdot}05]\rho X^2 T^4 + [-112{\cdot}1]\rho X x_{CN} T^{16}, \tag{12}$$

where x_{CN} = fraction by mass of stellar material in the form of carbon or nitrogen.

$$\beta = 2, \; U = 10^{35} \frac{X^3 \rho}{T^3} \exp\left\{\frac{-4{\cdot}32 \times 10^9}{T}\right\} \tag{13}$$

With ρ in g cm^{-3} and T in deg. K these formulae give the rate of energy generation in ergs per gram per sec. The formula for $\beta = 1$ includes the energy generated both by the "proton chain" and by the "carbon–nitrogen cycle". Over the range from $T = 10^6$ deg. K to $T = 5 \times 10^6$ deg. K the expression for U in (12) does not differ by more than 0·1 in $\log_{10} U$ from the accurate but more complicated formulae given by Borman-Crespin, Fowler and Humblet (1954). The formula for U in (13) is taken from Hoyle (1954). If temperatures exceeding 5×10^8 deg. K are encountered, nuclear fuels other than hydrogen ($\beta = 1$) and helium ($\beta = 2$) must be considered. Not enough is known at present of the energy levels of medium light nuclei for precise formulae to be given, but some account must nevertheless be taken at very high temperatures of the conversion of oxygen, neon, carbon, magnesium, etc. into heavier nuclei (Hoyle 1954), even though this has to be done in a very approximate way. Approximate formulae for $\beta > 2$ can be constructed as follows:

$$U = A_\beta \rho X^2 T^{n_\beta}, \qquad \beta > 2. \tag{14}$$

The index n_β must be large, and can be set tentatively at some assigned value, 30 for example. Then for given β the coefficient A_β is determined by the condition that U must become of order unity at a value of T determined by considerations of nuclear physics. Thus for neon as a nuclear fuel the value of T in question is about 8×10^8 deg. K, for oxygen the value is about $1{\cdot}5 \times 10^9$ deg. K, for magnesium and silicon about 2×10^9 deg. K. For T close to 5×10^9 deg. K the value of U becomes of order -1, corresponding to the break-down of nuclei into helium (Hoyle, 1954). This is probably the last nuclear process that needs consideration since it seems likely that a major instability must arise in a star once U becomes large and negative.

(ii) *Procedure for obtaining* $\partial\epsilon/\partial t$.—The derivative $\partial\epsilon/\partial t$ appears in the equations in order to take account of the slow changes of gravitational potential energy and of the heat content of stellar material that takes place during stellar evolution. The quantity $d\epsilon$ occurring in any small change is given by

$$d\epsilon = -\frac{3}{2}\rho^{2/3} d\left(\frac{P'}{\rho^{5/3}}\right) \tag{15}$$

provided relativistic degeneracy of the electrons is not important.

The following procedure enables $\partial\epsilon/\partial t$ to be estimated. Denote the evolutionary steps by 1, 2, ..., the number 1 referring to the star when it first forms and reaches approximate thermal and gravitational equilibrium, and the remaining numbers being taken in the order of evolution. Then we write

$$\left.\begin{aligned} \left(\frac{\partial\epsilon}{\partial t}\right)_n &= \frac{\epsilon_n - \epsilon_{n-1}}{t_n - t_{n-1}}, \qquad n = 2, 3, \ldots, \\ \left(\frac{\partial\epsilon}{\partial t}\right)_1 &= 0. \end{aligned}\right\} \tag{16}$$

* Throughout this paper we use the notation $[x]$ for the quantity 10^x = antilog$_{10}x$.

The adoption of (16) requires $\partial\epsilon/\partial t$ to be omitted for the initial state. This is an excellent approximation since $\partial\epsilon/\partial t$ has only a very slight effect on the structure of the star during the early stages of the evolution. Therefore in determining $(\partial\epsilon/\partial t)_2$, $\epsilon_1(M)$ is a known quantity. The time difference t_2-t_1 is also known, since it is the time difference that specifies the evolutionary step. Hence $\partial\epsilon/\partial t$ is determined in terms of M, P, T for the stage 2, and so on for subsequent steps.

The inclusion of $\partial\epsilon/\partial t$ emphasizes that the basic equations are of the partial type. Impressions to the contrary sometimes arise from the circumstance that $\partial\epsilon/\partial t$ is usually small compared with U. In such cases $\partial\epsilon/\partial t$ can be omitted as a reasonable approximation. Even when $\partial\epsilon/\partial t$ needs to be included, a satisfactory approximation can often be obtained from a less accurate procedure than (16), namely from

$$\left.\begin{aligned}\left(\frac{\partial\epsilon}{\partial t}\right)_n &= \frac{\epsilon_{n-1}-\epsilon_{n-2}}{t_{n-1}-t_{n-2}}, \qquad n=3,\ 4,\ \ldots,\\ \left(\frac{\partial\epsilon}{\partial t}\right)_1 &= \left(\frac{\partial\epsilon}{\partial t}\right)_2 = 0.\end{aligned}\right\} \tag{17}$$

(iii) *Determination of* K.—The opacity K must include energy transfer by both radiation and conduction. We require formulae for $K_{\rm rad}$, $K_{\rm cond}$, defined by

$$\left.\begin{aligned}Q_{\rm rad} &= -\frac{64}{3}\pi^2 ac\rho T^3 K_{\rm rad}^{-1}.R^4\frac{dT}{dM},\\ Q_{\rm cond} &= -\frac{64}{3}\pi^2 ac\rho T^3 K_{\rm cond}^{-1}.R^4\frac{dT}{dM},\end{aligned}\right\} \tag{18}$$

where $Q_{\rm rad}$, $Q_{\rm cond}$ represent the energy transferred by radiation and by conduction respectively. Since Q in (10) is the total flux, equal to $Q_{\rm rad}+Q_{\rm cond}$ when convection is absent (if convection occurs then (10) is not required), it follows that

$$K^{-1}=K_{\rm rad}^{-1}+K_{\rm cond}^{-1}. \tag{19}$$

We start a discussion of K by considering the case in which there is no degeneracy of the electrons. Then $K_{\rm cond}$ can be neglected since conduction in a non-degenerate star is very slow indeed (Eddington, 1930). Even in this case the determination of a highly accurate value of K is a formidable task, requiring the evaluation of very complicated series (Morse, 1940). In the hand computation of stellar models it has been the practice to use tables for determining K when ρ, T and the chemical composition are specified. Tabular information, such as that given by Morse or more recently by Keller and Meyerott (1955), is not well suited to calculation with an automatic computer however. Given a machine of large capacity and great speed, the ideal procedure would be to calculate the opacity *ab initio*, using a programme in which the relevant atomic theory was incorporated. This unfortunately lies far outside our resources. We have therefore been obliged to use a simple algebraic representation for $K_{\rm rad}$. We have followed Hoyle and Schwarzschild (1955), in using

$$K_{\rm rad}=0{\cdot}19\rho(1+X)\{1+[23{\cdot}287]\rho/T^{3{\cdot}5}\}, \tag{20}$$

for $\beta=1$, and have used

$$K_{\rm rad}=0{\cdot}19\rho\{1+[23{\cdot}287]\rho/T^{3{\cdot}5}\}, \tag{21}$$

for $\beta>1$. We have found that (20) and (21) give a better approximation for K_{rad} than might perhaps be expected. The approximation is tolerable for Type II stars on account of the small metal content of these stars. For massive Type I stars, electron scattering is the main source of opacity, and this is correctly given by (20) and (21). The main source of opacity in the deep interiors of evolving stars of moderate mass is also electron scattering.

At first sight it seems as if our expressions must fail badly on account of the neglect of free–bound transitions in the outer regions of both dwarf and giant stars of Type I, but this is not so, because such regions are convective (Osterbrock, 1953; Hoyle and Schwarzschild, 1955). Another fortunate point is that, although (21) gives a poor value for $\beta>2$ (but not for $\beta=2$), we have always encountered electron degeneracy when $\beta>2$, and the important mode of energy transfer is then by conduction. It seems then as if (20), (21) give a just tolerable approximation in all cases where reasonable accuracy in K_{rad} is required. A better approximation would, however, be desirable if a computer of greater speed and storage capacity were available.

It is important to choose an expression for K_{cond} that gives a suitably high conduction rate when there is electron degeneracy, and which represents K_{cond} with reasonable precision in the region of partial degeneracy. Using conductivity values given by Mestel (1950) we have obtained the following algebraic representation

$$K_{\text{cond}}=[-5{\cdot}3710](T/\rho)^{1{\cdot}8571}. \tag{22}$$

When there is no electron degeneracy (19) gives $K\simeq K_{\text{rad}}$, with conduction negligible, as it should be. When the electrons are highly degenerate (19) gives $K\simeq K_{\text{cond}}$, which is again correct. The combined expression (19) is also reasonably good in the range of partial degeneracy for values of T between 2×10^7 deg. K and 10^8 deg. K, the errors in $\log_{10}K$ being never more than about 0·05.

(iv) *The determination of* Γ.—With P' defined by (1), Γ can be expressed in the form (Chandrasekhar, 1938)

$$\Gamma=\frac{1}{3}\,\frac{32P^2-24PP'-3(P')^2}{8P^2-6PP'-(P')^2}. \tag{23}$$

Boundary conditions at the centre of a star

Starting values of P, T must be specified. Since $R=0$, $Q=0$ at $M=0$, the integration of the above equations can then be performed outwards from the centre.

Boundary conditions at the surface of a star

(i) *Surface temperatures less than 6000 deg. K.*—Opacity in the photospheric layers arises mainly from negative hydrogen ions in this case—except possibly for very low surface temperatures when molecular band absorption may become dominant. The theory of the outer layers of a star must then be very intricate and is not considered here. We have adapted the analysis of the negative ion case due to Hoyle and Schwarzschild (1955) to give a routine whereby R, Q, P are determined at $T=10^5$ deg. K. Inward integration of the equations can then be performed. To effect such a determination two quantities must be specified at the photosphere. These can be chosen in a number of ways; the most convenient were found to be the effective surface temperature of the star, T_e and the photospheric electron pressure, P_e. The choice of $T=10^5$ deg. K as a

starting point of the inward run of the differential equations was dictated by the following considerations. It is desirable that the starting temperature shall be high enough for all the hydrogen of the stellar material to be considered as ionized. On the other hand it is convenient to be able to neglect the thickness of the sub-photospheric zone from T_s down to the starting temperature of the run of the differential equations. This means that the starting temperature should not be set too high. A starting temperature of $T = 10^5$ deg. K was thought to give a suitable compromise between these two requirements.

Writing Q_s, R_s for the photospheric flux and radius, we make the very slight approximation of putting Q, R at $T = 10^5$ deg. K equal to Q_s, R_s. Our problem is therefore to determine Q_s, R_s, and P at $T = 10^5$ deg. K, when T_s, P_e are specified. Evidently we have

$$Q_s = \pi a c R_s^2 T_s^4. \tag{24}$$

The following equations were constructed from the analysis of Hoyle and Schwarzschild, the meanings of the symbols being: A_1, A_2, A_3, A_4 are the concentrations of hydrogen, magnesium, sodium and potassium, concentrations being in terms of numbers of atoms, not in terms of mass. These are the elements that make the main contributions to the density of free electrons. C_1, C_2, C_3, C_4 are the corresponding ionization potentials (13·54 eV for hydrogen, 7·61 eV for magnesium, 5·12 for sodium, 4·32 for potassium).

$$\alpha_i = C_i/T_s + \tfrac{5}{2}\log_{10} T_s + d_i - \log_{10} P_e, \quad i = 1, 2, 3, 4, \tag{25}$$

defines α_i, where d_i is a statistical weight factor ($d_1 = -0{\cdot}48$, $d_2 = 0{\cdot}04$, $d_3 = -0{\cdot}64$, $d_4 = -0{\cdot}92$). R_s, Q_s are obtained from (24) together with

$$2\log_{10} P_e - \log_{10}\left\{\sum_{i=1}^{4} \frac{\alpha_i A_i}{1+\alpha_i}\right\} - 2{\cdot}8 + 1{\cdot}55\,\frac{5040}{T_s} - \log_{10}\left(\frac{GM_s}{R_s^2}\right) = 0, \tag{26}$$

the total mass of the star, M_s, being regarded as known. The photospheric density is given by

$$\mathfrak{R}\rho_s T_s \sum_{i=1}^{4} \frac{\alpha_i A_i}{1+\alpha_i} = P_e. \tag{27}$$

The quantities ρ_s' and x are determined from

$$\mathfrak{R}\rho_s' T_s \frac{\alpha_1 A_1}{1+\alpha_1} = P_e, \tag{28}$$

$$\log_{10}(x + 0{\cdot}1373) = -13{\cdot}2783 - \tfrac{2}{3}\log_{10}(GM_s/R_s^2) + \tfrac{29}{6}\log_{10} T_s - 3{\cdot}48(5040/T_s) + \log_{10}(\rho_s'/\rho_s). \tag{29}$$

Value of P at $T = 10^5$ deg. K

$$\left.\begin{aligned} &\text{If } x < 0, \quad \log_{10} P = 16{\cdot}7561 + \tfrac{1}{2}\log_{10}\rho_s - \tfrac{3}{4}\log_{10} T_s - \log_{10}\mu_s. \\ &\text{If } x \geqslant 0, \quad \log_{10} P = 11{\cdot}855 + \tfrac{1}{2}\log_{10}\rho_s + \tfrac{1}{2}\log_{10} T_s - 4{\cdot}169x - \log_{10}\mu_s \end{aligned}\right\} \tag{30}$$

where $\mu_s = 4/(5X_s + 3)$, X_s being the value of X at the photosphere.

Values of R, Q at $T = 10^5$ deg. K

$$R = R_s, \qquad Q = Q_s. \tag{31}$$

This treatment assumes that $\beta = 1$ in the surface layers and that

(*a*) the ionization of hydrogen is effectively complete at $T = 10^5$ deg. K,

(*b*) the ionization energy of helium may be neglected. The procedure should be regarded as very approximate for $T_s < 3500$ deg. K on account of the neglect of molecular absorption.

(ii) *Surface temperatures greater than 6000 deg. K.*—In all cases we have encountered ρ/T^3 is a slowly varying function of M in the outer parts of the star. An excellent approximation is given by neglecting the derivative of ρ/T^3 with respect to M. It can then be shown, after some calculation, that the value of P at $T = 10^5$ deg. K is given by

$$\log_{10} P = 5 + \log_{10}\{[0{\cdot}4008] + [0{\cdot}9161]\chi/\mu_s\}, \tag{32}$$

χ being the positive root of the quadratic

$$[-0{\cdot}6977]\frac{\chi^2}{\mu_s} + \chi\left\{\frac{[0{\cdot}5153]}{\mu_s} + [-1{\cdot}2130]\right\} + 1 - \frac{[5{\cdot}1213]M_s}{(1+X_s)Q_s} = 0. \tag{33}$$

As before we put

$$R = R_s, \qquad Q = Q_s \quad \text{at} \quad T = 10^5 \text{ deg. K}.$$

In this case R_s, Q_s are the most convenient quantities to specify at the beginning of an inward run of the differential equations.

It is implicitly assumed in these equations that $\beta = 1$ in the surface layers of the star.

Condition of fit

Two parameters (P, T) have to be specified at the centre of a star in order that the differential equations can be integrated outwards, and two parameters, (R, Q) or (P_e, T_e) have to be specified at the photosphere for integration inwards from the surface. Thus a pair of integrations, one from the centre outwards and one from the surface inwards require the specification of four parameters. The condition for the existence of a possible stellar structure is that the inward and outward integrations can be made to give the same values of R, Q, P, T at the value of M at which the two integrations meet.

It is emphasized that with $X(M)$, $\beta(M)$, $\partial\epsilon/\partial t$ arbitrarily specified there is no existence theorem requiring a solution. Indeed we have found cases where no solution exists. Nor is there any guarantee that there shall be only one solution—we have found cases where there are two.

7. *Equations for an evolutionary step when X is a slowly varying function of M.*—In non-convective material we have

$$\partial X/\partial t = -q^{-1}U \tag{34}$$

which can be expressed in finite differences as

$$X(M, t_{n+1}) = X(M, t_n) - q^{-1}U(M, t_n)(t_{n+1} - t_n) + O(t_{n+1} - t_n)^2, \tag{34'}$$

provided $X(M, t_{n+1}) > 0$, where $t_n \to t_{n+1}$ represents the evolutionary step, and q is the energy released by the transformation of one mass unit of nuclear fuel. For $\beta = 1$, $q = 6{\cdot}2 \times 10^{18}$ ergs, while for $\beta = 2$, $q = 8{\cdot}6 \times 10^{17}$ ergs. If the right-hand side of (34′) turns out to be less than zero, when some particular time step is specified, then the value of β must be changed and X must be reset in accordance with the discussions of Section 3.

The determination of $X(M, t_{n+1})$ for convective material is a more complicated problem. Let the boundaries of the convective zone be denoted by M', M''. Provided M', M'' vary slowly with time the following approximate equation may be used

$$X(M, t_{n+1}) = (M'' - M')^{-1}\left\{\int_{M'(t_n)}^{M''(t_n)} X(M, t_n)\,dM - q^{-1}\int_{M'(t_n)}^{M''(t_n)} U(M, t_n)\,dM\right\}. \tag{35}$$

This equation neglects terms involving the time derivatives of M', M''. It has been found adequate in the cases we have encountered.

8. *Evolution when X or β is a rapidly varying function of M.*—Cases in which X and β vary extremely rapidly with M occur when nuclear energy is produced in one or more thin shells within a star. For example a star may possess a core with $\beta=2$, surrounded by an envelope with $\beta=1$. Energy generation may then be confined to an extremely thin shell immediately surrounding the core. Examples have been obtained in which the shell contains only a very tiny proportion of the mass of the star: in one instance we have found a shell containing less than $10^{-5} M_s$. It is then impracticable to follow the evolution by the method discussed in Section 5, since this would require extremely small time steps to be taken.

We proceed in such a situation by an alternative method. In the case of a $\beta=2$ core surrounded by a $\beta=1$ envelope, in which evolution is proceeding by successive layers of helium being added to the core, we simply extend the core to larger mass, the amount of the extension determining the time interval of the evolutionary step. That is to say, the mass of the core is used as the evolutionary parameter instead of the time. If $(M_c)_n$ denotes the mass of the core at step n and $(Q_s)_n$ is the corresponding luminosity then the time associated with the step $(M_c)_n \rightarrow (M_c)_{n+1}$ is given by

$$q\{(M_c)_{n+1}-(M_c)_n\}/(Q_s)_n \tag{36}$$

with satisfactory accuracy, provided the evolutionary steps are not too widely spaced.

It must be emphasized that (36) can only be used in the case where just one nuclear fuel is being burned in the star. If in the case just discussed, appreciable energy were also being generated by "helium burning" at the centre of the star, as well as in a hydrogen shell, then more careful considerations are needed. We can still use the mass of the core as the evolutionary parameter, but the time must be calculated from

$$q\{(M_c)_{n+1}-(M_c)_n\}/Q_n' \tag{37}$$

where q corresponds to the burning of hydrogen, and Q_n' is the energy generated in the shell alone (equal to Q_s minus the energy generated by the helium). The quantity $X(M,t)$, $\beta=2$ in this case may or may not be a slowly varying function of M. If it is slowly varying, then the equations of Section 7 can be used to determine the change of $X(M,t)$, $\beta=2$ in an evolutionary step, the time interval of the step being determined by (37). This keeps the burning of the helium commensurate with the burning of the hydrogen.

A still more awkward case arises if the helium core contains an inner core of carbon, oxygen, and neon, for in that case helium burning also occurs in a shell, and $X(M,t)$, $\beta=2$ is also a rapidly varying function of M. We can then make an evolutionary step by extending both the helium zone and the inner core, but the two extensions must be commensurate with each other. This can be ensured by using (37) for the extension of both shells, and by arranging that the time given by (37) is the same in both cases. When (37) is used for the extension of the helium burning shell the value of q for $\beta=2$ must be used, M_c must be interpreted as the mass of the inner core and Q_n' must be replaced by Q_s-Q_n'.

Still more complicated structures involving three or more shells can be treated in a like fashion.

9. *The conversion of the equations to a form suitable for the EDSAC I.*—In the EDSAC I any number is treated as if it is in the range -1 to 1, and is stored

so that it may have a rounding error of the order of 2^{-35}. Thus since the variables in the equations above may change during the course of the calculation by a factor much greater than 2^{35}, the numbers cannot be stored with accuracy even if they are scaled by an appropriate fixed factor.

The equations themselves suggest a method of overcoming this difficulty. It will be observed that most of the operations involved in the calculation of the derivatives are those of multiplication and division and of obtaining powers of quantities. The operations of addition and subtraction are comparatively rare. This suggests that we should represent the numbers by their logarithms (scaled by a certain constant factor) in the machine. We therefore write $\boldsymbol{M} = \log M$, $\boldsymbol{R} = \log R$ and similarly for all other variables and constants which may occur.

If $A + B = C$ and if A and B are both positive we define addition and subtraction logarithms by

$$\boldsymbol{C} = \mathrm{al}\,(\boldsymbol{A}, \boldsymbol{B}),$$

and

$$\boldsymbol{B} = \mathrm{sl}\,(\boldsymbol{C}, \boldsymbol{A}).$$

We give the following specimen equations derived from those above

$$\frac{d\boldsymbol{R}}{d\boldsymbol{M}} = \exp\{\boldsymbol{M} - 3\boldsymbol{R} - \boldsymbol{\rho} - \log_e 4\pi\},$$

$$\frac{d\boldsymbol{P}}{d\boldsymbol{M}} = -\exp\{2\boldsymbol{M} - 4\boldsymbol{R} - \boldsymbol{\rho} + \log_e G/4\pi\}.$$

In this representation of the problem to the machine the operations of division and of forming powers of numbers are replaced by the much faster operations of subtraction and multiplication respectively. It is necessary however to provide the machine with subroutines for calculating logarithms and exponentials, and the quantities defined by $\mathrm{al}\,(\boldsymbol{A}, \boldsymbol{B})$ and $\mathrm{sl}\,(\boldsymbol{A}, \boldsymbol{B})$.

For the integration we have used a programme which is available in the EDSAC library of subroutines. This programme (Gill, 1951) uses a Runge–Kutta process to integrate a set of differential equations of the form

$$dy_i/dt = f_i(y_1, y_2, \ldots, y_n).$$

It was necessary to exercise great care concerning the size of the step in the independent variable $\boldsymbol{M}$. It seemed reasonable to restrict the step $\delta\boldsymbol{M}$ to be such that the corresponding changes in the dependent logarithmic variables were less than a certain fixed amount. The machine was therefore programmed to halve or double the step of integration according to the size of the derivatives. In order to be able to print the variables at specified tabular intervals the doubling of the step was only permitted when the equivalent of an even number of steps of the current size had been performed. This ensures that every tabular point is reached. As it was not possible to give the machine the values $M = 0$, $R = 0$, $Q = 0$ (i.e. $\boldsymbol{M} = -\infty$, $\boldsymbol{R} = -\infty$, $\boldsymbol{Q} = -\infty$) as the starting conditions for the integration at the centre of the star the integrations were started at a small value of $M = M_0$ say. The corresponding R_0 and Q_0 were then calculated by assuming that the density and the rate of energy generation were both constant in the region $R \leqslant R_0$. M_0 was taken to be $e^{-8}M_s$.

Solutions of the differential equations which satisfy the boundary conditions both at the surface and at the centre are obtained by the following iterative process.

A set I_α, I_β, I_γ of three inward integrations is performed. I_α is regarded as basic and I_β and I_γ have small increments of the starting parameters, say R_s

and Q_s respectively. The integrations are stopped at an assigned value of the mass $M = M_i$ say. A similar set of outward integrations O_α, O_β, O_γ is also performed from $M = M_0$ to $M = M_i$, O_β and O_γ having small increments in P_0 and T_0 respectively. The two sets of values of R, Q, P and T at $M = M_i$ are then compared and it is assumed that the differences between the values obtained by inward and outward integration are approximately linear functions of variations in the starting parameters. Under this assumption it is possible to find a better set of initial values of the variables for the inward and outward integrations, by solving, using the machine, a set of four simultaneous equations.

We then integrate the equations with the new set of initial conditions. If there is substantial improvement in the "fitting" of the inward and outward solutions we may obtain a better set of initial conditions by assuming that the same linear dependence on the initial conditions will still hold. This gives us a method of first order numerical iteration for the solution we require.

If, however, the increments are large it may be necessary to carry out a further set of six integrations. There is no guarantee that either of these processes will converge but if we start with initial conditions which are reasonably good we find that three or four iterations give a fit in the solutions to an accuracy of one part in the fourth decimal of the logarithm.

The EDSAC I performs an integration, inward or outward, in about 15 minutes. This means that the machine is theoretically capable of obtaining a sufficiently accurate solution to the equations in a few hours, but in practice the actual time depends very much on the original estimates of the initial conditions.

The time taken to calculate the change in the constitution of a star and to estimate $\partial\epsilon/\partial t$ is negligible in comparison with the time taken for the solution of the differential equations.

University Mathematical Laboratory,
Cambridge:
1956 *May* 10.

St. John's College,
Cambridge.

References

Borman-Crespin, D., Fowler, W. A. and Humblet, J. (1954), *Bull. Soc. Sci. Liège*, **9–10**, 327.
Chandrasekhar, S. (1938), *Introduction to the Study of Stellar Structure*, University of Chicago Press, p. 56.
Eddington, A. S. (1930), *Internal Constitution of the Stars*, Cambridge University Press, p. 276.
Gill, S. (1951), *Proc. Camb. Phil. Soc.*, **47**, 96.
Hoyle, F. (1954), *Ap. J. Supp.*, **1**, No. 5, 121.
Hoyle, F. and Schwarzschild, M. (1955), *Ap. J. Supp.*, **2**, No. 13, 1.
Keller, G. and Meyerott, R. E. (1955), *Ap. J.*, **122**, 32.
Mestel, L. (1950), *Proc. Camb. Phil. Soc.*, **46**, 331.
Mestel, L. (1953), *M.N.*, **113**, 716.
Morse, P. M. (1940), *Ap. J.*, **92**, 27.
Osterbrock, D. E. (1953), *Ap. J.*, **118**, 529.

A PRELIMINARY DETERMINATION OF THE AGE OF TYPE II STARS

C. B. Haselgrove and F. Hoyle

(Received 1956 May 10)

Summary

Fifteen evolutionary steps have been computed for a star of mass $2{\cdot}512 \times 10^{33}$ grams. Comparison of the results with the colour-magnitude diagram of M3 suggests that this globular cluster has an approximate age of $6{\cdot}5 \times 10^{9}$ years.

Fifteen evolutionary steps have been calculated by the method described in the previous paper for a star of mass $2{\cdot}512 \times 10^{33}$ grams. The following initial composition, taken to be uniform throughout the star was used:—

Hydrogen concentration	0·9309
Helium concentration	0·0666
Carbon–nitrogen concentration	0·0025

Small concentrations of other elements could be introduced, but would have no appreciable effect on the results. Carbon and nitrogen are included in the above list because of their importance in the thermonuclear transformation of hydrogen into helium. The present initial composition is regarded as a reasonable estimate of the composition of Type II stars. Metals have an important influence on conditions at the photosphere in the later evolutionary stages of the star, but have

TABLE I

Solution	$\log_{10}R$	$\log_{10}L$	$\log_{10}P_0$	$\log_{10}T_0$	$\bar{X}$
1	10·825	33·837	17·183	7·140	0·93090
2	10·829	33·870	17·201	7·153	0·91928
3	10·840	33·904	17·218	7·166	0·90642
4	10·856	33·941	17·233	7·182	0·89241
5	10·881	33·995	17·236	7·197	0·87256
6	10·915	34·048	17·238	7·217	0·85356
7	10·972	34·114	17·239	7·245	0·83126
8	11·017	34·155	17·307	7·289	0·81817
9	10·975	34·215	18·231	7·228	0·81255
10	11·070	34·300	19·114	7·282	0·80063
11	11·201	34·334	19·881	7·323	0·79809
12	11·212	34·356	20·170	7·343	0·79523
13	11·277	34·407	20·481	7·366	0·78917
14	11·338	34·487	20·661	7·377	0·78401
15	11·417	34·617	20·823	7·396	0·77620
16	11·576	34·893	21·028	7·414	0·76388

R in cm.
L in ergs per sec.
P_0, the central pressure in dynes per cm^2.
T_0, the central temperature in deg. K.
$\bar{X}$ the hydrogen concentration *averaged over the whole star*.

little effect in the early stages considered in the present paper (Hoyle and Schwarzschild 1955).

The calculations were performed with the aid of the computer EDSAC I at the Cambridge University Mathematical Laboratory. Results for the radius R, luminosity L, central pressure P_0 and central temperature T_0 are given in Table I. The mean hydrogen concentrations for the whole star at the various evolutionary stages are also given.*

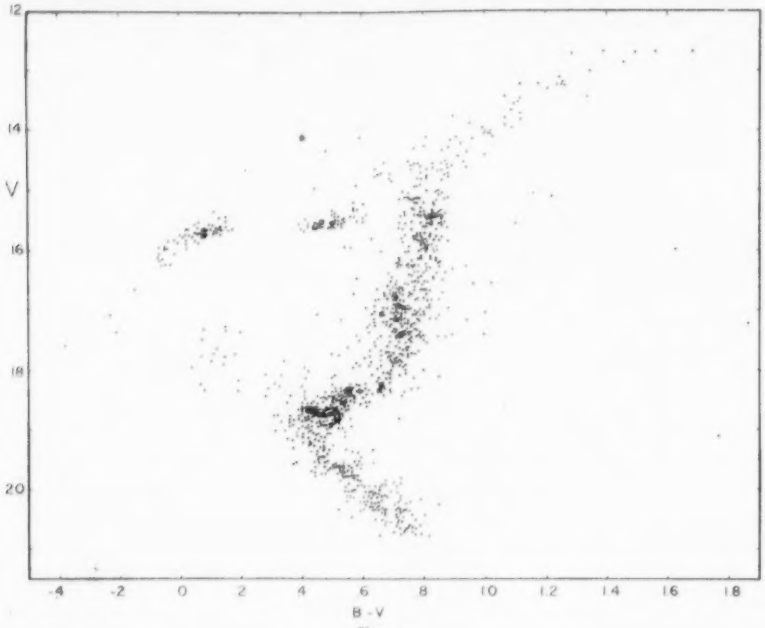

FIG. 1.

The solutions 1 to 8 were found to possess a central convective region containing approximately 8 per cent of the mass of the star. This convective core does not retreat substantially until essentially all its hydrogen content becomes exhausted. This occurs between solutions 8 and 9. Thus although there is little change in X (the mean proportion of hydrogen in the star) between these solutions, there is a highly important change in the structure of the star. At stage 8 the central regions still contain some hydrogen and the thermonuclear production of energy still occurs mainly in the central regions. But at stage 9 the production of energy takes place in a shell zone surrounding a nearly isothermal inert core. The mathematical structure of the problem is thereby altered, almost discontinuously. It is this change of mathematical structure that explains the marked change in the numbers given in Table I. The present results may possibly depend in this respect on the concentrations of carbon and nitrogen used in our calculations. With lower concentrations the importance of the carbon–nitrogen cycle would be lessened, and this would decrease the extent of the inner convective region. It may also be noted that the formula we have used for energy production by the carbon–nitrogen cycle is based on the work of Bosman-Crespin, Fowler, and Humblet (1954), and

* The full tables of solutions have been deposited with the Royal Astronomical Society.

that we have chosen the more rapid of the two energy production formulae discussed by these authors, depending on there being a favourably placed resonance level in the nucleus of O^{15}. If there is no such level, the slower formula for

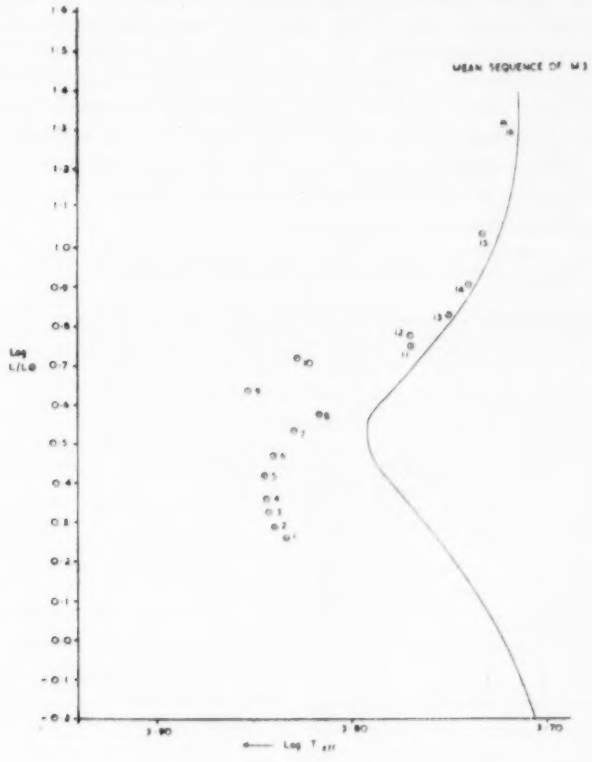

FIG. 2.

Values adopted in obtaining Fig. 2.

Observational points (mean values for M3 sequence).

log $L/L_\odot$	−0·108	0·048	0·252	0·448	0·568
log T_{eff}	3·713	3·730	3·757	3·782	3·791
log $L/L_\odot$	0·656	0·864	1·112	1·320	1·512
log T_{eff}	3·777	3·745	3·720	3·715	3·710

Theoretical points:

log $L/L_\odot$	0·260	0·292	0·326	0·363	0·418	0·470	0·536	0·577
log T_{eff}	3·834	3·840	3·843	3·844	3·845	3·841	3·830	3·817
log $L/L_\odot$	0·637	0·722	0·756	0·779	0·830	0·910	1·040	1·316
log T_{eff}	3·853	3·827	3·770	3·770	3·750	3·740	3·733	3·722

carbon-nitrogen energy production would have to be used, and this again could modify the details of our solutions, especially solutions 8 and 9.

The surface boundary condition of the star was treated in the manner discussed previously (1956), the switch to the surface condition of Hoyle and Schwarzschild being made at solution 12.

To facilitate comparison with our results, the stars of the globular cluster M_3 are represented in a colour-magnitude diagram in Fig. 1.* From this diagram a mean curve can be drawn. This is given in Fig. 2, together with our results. It will be noticed that the scales used in Figs 1 and 2 are different. The conversion was made in the following way: First, apparent magnitudes m_{pv} were converted to absolute photovisual magnitudes M_{pv} by taking the horizontal branch stars of Fig. 1 as having $M_{pv} = 0{\cdot}0$. This gives 0·0 for the absolute photovisual magnitude of the RR Lyrae stars, a value that is generally accepted by astronomers and which is not likely to be in error by more than about two tenths of a magnitude. The magnitude-luminosity conversion between Figs 1 and 2 is then made by putting the photovisual magnitude of the Sun equal to $+4{\cdot}62$ (Kuiper 1938). We then have

$$\log_{10}\frac{L}{L_0} = 0{\cdot}4\,\{(4{\cdot}62 - M_{pv}) + \text{bolometric correction}\}.$$

Bolometric corrections are given as a function of colour index in Table II. The conversion from colour index to effective surface temperature is also given in Table II.

TABLE II

Colour index	Logarithm of effective surface Temperature (deg. K)	Bolometric correction
0·0	3·9550	0·400
0·1	3·9075	0·220
0·2	3·8680	0·100
0·3	3·8285	0·020
0·4	3·7970	0·080
0·5	3·7680	0·150
0·6	3·7440	0·210
0·7	3·7200	0·270
0·8	3·7000	0·310
0·9	3·6810	0·380
1·0	3·6550	0·460

Discussion of Results.—The first point requiring emphasis is that our calculated points ought not to fall entirely on the observed sequence, since the observed sequence concerns stars of variable mass presumably of essentially the same age, whereas our calculated points refer to a star of fixed mass at various evolutionary phases.

We next note that evolution is an accelerating process. Consider a series of time $t_1, \ldots, t_n, \ldots$ in the evolution, t_0 representing the initial state. Then we have

$$t_n - t_1 = qM \int_{\overline{X}_1}^{\overline{X}_n} \frac{d\overline{X}}{\overline{L}}$$

where $\overline{X}_1$, $\overline{X}_n$ are the mean hydrogen concentrations for the initial state and for the stage t_n respectively, M is the mass of the star, and q is the energy obtained from the transformation of one mass unit of hydrogen into helium ($q = 6{\cdot}2 \times 10^{18}$ ergs per gram). Computations of this integral (which can be performed by simple

* We are much in debt to Dr A. R. Sandage for providing the observational material of this paper, and also for allowing us to reproduce it.

quadratures with the aid of the information given in Table 1) show that t_n increases only slightly beyond stage 13. The steps 1–2, 2–3, 3–4, 4–5, 5–6, 6–7, require nearly equal time, each amounting to approximately $2{\cdot}5 \times 10^{16}$ seconds. The step 7–8 requires about $1{\cdot}5 \times 10^{16}$ seconds, while thereafter the steps up to stage 13 average somewhat less than 10^{16} seconds. After stage 13 the evolution becomes progressively even more rapid. Thus by the time the giant branch is reached significant evolution takes place in as little as 10^{15} seconds. The acceleration is of course promoted by the increasing luminosity.

This phase of the evolution therefore occupies a very short time in the life of a star. As the rate of evolution of a star depends strongly on its initial mass, stars of different masses reach this phase at fairly widely differing ages. The cluster stars observed in this part of the sequence, supposed of equal age, must therefore have closely similar masses, although there will be a wider variation in the masses of stars observed in lower parts of the sequence.* Hence the higher parts of the sequence should differ little from the evolutionary track of a star of fixed mass—the mass being taken equal to the average mass of the stars that populate the upper part of the sequence. Our results, shown in Fig. 2, confirm this expectation.

The present interpretation (which it will eventually be possible to test when more evolutionary tracks have been computed—particularly for stars of smaller masses) requires the stars of the observed sequence at and beyond point 13 to have masses close to the mass for which our calculations were performed—$2{\cdot}512 \times 10^{33}$ grams. Evolution beyond point 13 is so rapid that the masses of the highly luminous giants of M3 and of the horizontal branch stars, including the RR Lyrae stars, should not be much different from this.

Our interpretation also requires the age of M3 to be close to the time of evolution to point 13, which when computed as indicated above is found to be $2{\cdot}049 \times 10^{17}$ seconds, or $6{\cdot}5 \times 10^{9}$ years, in good agreement with the estimate of $6{\cdot}2 \times 10^{9}$ years by Hoyle and Schwarzschild (1955).

In conclusion it is worth remarking once again that the swing left between solution 8 and 9 is probably dependent on the existence of a resonance level in the O^{15} nucleus. If such a level does not exist, energy production by the carbon-nitrogen cycle would be much weaker in these stars (approximately half the energy is produced by the carbon-nitrogen cycle in our computations) and this might well affect the form of the solutions between points 8 and 11, although probably not much otherwise. This again is a point that can be checked by further computations.

It is also worth noting that evolution from 8 to 9 is very rapid indeed, as also is the evolution across from 9 to 10. Consequently not many stars should be found at these particular stages, especially the step 8–9.

While there is some theoretical doubt whether the swing left at stage 8 ought to occur in the globular cluster stars, there should be no such doubt for appreciably more massive stars in which the carbon–nitrogen cycle is certainly the main source of thermonuclear energy. Hence some similar phenomenon corresponding to the exhaustion of a convective core ought to occur in more massive stars. One might hazard the guess that rapid evolution taking place at this stage will move the stars very markedly towards the right in a colour-magnitude diagram. Such a rapid sequence of changes is exactly what is required to explain the existence of the

* This point is discussed in detail by Sandage (1953).

well-known Hertzsprung gap. This again is a possibility that can be decided only by further computations.

It is a pleasure to acknowledge our gratitude to the Director of the University Mathematical Laboratory, Cambridge, for the facilities that have been given to us, and particularly for the use of EDSAC.

University Mathematical Laboratory,
Cambridge:
1956 *May* 10.

St. John's College,
Cambridge.

References

Bosman-Crespin, D., Fowler, W. A. and Humblet, J. (1954), *Bull. Soc. R. Sci. Liège*, **9–10**, 327.
Haselgrove, C. B. and Hoyle, F. (1956), *M.N.*, **116**, 515.
Hoyle, F. and Schwarzschild, M. (1955), *Ap. J. Supp.*, **2**, 1.
Sandage A. R. (1953), *Mém. Soc. R. Sci. Liège*, 4th Series, **14**, 254.

THE PERIOD-LUMINOSITY RELATION AND STELLAR COMPOSITION

V. C. Reddish

(Received 1956 March 12)

Summary

The structure of cepheids and the effect on the period-luminosity relation of a change in the composition of the material out of which variables are formed, is considered. It is shown that if a difference ΔM_{pg} is observed between the period-luminosity relations of two groups of cepheids, the maximum difference dX of the hydrogen abundances in the initial composition is given by the inequality

$$\left[\frac{4}{X+0{\cdot}6q}-\frac{1}{X+q}\right]dX<0{\cdot}9\Delta M_{pg},$$

where $Q=1-q^{-1}$ is the fraction of the mass of a cepheid contained in its core exhausted of hydrogen.

It is probable that the hydrogen abundance in the interstellar gas in M31 does not vary by more than 15 per cent across the galaxy, and the variation may actually be very much less than this.

Investigations by Baade and Swope (**1**) into the period-luminosity relations for cepheid variables in various regions of the Andromeda Nebula M31 suggest that any difference in the zero points of the relations are small, say less than 0·25 magnitude (**2**).

These observations lead to the conclusion either that there are only small differences in composition between the cepheids of a given period or that any differences which do exist displace the period-luminosity relation parallel to itself.

The considerations which follow show that a change of only a few percent in the hydrogen abundance in the material out of which the cepheids formed would cause a measurable displacement in magnitude of the period-luminosity relation. It is concluded that any differences between the hydrogen abundances in the interstellar gas near the centre and towards the edge of M31 is less, probably much less, than 15 per cent.

Theories of the structure of stars lead generally to an equation for the luminosity in the form

$$L=A\mu^{k}M^{l}R^{m}Z^{n}(1+X)^{-1}, \qquad (1)$$

where μ denotes molecular weight, M and R mass and radius, Z and X abundances of heavy elements and hydrogen respectively. With opacity due to photoelectric absorption, usually $k=7{\cdot}5$, $l=5{\cdot}5$, $m=-0{\cdot}5$ and $n=-1$, while if opacity is due solely to electron scattering $k=4$, $l=3$, $m=n=0$. A varies with the structure but is a constant for all stars of similar structure.

The theory of pulsation gives the equation for the period

$$P=BR^{1{\cdot}5}M^{-0{\cdot}5}, \qquad (2)$$

where B also is a constant for all stars of similar structure.

Observations of cepheid variables give a relation between P and R (**3**) which may be written

$$P = CR^q, \tag{3}$$

where C is a constant.

Eliminating M and R between these three equations gives

$$\log L = \log A + 2l \log B - (3l/q + m/q) \log C + \{l(3/q - 2) + m/q\} \log P + k \log \mu + n \log Z - \log (1 + X). \tag{4}$$

Neglecting the effect of variations in Z and X we have

$$2l\Delta \log B + \Delta \log A + k\Delta \log \mu = \Delta \log L - \{l(3/q - 2) + m/q\} \Delta \log P. \tag{5}$$

The empirical mass-luminosity relation (**5**) gives $l \approx 3{\cdot}5$, close to the theoretical value for electron-scattering opacity. If the luminosity is almost independent of radius (as in the Hoyle-Lyttleton type of giant models (**4**)) then $m \approx 0$ and

$$7\Delta \log B + \Delta \log A + k\Delta \log \mu = \Delta \log L - 3{\cdot}5\,(3/q - 2)\,\Delta \log P. \tag{6}$$

With the exception of the two points of largest P, the values of $\log P$ and $\log R$ given by Allen (**3**) are fitted well with a line of slope $q = 1{\cdot}0$. If the two highest points are included and if all the points had the same errors, a line of slope as high as $1{\cdot}18$ could be fitted. However, it is well known that the error of determining effective temperatures and thus stellar radii increases with higher luminosity class and thus in this case with increasing R. Consequently the slope will not be far from $1{\cdot}0$ (providing there are not unknown systematic errors in the data which Allen used).

As the effective polytropic index n_{eff} increases, B decreases. An increase in n_{eff}, an increase in the central concentration of mass, usually (but not necessarily) implies higher luminosity, a more advanced stage of evolution and greater average molecular weight. Consequently $\Delta \log A$ and $\Delta \log \mu$ usually have opposite signs to $\Delta \log B$.

With $\Delta \log P = 1{\cdot}6$ (P increasing from $2\frac{1}{2}$ to 100 days), $\Delta \log L \approx 1{\cdot}6$, and $q = 1{\cdot}0$, if $\Delta \log B$ is negative

$$7\Delta \log B < -4{\cdot}0, \qquad \Delta \log B < -0{\cdot}57,$$

or B decreases by a factor of more than $3{\cdot}7$ as P increases from $2\frac{1}{2}$ to 100 days.

With $q = 1{\cdot}18$ $\qquad 7\Delta \log B < -1{\cdot}4, \qquad \Delta \log B < -0{\cdot}2,$

or B decreases by a factor of more than $1{\cdot}6$. Thus as P increases from $2\frac{1}{2}$ to100 days B decreases by a factor between $1{\cdot}6$ and $3{\cdot}7$. This suggests that convective transport of energy becomes more important as the period shortens. Epstein has shown (**6**) that B decreases by a factor $2{\cdot}5$ as the effective polytropic index n_{eff} increases from $1{\cdot}5$ to 4; this seems to be about the largest probable increase, and if that is the case then with $q \leqslant 1{\cdot}18$ it follows that

$$\Delta \log A + k\Delta \log \mu \leqslant 1{\cdot}4,$$

or the increase in luminosity due to increasing central concentration (A) and increasing molecular weight is by less than a factor of 25. If the luminosity increases with radius so that m is positive, $\Delta \log A + k\Delta \log \mu$ becomes smaller still. An increase in μ implies a decrease in X and sometimes an increase in Z. With n in the range 0 to -1, $Z^n(1 + X)^{-1}$ may increase or decrease; but the change is almost certainly fairly small as there is no evidence of large differences in Z along the cepheid sequence and n is probably close to zero.

The alternative of $\Delta \log B$ positive would imply (with $k = 4$ for electron-scattering models) $\qquad \Delta \log A + 4\Delta \log \mu < -4{\cdot}0.$

μ is unlikely to decrease more than by a factor 3/8 (all He to all H) so that

$$\Delta \log A < -2{\cdot}3$$

An increase in B would imply an even larger decrease in A than this factor of more than 200. Such large changes in A and μ suggest enormous differences in the structure, composition and masses of the cepheids along the sequence, and do not appear to be as probable as the comparatively small changes which result from assuming that B decreases as P increases.

A decrease in B by a factor between 1·6 and 2·5 implies an increase in effective polytropic index (**6**) of between 1·3 and 2·5. The larger increase would imply an increase in central concentration which would largely offset the effect of decreasing mean density to give similar central densities along the sequence of cepheids. If that is the case, the connection between variability and particular central conditions would suggest that the onset of degeneracy may be a cause of pulsation. But changes in central concentration determined from the above equations depend critically on q through n_{eff} and B, and the figures merely suggest a possibility.

The problem now to be considered is the effect on the period-luminosity relation of a change in the composition of the matter from which the cepheids are formed.

At the low densities which exist in these extended stars, the opacity is due to electron scattering except in the outer layers which contain only a small proportion of the mass and have little effect on the luminosity. Hence in equation (1) $n \sim 0$ and $k \sim 4$.

Now $\mu = 4/(5X+3)$ for small Z, and if a fraction Q of the mass of a star is contained in a hydrogen-exhausted core, and X was the hydrogen abundance in the gas from which the star formed and is equal to the value in the envelope of the star, then writing $q = (1-Q)^{-1}$ we have

$$\Delta\left(k \log \bar{\mu} - \log\left(1+\bar{X}\right)\right) = -0{\cdot}43\left\{4/(X+0{\cdot}6q) - 1/(X+q)\right\} dX, \qquad (7)$$

where bars denote present mean values in the star. Thus the displacement of the period-luminosity relation in bolometric magnitude resulting directly from a change in the initial composition of the stars is

$$\Delta M_{\text{bol}} = 1{\cdot}1\left\{4/(X+0{\cdot}6q) - 1/(X+q)\right\} dX. \qquad (8)$$

An increase in the molecular weight of the matter from which the variables are formed means that the ratio of the molecular weight in the envelope to that in the hydrogen-exhausted core will be increased and the radius will decrease (**4**). Thus the period will shorten, $\Delta \log P$ will be negative and the displacement of the period-luminosity relation will be increased.* The surface temperature will rise

* It may be that variability occurs at different stages in the evolution of stars of different mass. Any change in the composition of the envelope may change the stage at which pulsation occurs. If pulsation occurs before maximum extension of the radius, it may be that an increase in the molecular weight in the envelope (which will cause it to contract) will retard the stage at which pulsation takes place to the point where more of the core has been burned out and the resulting further expansion of the envelope produces a similar distribution of gravitational potential energy to that which would have existed at the pulsation stage had the composition of the envelope not been changed. The overall molecular weight, and the luminosity, will have been increased still further; provided the envelope is not *more* extended at the pulsation stage as a result of the change in composition (this is evidently unlikely) the preceding equations will remain valid. Conversely, if pulsation occurs after maximum extension of the radius, the stage at which pulsation occurs may be advanced. Proper consideration of this matter will have to await a more complete knowledge of the structure of cepheids.

and the star will become photographically brighter on that account, i.e. $\Delta M_{pg} > \Delta M_{bol}$.

Any increase in the abundance of heavy elements besides helium accompanying the decrease of hydrogen abundance would affect the effective radius of the star and the depth of the outer convective region (and thus the effective polytropic index of the star). Hoyle and Schwarzschild have considered such an effect in Population II red giants (**7**). An increase in the opacity in the outer layers due to increased abundance of heavy elements would have little effect on the luminosity but would tend to raise the photosphere to a higher level. With constant luminosity $L = R^2 T_e^4$ requires that $T \propto R^{-1/2}$ in the outer layers; but T falls off more quickly than this. Consequently the surface temperature would fall too quickly as the photosphere was raised and the star would be unable to radiate the energy coming from below. The density of the outer layers must decrease to allow radiation to escape from deeper in the star—that is to say the effective polytropic index would increase. The constant B in equation (2) would decrease and the period shorten. The luminosity would decrease slightly and the radius increase somewhat. In the case of polytropes, both uniform and composite, the effect on the period of the change in B usually outweighs the opposite effect of the change in radius, and the difference is enhanced by the fact that the outer half of the star is most important in determining B (**6**). Although the cepheids will differ in structure from simple polytrope models it is likely that these changes will be similar in effect. The effect of an increase in heavy elements accompanying an increase in helium content would therefore probably increase rather than decrease the displacement given by equation (8).

The conclusion is therefore reached that if the period-luminosity relations of two groups of cepheids differ in magnitude by ΔM_{pg}, the maximum difference of the hydrogen abundances in the material out of which these stars condensed is given by the inequality

$$\{4/(X + 0{\cdot}6q) - 1/(X + q)\}\, dX < 0{\cdot}9\, \Delta M_{pg}, \qquad (9)$$

where q is probably about 2, ($Q \sim \frac{1}{2}$).

With a maximum difference of 0·25 in M_{pg} between the cepheids near the centre and those half way to the edge of M31, the corresponding maximum difference in hydrogen abundances is 15 per cent.

Department of Astronomy,
University of Edinburgh:
1956 *March* 9.

References

(1) W. Baade and H. H. Swope, *A. J.*, **60**, 151, 1955.
(2) W. Baade, I.A.U. Commission 28, 1955.
(3) C. W. Allen, *Astrophysical Quantities*, p. 190, London, 1955.
(4) C. M. Bondi and H. Bondi, *M.N.*, **110**, 287, 1950; *ibid.*, **111**, 397, 1951.
(5) C. W. Allen, *Astrophysical Quantities*, p. 184, London, 1955.
(6) I. Epstein, *Ap. J.*, **112**, 6, 1950.
(7) F. Hoyle and M. Schwarzschild, *Ap. J.*, Supplement II, 1, 1955.

THE SYSTEM OF p VELORUM

David S. Evans

(Communicated by H.M. Astronomer at the Cape)

(Received 1956 May 16)

Summary

The star p Velorum is a visual binary, one component of which is a spectroscopic binary. In a period of four years, commencing at the beginning of 1952, a total of 56 spectra has been obtained with the Cassegrain spectrograph attached to the Radcliffe reflector. The measures by the author have been combined with the earlier observations by Sanford. Using the solution for the visual orbit given by van den Bos, it has proved possible to eliminate the effects of motion in the visual orbit from velocity observations of the spectroscopic binary. A new solution for the spectroscopic orbit is obtained. Three equations are obtained giving the values for the individual masses in terms of the parallax. Using spectra obtained at epochs of large velocity difference the spectral types of the components of the spectroscopic binary are estimated. Microphotometer tracings of all suitable spectra have been examined in an attempt to detect lines due to the visual companion. The failure of this attempt enables the spectral type of the visual companion to be estimated. The spectroscopic data are compared with the photometric observations of colour and magnitude obtained at the Cape. A value for the parallax not inconsistent with the trigonometrical and spectroscopic results is adopted and the masses of the individual stars inferred. There seems no escape from the conclusion that the visual companion, the most massive of the three components, is markedly under-luminous.

Introduction.—The star, p Velorum, R.A., $10^h\ 33^m.1$, Declination, $-47°42'$ (1900), is a close visual binary, for which an orbit has been given by van den Bos (**1**), (**2**). He quotes the magnitudes as 4·49 and 5·3, the spectral types as F2, A3, finds a period of 16·00 years, a semi-axis major of $0''.316$ and an eccentricity of 0·70. The spectrum shows the characteristics of a spectroscopic binary, and, as long ago as 1918, Sanford (**3**), found a period of 10·210955 days and an eccentricity in the spectroscopic orbit of 0·541. The system is, therefore, a triple one, with one component of the visual binary itself a spectroscopic binary. In his analysis, Sanford failed to take account of the variation in the velocity of the centre of gravity of the spectroscopic binary due to motion in the visual orbit, and, as van den Bos has pointed out, this variation is too large to be negligible, so that new observations and a fresh discussion became desirable. Sanford mentions the existence of the visual companion, but, lest it be thought that the foregoing remarks imply any criticism of him, it should be stated at once that he was the victim of a double observational coincidence. The two observations of the visual double then available were 18 years apart, which is so nearly the visual period that there had, apparently, been only a small change in relative position during this interval. His radial velocity observations fell into two groups, one near 1905 with a three-prism spectrograph, the other near 1914 with a two-prism instrument.

At both epochs the velocity corrections for motion in the visual orbit chanced to be rather small. Sanford did find a fairly small systematic difference between the two groups of velocities, but he evidently put it down to systematic differences between the two spectrographs, and applied a correction of −2·84 km/sec to correct the second group to the first. In handling Sanford's results we now remove this correction.

As the result of the suggestion by Dr van den Bos, special attention has been paid to p Velorum in the radial velocity programme undertaken by

TABLE I

Sanford's Observations

Julian Date 2 400 000 +	Velocities P	Velocities S	*F*	Corrected Velocities P	Corrected Velocities S	Phase	Corr.	Wt.
Three-prism spectrograph								
16 463·845	+35·3	− 4	−0·347	+30·4	− 9	2590	− 4	2
16 517·853	+38·4	−10	−0·320	+33·9	−15	5486	− 4	2
16 846·797	+21·4		+0·560	+29·2		7651	− 5	2
16 871·744	+25·4		+0·665	+34·7		2084	− 4	2*
16 872·701	+39·2	− 6	+0·665	+48·5	+ 3	3021	− 4	2
17 605·861	+13·7		+0·388	+19·1		1074	+17	2
17 611·810	+33·3		+0·385	+38·7		6900	+17	2
17 613·714	+ 0·5		+0·385	+ 5·9		8765	+17	2
17 654·716	− 5·5		+0·367	− 0·4		8922	+18	2
Two-prism spectrograph								
20 120·837	+42·7		−0·147	+40·6		4225	+24	1
20 121·853	+39·3		−0·148	+37·2		5220	+24	1
20 122·851	+38·6		−0·148	+36·5		6198	+24	1
20 124·819	+27·3		−0·149	+25·2		8125	+24	1
20 128·804	+31·7		−0.149	+29·6		2028	+24	1
20 252·567	+40·7	− 8	−0·164	+38·4	−10	3241	+23	1
20 255·609	+40·7		−0·164	+38·4		6220	+23	1
20 257·465	+26·4		−0·165	+24·1		8038	+23	1
20 260·668	+20·2		−0·165	+17·9		1175	+23	1
20 261·671	+33·1		−0·165	+30·8		2157	+23	1
20 265·572	+41·4		−0·165	+39·1		5978	+23	1
20 266·612	+31·8		−0·165	+29·5		6996	+23	1
20 267·572	+24·9		−0·165	+22·6		7936	+23	1
20 270·596	+ 8·5		−0·166	+ 6·2		0898	+23	1
20 271·628	+26·0		−0·166	+23·7		1909	+23	1
20 272·506	+40·2		−0·166	+37·9		2769	+23	1
20 294·432	+44·3		−0·169	+41·9		4243	+23	1
20 296·522	+38·3		−0·170	+35·9		6200	+23	1
20 308·424	+27·8		−0·170	+25·4		7947	+23	1
20 309·451	− 1·8	+63	−0·170	− 4·2	+61	8952	+23	1
20 340·473	−17·3	+65	−0·175	−19·8	+63	9335	+23	1
20 349·469	+23·6		−0·175	+21·1		8146	+23	1
20 350·473	− 6·9	+64	−0·175	− 9·4	+62	9129	+23	1
20 351·462	−36·6	+83	−0·176	−39·1	+81	0098	+23	1
21 260·832	− 0·5		−0·290	− 4·6		0729	+13	1
21 280·760	−33·9	+87	−0·293	−38·0	+83	0246	+13	1
21 290·719	−40·4	+105	−0·295	−44·5	+101	0000	+13	1
21 321·662	−29·2	+85	−0·297	−33·4	+81	0305	+12	1

* Sanford regards this observation as uncertain.

TABLE II

The Cape Observations

Julian Date 2 400 000+	Velocities P	Velocities S	*F*	Corrected Velocities P	Corrected Velocities S	Phase	Corr.	Wt.
34 069·475	+27·2		−0·306	+22·9		5432	− 5	oc*
34 196·174	−23·1	+91·4	−0·145	−25·1	+89·4	9520	− 6	1a
34 351·592	+28·7		+0·460	+35·1		1735	− 5	1a
34 374·557	+39·2		+0·553	+46·9		4227	− 5	2a
34 427·433	+29·8		+0·734	+40·1		6014	− 3	4a
34 436·449	+32·9		+0·757	+43·5		4844	− 3	3a
34 448·365	+22·1		+0·783	+33·1		6514	− 2	2a
34 457·348	+30·8		+0·800	+42·0		5312	− 1	2a
34 475·280	+25·4		+0·822	+36·9		2875	− 1	2b
34 487·326	+27·7		+0·831	+39·3		4672	− 1	3a
34 499·293	+23·2		+0·835	+34·9		6393	0	4b
34 508·258	+27·6		+0·836	+39·3		5173	0	3b
34 519·221	+27·3		+0·836	+39·0		5910	0	3b
34 547·169	+26·6		+0·827	+38·2		3282	+ 1	1b
34 740·527	+24·7		+0·661	+34·0		2656	+ 8	2b
34 755·569	+21·0		+0·647	+30·1		7388	+ 8	2b
34 770·498	+24·8		+0·634	+33·7		2009	+ 9	2b
34 788·495	−37·6	+74·2	+0·618	−28·9	+82·9	9635	+ 9	2b
34 791·466	+26·1		+0·614	+34·7		2545	+ 9	2b
35 108·582	+24·7		+0·402	+30·3		3127	+17	1b
35 123·584	+20·5		+0·396	+26·0		7819	+17	1b
35 156·423	−42·4	+90·8	+0·380	−37·1	+96·1	9982	+18	1b
35 171·366	+31·9		+0·374	+37·1		4617	+18	1b
35 191·290	+32·9		+0·363	+38·0		4130	+18	1b
35 191·453	+24·8		+0·363	+29·9		4290	+18	1b
35 196·272	− 6·2		+0·361	− 1·1		9010	+18	1b
35 196·365	−16·2	+58·7	+0·361	−11·1	+63·8	9101	+18	1b
35 196·471	−17·4	+71·2	+0·361	−12·3	+76·3	9205	+18	1b
35 441·595	−15·0	+69·3	+0·268	−11·2	+73·1	9277	+21	1b
35 483·538	−30·2	+82·3	+0·252	−26·7	+87·8	0356	+22	4b

* This observation was obtained with the "c" camera, *f*/3·7, giving a dispersion of 50 A/mm. It is discordant and is omitted from the discussion.

the Cape Observatory using the equipment of the Radcliffe Observatory, Pretoria.

The observations.—Tables I and II above give complete schedules of the observed radial velocities. In the case of Sanford's observations, results from the three-prism spectrograph are counted with double weight. The high resolution of this instrument, which had a dispersion of 10·4 A/mm at Hγ (**4**), enabled him to resolve the stellar lines near the minor maximum of the velocity difference between the components of the spectroscopic binary. This has not been possible with the two-prism Pretoria instrument. The Pretoria spectra have been taken either with the "a" camera, *f*/8, giving a dispersion of 21 A/mm at Hγ, or with the "b" camera, *f*/6, giving 29 A/mm (**5**). Spectra on each of these dispersions have been given unit weight.

Comments on the tables.—The results used in Table I are extracted from Sanford's paper, and have been changed only by the removal of the systematic correction which he applied. The velocities in this form are given in the second

and third columns of the table. In Table II are the Cape results, all the measures being by the author. A discussion of the systematic errors of the Cape radial velocities, to be published elsewhere, indicates that, to correct velocities measured by D. S. E. to the Lick three-prism system, the following corrections should be applied: "a" camera, +1·7 km/sec; "b" camera, +0·7 km/sec. These corrections have already been applied to the data exhibited in Table II. It frequently happened that several spectra of p Velorum were obtained on one plate. In such a case a mean result for the several spectra has been used. This is indicated in the last column of Table II, where a designation such as 3b indicates the mean from three "b" camera spectra. Means have not been taken when the velocities were changing rapidly.

It will be noted that the modern observations do not agree as they stand with those of Sanford. This is interpreted as being due to orbital motion in the visual orbit. The two sets of observations are capable of being reconciled within the observational uncertainties in the following way. Van den Bos (**2**) has given a table of the function pV, p being the parallax in seconds of arc, and V the radial velocity in km/sec of one component relative to the other in the visual orbit. For the epoch of each radial velocity observation the corresponding value of pV can be found by interpolation from van den Bos' table. These are the values denoted by F which appear in the fourth columns of Tables I and II. The upper signs in van den Bos' table have been used throughout. By trial and error some multiple of these numbers, F, must be found, so that when these multiples of F are applied to the observed velocities, the old and the new values agree. At the same time the period must be redetermined on the basis of all the available observations. The solution was reached by trial and error. The period is very closely determined from the epochs of large velocity difference. Adopting the period so determined the phases can be computed and a first value of the multiplier of F which best reconciles the old and new observations can be found. Application of these corrections leads to changes in the velocities near maximum velocity difference, requiring a slight revision of the period, followed by a slight revision of the value of the multiplier. These procedures lead to a value for the period of 10·21040 days (compared with Sanford's value of 10·210955 days) and the phases given in the seventh column are computed using this period and the epoch J.D. 2421290·719 as corresponding to zero phase. The period is not introduced as an unknown in the computations which follow. The value of the factor adopted in the correction for motion in the visual orbit is +14. It is not very closely determined, but it is thought that it could not be in error by as much as 20 per cent either way. Certainly values of +12 and +16 when tried gave an accordance noticably worse than the value adopted. The corrected velocities in the fifth and sixth columns are the values obtained after the application of this correction. The element which has been removed is the velocity of the centre of gravity of the spectroscopic binary relative to the centre of gravity of the triple system. If we assume for the present (the opposite assumption will be discussed later) that the spectroscopic binary is the visual primary, then the fact that the correction factor is positive identifies 43° as the longitude of the *ascending* node in the visual orbit. Moreover, we clearly have the relation

$$\frac{1}{p}\,\frac{m_3}{m_1+m_2+m_3} = 14 \qquad (1)$$

where m_1 and m_2 are the masses of the spectroscopic components, and m_3 the mass of the visual companion.

The data of Tables I and II with these corrections applied are plotted in Fig. 1. The probable error of a single observation is usually between 1·0 and 1·5 km/sec, and, since the observations are numerous, one or two deviations from the mean which amount to several times the standard error occur, but the consistency is quite in accord with the usual statistical behaviour of radial velocity measures.

From this figure it will be seen that there are parts of the empirical velocity curves where the velocity difference between the components is changing at the rate of roughly 6 km/sec per hour. With a trigonometric parallax according to the Yale Catalogue of $0''{\cdot}033 \pm 0''{\cdot}007$ and a semi-axis major in the visual orbit of $0''{\cdot}316$ according to van den Bos (**1**) the light-time across the relative visual orbit approximates to $2\frac{1}{2}$ hours. The light-time from the centre of gravity of the spectroscopic system to the plane though the centre of gravity of the triple system parallel to the plane of the sky is some fraction of this, but is not so small as to be negligible on the steeper parts of the velocity curves. I am indebted to the kindness of Dr van den Bos for providing a correction curve for this effect. The scale of this curve is determined by the empirical relation of equation (1) for the same combination of symbols occurs in the formulae. The total range of light-time involved is 50 minutes. From Dr van den Bos' curve the corrections of Column 8 in the tables are derived. These are corrections to the phases in units of the fourth place of decimals.

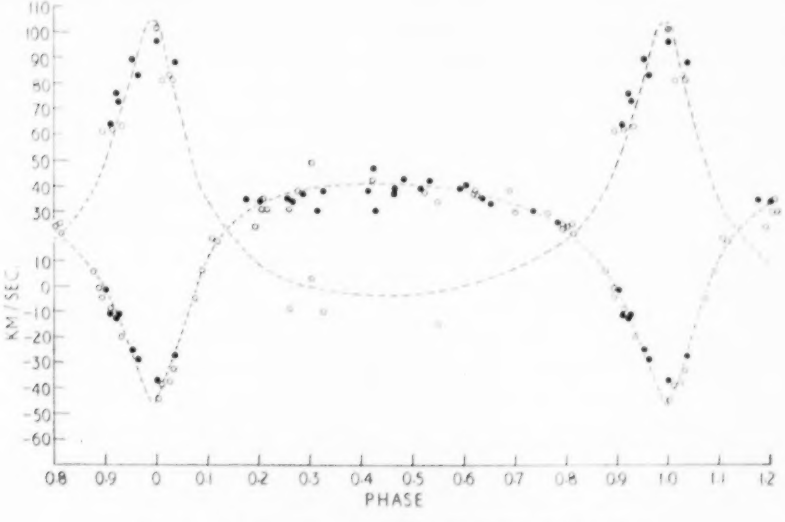

FIG. 1.—*Observed velocities corrected for motion in visual orbit*
○ : *Sanford*
● : *Cape*

The determination of the elements.—The following table gives the normal points used in the solution for the elements of the primary. The corrections to velocities and phases described above are included.

TABLE III

Normal Points

Phase (ϕ)	Observed Velocity	Computed Velocity	Residuals O−C	No. of Observations
1005	+11·54	+11·25	+0·29	5
2011	+32·00	+31·53	+0·47	8
2848	+36·70	+37·53	−0·83	14
4236	+40·70	+40·54	+0·16	6
5035	+39·49	+40·14	−0·65	15
6142	+37·79	+37·43	+0·36	15
6953	+33·33	+33·35	−0·02	7
7930	+25·35	+24·06	+1·29	8
8908	+ 0·95	+ 2·37	−1·42	6
9369	−18·34	−18·95	+0·61	8
0247	−33·21	−32·98	−0·23	9

The computed velocities are derived from the final elements given below. They were obtained by the customary least-squares procedure for the derivation of corrections to the initial elements stated. The value of γ found from the least squares solution has been increased by 0·03 km/sec to give the adopted final value. In carrying out the solution it was found best, after some trials, to give each of the normal points the same weight. The strictly correct statistical procedure produces a solution which passes very exactly through the normal points near phase 0·5 at the expense of rather large residuals for the points near zero phase. Since the former group exercises much less influence on the determination of the elements than the latter does, given the large eccentricity and the orientation of the orbit, the policy of uniform weights seemed best, even though the formal probable errors of the solution are probably somewhat increased in consequence.

TABLE IV

Solution : Primary

	Initial	Final	Sanford
γ	+21·22 km/sec	+21·30 km/sec	+19·25 km/sec
K	42·70 km/sec	+43·33 ± 0·76 km/sec	+42·34 km/sec
e	0·56	0·5597 ± 0·0088	0·541
ω	186°	187°·32 ± 0°·71	184°·62
ϕ_0	−0·0044	−0·0017 ± 0·0010	
	equivalent to J.D.	2 420 259·452	2 420 259·381
P		10·21040 days	10·210955
$a \sin i$		$5{\cdot}042 \times 10^6$ km	$4{\cdot}981 \times 10^6$ km
$m \sin^3 i$		0·304 × sun	0·281 × sun

The average probable error of a single radial velocity observation of unit weight is ± 2·0 km/sec. The formal probable errors deduced from the interagreement of lines for the Radcliffe plates range from ± 0·7 km/sec to ± 2·1 km/sec. Phases in our solution are computed from the arbitrary epoch J.D. 2 421 290·719 and ϕ_0 denotes the phase of periastron passage in this system.

For the spectroscopic secondary we merely have to find that value of K', ω being increased by 180°, which fits the observations best. As Sanford remarked in his paper he found some discrepancies, and we naturally meet difficulties of the same type. The best value of K' is 53·6 km/sec. This is the value which makes the sum of the squares of the residuals, " Observed *minus* Calculated ", a minimum.

The value which makes the sum of the residuals, with their proper signs, zero, is 52·2 km/sec. If, from Tables I and II, we extract the observations of the secondary in order as given there, we have the following table of residuals and data for the secondary.

TABLE V

Data for spectroscopic secondary

Residuals: Observed *minus* Calculated

Sanford's Observations	Cape Observations
−16·7	+ 7·5
−13·9	− 8·9
+ 2·7	− 7·7
− 9·3	+ 8·6
+13·2	+15·0
− 7·3	+ 7·0
+ 5·0	+11·3
−17·2	
− 4·3	
− 2·4	
− 1·1	

Elements

	Sanford's values
K' = 53·6 km/sec	52 km/sec
$a \sin i$ = 6·237 × 10^6 km	6·107 × 10^6 km
$m \sin^3 i$ = 0·245 ☉	0·235 ☉

The foregoing tables constitute the ordinary solution of the spectroscopic orbit. The probable errors of the elements are rather disappointingly large, but there seems no point in attempting a closer fit. In any case, as can be seen, a high formal accuracy does not necessarily imply that the solution will give correct predictions. So far as this solution goes we can probably assume quite safely that the mass ratio in the spectroscopic primary could not possibly be in error by as much as 10 per cent, while the figure in equation (1) can hardly be as much as 20 per cent in error.

Discussion of the components of the triple system.—It was initially hoped to discover from the spectrograms evidence of the spectrum of the third star, the visual companion, and, to that end all suitable plates were put through the Radcliffe microphotometer. Special attention was paid to the Balmer lines in the hope that a careful study at different phases of the spectroscopic binary might lead to a determination of the relative positions of the lines of the third star, and thus to a velocity measurement and a parallax determination. This hope has not been realised. A careful study of the spectra and tracings has failed to show any metallic lines due to the visual companion. However, this negative result allows us to make a positive deduction concerning the spectrum of the companion. The spectroscopic secondary has a spectrum rather similar to the spectroscopic primary, and, speaking at this stage, roughly, must be of the order of one magnitude fainter than the primary. The visual secondary is roughly half a magnitude to one magnitude fainter than the visual primary. In other words, the visual companion must be intermediate in brightness between the other two stars, and, if it had a spectrum containing strong metallic lines, or if it were similar to the spectra of the other two stars, we should have no difficulty in detecting it. The only possible solution would seem to be to designate the visual

companion as an early A-type dwarf, the spectrum of which consists of nothing but broad hydrogen and calcium lines which are too broad to be distinguished in the joint spectrum. The joint spectrum does have broad hydrogen lines—a fact noted so long ago as the compilation of the Henry Draper Catalogue—and these we ascribe to the visual secondary. The hydrogen lines of the other two stars appear as narrow absorptions, readily separable at high velocity differences, on top of these broad lines.

The spectra at maximum velocity difference have been classified according to the MK system (**6**), a task of some difficulty in view of their complexity. What emerges is that the two components of the spectroscopic binary are of nearly the same spectral class with the fainter, possibly, very slightly the earlier and the brighter, one luminosity class higher than the fainter. It does not seem possible for the types to be earlier than F3 or later than F5. Provisionally they are denoted as F3 – 5 IV and F3 – 5 V. In terms of a calibration to be published elsewhere, we have, on the *S* system for stars on this part of the Russell–Hertzsprung diagram, absolute magnitudes near +2·5 and +3·5 and colours near +0·12 and +0·17 for these stars. These values of the magnitudes give for the spectroscopic pair together the absolute magnitude of 2·14. The visual companion is certainly fainter than the primary by an amount variously quoted as 0·5 and 0·8 magnitudes. If we take a value of 0·65 the absolute magnitude of the companion is +2·79. The observed joint colour of all three is +0·02, so that the colour index of the companion on this set of assumptions must be −0·21, the colour of an A0 V star. If the difference is taken as 0·5 magnitudes, the companion must have absolute magnitude 2·64 and colour −0·19, which is that of an A1 V star.

The result of this discussion is more closely determined than the uncertainties of the data might suggest. The components of the spectroscopic binary certainly have positive colour indices. The visual companion is fainter than the primary and the joint colour index is small and positive. Hence the visual secondary must have a negative colour index, which is what we infer both from this argument and from the appearance of the joint spectrum. The relative luminosities of the components of the spectroscopic binary are also fixed within limits, at roughly the value adopted, by the observed line-strengths in the two spectra. An important consequence of this discussion is that the visual companion is under-luminous for its type, according to the foregoing figures, by about a magnitude and a half.

It might seem more plausible to make the visual secondary the spectroscopic binary to avoid this conclusion of under-luminosity. Taking rough figures we may argue the hypothesis through as follows:—The magnitude difference between primary and secondary (visual) is, say, half a magnitude. The difference between the two components of the spectroscopic pair is one magnitude. If the visual primary is of magnitude +2·0, the visual secondary is +2·5, and this now being assumed to be the spectroscopic binary is composed of stars of magnitudes +2·9 and +3·9. The two brighter stars are together equivalent to a star of about magnitude +1·5. The lines of the spectroscopic companion are therefore seen against a total light from other sources of a star of this magnitude, and the minimum possible residual intensity even for a perfectly black line is over 90 per cent. This does not seem to accord with the fact that the lines of the secondary are, though fairly faint, perfectly easily visible in the joint spectrum.

We therefore are confirmed in our original assumption that the visual primary is the spectroscopic binary and we have in consequence the following system of data:

Spectroscopic pair

F3 – 5 IV $M = 2{\cdot}5$, $C.I. = +0{\cdot}12$

F3 – 5 V $M = 3{\cdot}5$, $C.I. = +0{\cdot}17$

Visual companion

A0 – 1 V $M = 2{\cdot}7$, $C.I. = -0{\cdot}2$

Total joint $M = +1{\cdot}65$

Observed $m = +3{\cdot}89$, observed $C.I. = +0{\cdot}02$

Spectroscopic parallax = 0″·036, from above data.

Trigonometric parallax = 0″·033, from Yale Catalogue.

If we adopt a value of 0″·035 for the parallax we have, from equation (1),

$$0{\cdot}51\ m_3 = 0{\cdot}49\ (m_1 + m_2)$$

and from the spectroscopic solution:—

$$m_1/m_2 = 0{\cdot}304/0{\cdot}245 = 1{\cdot}241.$$

Van den Bos' data give,

$$m_1 + m_2 + m_3 = (0{\cdot}316)^3/(0{\cdot}035)^3(16{\cdot}0)^2 = 2{\cdot}875.$$

These lead to the following values for the massest:—

$$m_1 = 0{\cdot}81 \quad m_2 = 0{\cdot}65 \quad m_3 = 1{\cdot}41,$$

and thence we have easily the values of sin i in the spectroscopic orbit, and of the semi-axes major of the orbits of the spectroscopic components.

Two points should, however, strike the reader. One is that the deduced values of the masses are rather low: the other is that the whole of the foregoing argument depends on the adopted value for the parallax in a rather sensitive way. Values which are quite indistinguishable in the field of trigonometric determinations of parallax produce a considerable change in the mass values. Even the method of spectroscopic parallaxes is not quite definitive enough. If we leave the parallax disposable and write $10p = 1/X$, we can express the masses in terms of X:

$$m_1 = 0{\cdot}0682X^3 - 0{\cdot}0959X^2$$
$$m_2 = 0{\cdot}0550X^3 - 0{\cdot}0772X^2$$
$$m_3 = 0{\cdot}1726X^2$$

giving the following system of values:

X	=	2·0	3·0	3·5	4·0
p	=	050	033	029	025
m_1	=	0·17	0·98	1·74	2·83
m_2	=	0·14	0·79	1·40	2·28
m_3	=	0·69	1·55	2·11	2·76

It is regrettable that we should have to exercise a choice, and the only method of avoiding this would be to find and measure the velocity of a narrow line or lines in the spectrum of the visual companion.

In seeking grounds on which the best choice of parallax may be based, we must first take note of an inescapable anomaly. The order of decreasing brightness of the stars is 1, 3, 2, but this is only the order of the inferred masses for values of

X from about 4·0 to 5·0. Thus the mass luminosity relation is certainly not satisfied by all the stars outside this range. Inside this range the assumption that they all satisfy the mass-luminosity relation leads to a contradiction. For example, take $X = 4{\cdot}0$. The bolometric magnitudes of the components inferred from the mass-luminosity relation are about $+0{\cdot}5$, $+1{\cdot}4$, $+0{\cdot}5$, which when combined and compared with the apparent bolometric magnitude give a parallax corresponding to $X = 6$.

If we decide that the one star which, according to current ideas, ought to satisfy the mass-luminosity relation, does in fact do so, we can obtain a very precise values of the parallax. This is the F3 – 5 V star. For it we have

$$M_{\text{bol}} = 5 - 10 \log (\text{mass}) = m_{\text{bol}} - 5 \log X$$

or, using the expression for the mass derived above

$$0{\cdot}5 - 0{\cdot}1\, m_{\text{bol}} = (3/2) \log X + \log (0{\cdot}0550\, X - 0{\cdot}0772).$$

The value of X which satisfies this equation depends on estimating the apparent bolometric magnitude of star No 2, but is not critically dependent on the value adopted. If we take $m_{\text{bol}} = 5{\cdot}7$ we have $X = 3{\cdot}6$. Slightly varying assumptions as to the magnitude differences between the components permit small variations in this value, up to about 0·1. We end by adopting $X = 3{\cdot}5$, corresponding to a parallax of 0″·029. If we maintain the magnitude difference between the Class V and Class IV stars at exactly 1·0 magnitudes this decision gives a total absolute magnitude for the system of $+1{\cdot}20$, and absolute magnitudes (photographic) for the components of 2·0, 3·0, and 2·2. On the other hand, as is explained in the following paper, an alternative is to hold star No 2 strictly on the main sequence and to solve for the magnitude difference as an unknown. The data do in fact hang together so well that this does not make differences which are important from the standpoint of the location of the stars on the Hertzsprung–Russell diagram. Adoption of 0″·029 for the parallax gives, for the spectroscopic pair, $i = 34^{\circ}00'$, $a_1 = 9{\cdot}02 \times 10^6$ km, $a_2 = 11{\cdot}15 \times 10^6$ km.

Acknowledgments.—I am indebted to colleagues at the Cape, Radcliffe and Union Observatories for helpful discussion: most particularly to Dr van den Bos for drawing our attention to this system and for wise counsel in the treatment of the more involved difficulties, and to Dr Halton C. Arp for his help in discussing the photometric data.

Royal Observatory,
Cape of Good Hope :
1956 *April.*

References

(1) Union Observatory Circulars, Vol. 5, No. 109, 367, 1950.
(2) *Ibid.*, Vol. 6, No. 113, 214, 1953.
(3) *L.O.B.*, **9**, 181, 1918.
(4) *Lick Obs. Pub.*, **9**, 58, 1905.
(5) Feast, Thackeray and Wesselink, *Mem. R.A.S.*, **67**, Part II, 1955.
(6) H. L. Johnson and W. W. Morgan, *Ap. J.*, **117**, 313, 1953.

p VELORUM AND STELLAR EVOLUTION

Halton C. Arp and David S. Evans

(Communicated by H.M. Astronomer at the Cape)

(Received 1956 May 16)

Summary

The data derived for p Velorum are in good agreement with the present theory of stellar evolution. The age of the system is about 10^8 years. It is concluded that, in that time, the faintest component has remained essentially unchanged, the brightest component has completed the first stage of its evolution, and the most massive component has advanced far in its evolution. The position of this third component on the Hertzsprung–Russell diagram is an indication of the probable course of the late stages of evolution of stars of this type.

Introduction.—The data for p Velorum deduced in the preceding paper are unusually complete, and provide an opportunity for discussion from the evolutionary standpoint. Two of the component stars lie off the main sequence and their masses do not satisfy the mass–luminosity relation. Present evolutionary theory demands just such divergences, and p Velorum provides an opportunity for observational test of the theory by comparison with data for a group of stars which have a common age.

Observed and derived parameters.—The data for the three components are listed in Table I. Photometric data have been converted from the 1953 *S* system used in the preceding paper to the *B*, *V* system. To the accuracy needed for this discussion this means that corrections of +0·2 have been applied to the magnitudes, +0·24 to the F star colours and +0·28 to the A star colour. The step which

TABLE I

	Adopted parallax : 0″·029 Star No. 1	Joint $M_V = +1{\cdot}12$ Star No. 2	Joint $B-V = +0{\cdot}28$ Star No. 3
Mass	1·74 ± 0·08	1·40	2·11 ± 0·40
M_V	1·90 ± 0·1	3·30 ± 0·3	2·40 ± 0·2
$B-V$	+0·37 ± 0·03	+0·41 ± 0·03	+0·06 ± 0·05
Sp	F3–5 IV	F3–5 V	(A)

fixes the masses given in this table is the choice of 0″·029 for the parallax. This point has been discussed at length in the preceding paper. It is the choice which puts the F3 – 5 V star in the position where it ought to lie on the Hertzsprung–Russell diagram, that is on the main sequence. The main sequence chosen is the main sequence for unevolved stars in galactic clusters determined by Johnson (**1**). The colour of star No. 1 was then chosen as that of an F3 – 5 IV star, and the difference in visual magnitude between star No. 3 and Nos. 1 and 2 together was chosen as 0·8 magnitudes. A solution is then made for the absolute visual magnitudes of Nos. 1 and 3 and for the colour of No. 3.

In Fig. 1, the filled circles represent the present positions of the stars on the absolute magnitude–colour diagram. The two open circles represent the positions on the main sequence from which stars Nos. 1 and 3 must have come if they have evolved without appreciable change of mass. Lines through these points show the range of uncertainty which represents the lack of definition of the empirical mass–luminosity relation over small segments.

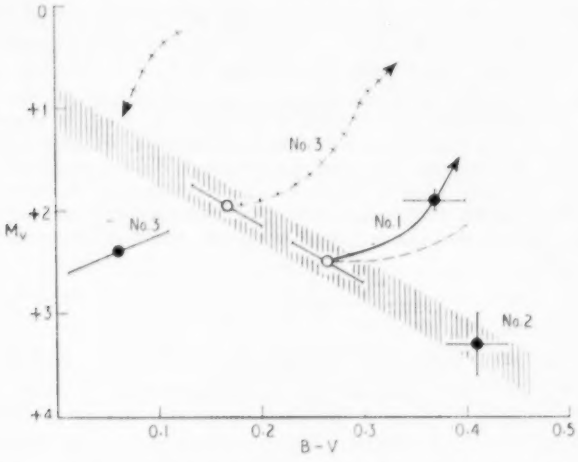

FIG. 1.—*The components of p Velorum on the Hertzsprung–Russell diagram.*
○ : *original positions.*
● : *present positions.*
Estimated limits of data indicated by horizontal and vertical lines.

Accuracy of the parameters.—The uncertainties associated with the quantities listed in Table I were estimated in the following way: the adopted parallax fixes the mass of star No. 2. The uncertainty in the mass of No. 1 is then the uncertainty of the ratio, K/K', of the velocity ranges in the previous paper, and this is fairly exactly known, whereas mass No. 3 comes from equation (1) of the previous paper, and the right-hand side might be uncertain by as much as 20 per cent. The accuracy with which star No. 2 may be placed, in absolute magnitude, on the main sequence, from its spectral class is estimated as $\pm 0{\cdot}3$ magnitudes. The uncertainties in the $B-V$ values correspond to the uncertainties in spectral classification.

Since No. 2 is the faintest of the three stars, the derived magnitudes of Nos. 1 and 3 are relatively insensitive to any error in the adopted magnitude of No. 2. The colour derived for No. 3 depends primarily on the adopted value of the magnitude difference between the visual primary and secondary. Van den Bos estimates that the difference is 0·8 and that it cannot lie outside the range from 0·5 to 1·0 magnitudes. In Fig. 1, the diagonal line drawn through the plotted position of No. 3 represents the range of solutions corresponding to the extreme assumptions of 0·6 and 1·0 magnitudes difference. The estimated uncertainties of placing the remaining two stars on the diagram of Fig. 1 are shown by the lines through them.

It should be emphasized that, although uncertainties exist, they are not so great as to cause any significant uncertainty in the place of the stars in the colour–absolute magnitude diagram.

In addition there is a check afforded by the spectrographic observations. Spectroscopically No. 1 is a luminosity class IV star and also, from the relative line strengths on the microphotometer tracings, a little more than a magnitude brighter than No. 2. No. 3 has broad hydrogen lines and metal lines which are either absent or very weak. In the preceding paper a solution was made, not on the assumption that No. 2 was a main sequence star, but instead on the assumption of 1·0 magnitude difference between No. 1 and No. 2. The derived magnitude of No. 2 agrees with the value used here within a few tenths of a magnitude.

It may be remarked that p Velorum lies at galactic latitude $+10°$ roughly in the direction of η Carinae. At a distance of only 35 parsecs, however, it is presumed to be unreddened.

Evolution.—A star, initially on the main sequence and chemically homogeneous, does not alter its luminosity or effective temperature rapidly until an appreciable proportion of the hydrogen in its interior has been transmuted into heavier elements. Schönberg and Chandrasekhar (**2**) have shown that the star then begins to evolve in one of two ways.

In the case where the diminution of hydrogen in the interior halts convection, the hydrogen-exhausted core is isothermal, and the star brightens by about one magnitude remaining at about the same effective surface temperature. It thereafter goes on to more rapid evolution through non-equilibrium configurations. In terms of Fig. 1, this type of evolution means a movement away from the initial position on the main sequence in an upward direction. This case has been applied by Sandage and Schwarzschild (**3**) and Sandage (**4**) to stars in globular clusters which are initially fainter than absolute magnitude +4. It is evident that this case does not apply to p Velorum, for, although star No. 1 has not become brighter by as much as a magnitude, it has become considerably redder.

In the case in which the stellar core remains convective, the luminosity increases somewhat in the early stages of evolution, but the radius increases rapidly, so that the predominant change is reddening of the star. This case fits the observed position of star No. 1 very well. During the time in which the ratio of the mean molecular weight inside the core to the mean molecular weight in the rest of the star increases from 1 to 2, the luminosity increases by a factor 1·41, and the effective temperature at the surface decreases by a factor 1·18. The actual evolutionary path of star No. 1 is roughly indicated by the solid line in Fig. 1. The dashed line immediately beneath it represents the approximate path computed by Schönberg and Chandrasekhar, and terminates at the above-mentioned limit. Schönberg and Chandrasekhar point out, however, that in a real star the reduction of the hydrogen content of the core will cause the central temperature to rise, and hence counteract the tendency of the radius to increase. They predict that the actual path should be similar to the dashed line in Fig. 1, but should lie somewhat above it. Roy (**5**) computes a similar initial evolutionary path. Since this corresponds closely with the observed path, the observational data for p Velorum confirm rather exactly the predictions of the theory for stars with initially convective cores.

It should be noted that this does not necessarily imply that stars of fainter absolute magnitude do not evolve by way of the initially isothermal core case. The rapidity of mixing would be expected to increase with the initial brightness of the star.

Since convection is impossible in an exhausted core, the growth of such a core slows and finally stops convection. The star then goes over to the isothermal core evolution and thereafter the principal change is an increase in luminosity. Although star No. 1 has, apparently, started its evolution with a convective core, it is not possible to decide whether it has yet gone over to the isothermal core case. For this star, an increase in luminosity by one magnitude from the initial conditions would bring it to $M_V = 1{\cdot}5$, and for the convective core case to something brighter than $M_V = 2{\cdot}1$. From the observed value, $M_V = 1{\cdot}9$, it is concluded that star No. 1 is approximately at the end of its initial evolutionary track in either case.

At the end of the initial evolutionary track, 12 per cent of the mass of the star is contained in the core (**3**). Placing star No. 1 at that limit enables us to compute the age of the system from the equation given by Sandage and Schwarzschild (**3**):

$$Lt = 0{\cdot}007c^2 X_c q_1 M. \qquad (1)$$

Taking the fraction of the mass in the core, $q_1 = 0{\cdot}12$, the abundance by weight of hydrogen outside the core, $X_c = 0{\cdot}596$, the mass of star No. 1, $M = 1{\cdot}74 \times$ Sun, and its initial luminosity, L, to correspond to an absolute bolometric magnitude of 2·4, we have

$$t \approx 1{\cdot}4 \times 10^9 \text{ years} = \text{age of p Velorum.}$$

This approximate age for the system enables us to compute an upper limit for the mass in the exhausted core of the main sequence star, No. 2. Since the evolution process proceeds faster as the star becomes brighter, the mass and luminosity of star No. 2 indicate that it must have less than 6 per cent of its mass in this core, and, possibly, considerably less than this. The star has thus not had enough time to evolve appreciably away from the main sequence because of its low luminosity. This is consistent with the original assumption that it still, in fact, lies on the main sequence.

Finally, star No. 3 may be discussed from the standpoint of its evolution. An observational extension of the theory now becomes possible from a consideration of this sub-luminous A star. In Fig. 1 the approximate initial path of its evolution is shown by the line of crosses, which is drawn approximately parallel to the observed path for star No. 1, taking into account the bolometric corrections necessary at these colour indices. The star rises from its initial position on the main sequence to about $M_V = +1$ at the Schönberg–Chandrasekhar limit. From this point onwards it must evolve rapidly. Its luminosity increases by a large factor while its effective temperature decreases somewhat. The beginning of this path, above $M_V = +1$ is roughly indicated by the extension, upwards and to the right, of the line of crosses in Fig. 1.

It is computed from equation (1) that this star requires 8×10^8 years to reach the Schönberg–Chandrasekhar limit. Hence only 6×10^8 years have been spent in the evolution through the upper parts of the colour–magnitude diagram down to its present position. This is in good agreement with the relative track times computed by Sandage (**3**) in the globular cluster M3.

Conclusions drawn from the observed colour–magnitude diagrams of globular clusters indicate that the stars in them reach $M_V = -3$ and $B-V = +1{\cdot}6$ in their evolutionary development. Thereafter they become less luminous and move toward bluer colour indices in the vicinity of the horizontal branch (region of $M_V = 0$ and $B-V = 0{\cdot}0$ to $0{\cdot}2$). Observations of globular cluster stars also indicate that, so far as those stars are concerned, the limit of evolution so far observed brings the stars to a region of the diagram lying to the left and below the region defined above. In M13 (**6**) the limit is in the region $M_V = +2{\cdot}5$ to $+3{\cdot}0$ and $B-V = -0{\cdot}4$.

Star No. 3 has, evidently, come down from the more luminous regions of the diagram in a way analagous to the behaviour of the globular cluster stars. The track is suggested by the downward line of crosses. The star, however, appears to be somewhat redder than corresponding stars in globular clusters at the same absolute visual magnitude.

Hoyle and Schwarzschild (**7**), however, have recently developed in detail the theoretical evolutionary behaviour of stars to the limit of the giant branch. On the basis of the higher metal to hydrogen ratio, believed to be characteristic of type I stars relative to type II, they also obtain the observed galactic cluster giant branches. The latter branches are a factor of about 10 less luminous. From consideration of the age and spectral characteristics of p Velorum it is probable that the component stars are of type I. Therefore the subsequent evolution from the giant branch is not necessarily exactly the same as that observed for type II, and in any case they start this phase from fainter luminosities.

The observational data thus suggest that, for a type I system of age around 10^9 years, the far-evolved stars pass through a stage analagous to that observed for globular cluster stars. They are, however, redder at the same absolute magnitude, and are best characterized at this stage of their evolution as A type sub-dwarfs.

Indiana University Observatory,
Indiana, U.S.A.:
1956 *April.*

Royal Observatory,
Cape of Good Hope.

References

(1) *Ap. J.*, **120**, 325, 1954.
(2) *Ap. J.*, **96**, 161, 1942.
(3) *Ap. J.*, **116**, 463, 1952.
(4) Comm. 5th Coll. Int. Astrophysique, Liege, p. 25, 1953.
(5) A. E. Roy, *M.N.*, **115**, 396, 1955.
(6) H. C. Arp and H. L. Johnson, *Ap. J.*, **122**, 171, 1955.
(7) *Ap. J. Supp.*, No. 13, Vol. II.

A STUDY OF THE FOUR ECLIPSING BINARY SYSTEMS: RW MONOCEROTIS, RW GEMINORUM, U CORONAE BOREALIS, AND TY PEGASI

Alan H. Batten

(Received 1956 June 22)

Summary

A new attempt at the determination of the photometric elements of the eclipsing binaries RW Monocerotis, RW Geminorum, U Coronae Borealis and TY Pegasi has been made from visual photometric light curves obtained by the late Drs Dugan and Pierce and published posthumously by Wood. The first three systems appear to exhibit total exclipses, and TY Pegasi is a partially eclipsing system. A notable difficulty in the solutions for RW Mon and RW Gem has been to reconcile the " shape " and " depth " ratios of the radii k of the two components ; and, in the latter part of the paper, an attempt has been made to demonstrate the possibility that this is a consequence of the considerable distortion of the secondary components which, in each case, probably nearly fill the largest closed equipotential capable of containing their mass.

The photometric observations are combined with spectroscopic evidence available for three of these systems, and the contact hypothesis is used to estimate the mass-ratio of the systems which leads to the determination of their absolute dimensions.

---

1. *Introduction.*—The immediate object of this investigation has been the analysis of light curves of the four eclipsing systems RW Monocerotis, RW Geminorum, U Coronae Borealis, and TY Pegasi. It has also been concerned, however, with a more general consideration of the problem presented by the light curves of highly distorted binary stars. These four systems were all chosen because it was suspected that their secondary components occupy completely the space enclosed by the largest closed equipotential surface capable of containing their mass. Throughout this paper such systems are termed "semi-detached systems" (**1**), and the secondary components are described as being at their respective *Roche limits* (**2**). Stars at their Roche limits are necessarily highly distorted, and do not possess symmetry about their axes of rotation. The question of the stability and evolution of these systems is at present of considerable interest, and new evidence of the dimensions and physical characteristics of the secondary components of additional systems of this type is very desirable.

2. *Previous investigations of the systems: source and description of the present investigation.*—All of these systems have been the subjects of previous analyses for their geometrical elements on the basis of less substantial photometric evidence. The best known of the four is U Coronae Borealis which has been investigated by, amongst others, Fetlaar (**3**), Baker (**4**), Shapley (**5**), and Dugan and Wright (**6**); this last investigation is also concerned with the evidence of variability of the period. All these analyses resulted in solutions corresponding to partial eclipses. On the other hand, the catalogues both of Schneller (**7**) and of Kukarkin and Parenago (**8**) list the system as exhibiting a total eclipse

at primary minimum. As will be seen, this latter alternative has been confirmed by the present investigation. A second notable feature of the system is the discrepancy between the spectral type of the secondary component, as computed from the depths of the minima of the light curve and as deduced from the spectroscopic observations. Sahade and Struve (**9**) argue that since both spectra of the system have been observed they must be closely similar in type (spectrum of brighter star: $B5$). Previous light curves, however, have shown very shallow and barely detectable secondary minima which lead to estimates of the spectral type, of the fainter star, as late as G or early K. Petrie (**10**), also, has determined the difference in visual magnitude, between the two stars, as $1^{m}.83 \pm 0^{m}.5$ by his spectrophotometric method, implying a late type for the secondary component. The curve used in the present investigation is notable for its deep and well-defined secondary minimum. The significance of this fact will be discussed later.

Analyses of light curves of RW Monocerotis have also been made by Shapley (**11**) and Fetlaar (**12**). The former is based on observations by Haynes and Seares (**13**), and the latter on the visual observations of Nijland. There is some divergence between the two sets of elements, but no greater than would be expected.

RW Geminorum has also been investigated by Shapley (**14**) and Fetlaar (**12**). A preliminary analysis has also been made by Pierce, and has been published posthumously by Wood (**15**), together with the observations used here. The various solutions are in tolerable agreement.

Only two analyses of light curves of TY Pegasi have been published. The first is by Dugan (**15**), which is based on the observations used here; the other by Dugan and Wright (**16**), based on observations made to investigate the variation of the period of this system. There is some divergence between the two sets of elements. Dugan, in the first of these analyses, met with some difficulty in fitting the calculated light curve to the observations, near the shoulders of primary minimum—the computed curve falls systematically below the observed curve. (The analysis was made on the assumption of zero darkening for the primary component.) No such difficulty is reported by Dugan and Wright.

The observations used in the present analyses were obtained with the visual polarizing photometer of the Princeton Observatory by the late Drs R. S. Dugan (TY Pegasi, U Coronae Borealis) and N. L. Pierce (RW Geminorum, RW Monocerotis), and published posthumously by Wood (**15**). The analysis followed the iterative least-squares procedure described by Kopal in Sections 3.5–3.9 and 3.13 of "The Computation of Elements of Eclipsing Binary Systems" (**17**) for the totally eclipsing systems, and Sections 3.14–3.16 and 3.18 for TY Pegasi. Owing to the comparatively limited accuracy of visual observations no attempt was made to go beyond the "intermediary" solutions for the elements of the several systems. The errors were calculated according to Section A4. Intrinsic weights were evaluated according to Kopal's equation 3.34*b* for RW Monocerotis and RW Geminorum, and equation 3.37*b* for U Coronae Borealis and equation 3.63 for TY Pegasi. For TY Pegasi only, were empirical weights included in the solution. For RW Geminorum, rectification of the light curve for ellipticity and reflection effects was found necessary, and Kopal's formula 6.7 was used, assuming $B = 0$.

For three of the systems, the assumption of a total eclipse at primary minimum converged to sets of elements representing the observations satisfactorily. For

the fourth—TY Pegasi—however, such a solution did not appear to converge to any specific value of the ratio of the radii, k, and a solution was eventually obtained on the hypothesis of a partial eclipse caused by an occultation of the early type component at the time of primary minimum.

Two of the light curves show unusual features. TY Pegasi displays what Dugan described as "an embarrassing series of observations from phase $2^d{\cdot}6876$ to $2^d{\cdot}8022$". These points, which are just before the beginning of secondary minimum, fall consistently below maximum light as determined by the remainder of the points between minima. As the difference between the two values of maximum light obtained by including and excluding these observations in the weighted mean amounts only to $0^m{\cdot}01$, they were included, although naturally this increases the error of the determination. It might also be remarked here that although Dugan rectified the light curve before analysing the primary minimum, such a course does not seem to be jutsified by the relatively low accuracy of observations between minima.

Irregularities of an even more serious nature appear in the light curve of U Coronae Borealis. About three-quarters of the way through primary minimum, near phase $+0^d{\cdot}15$, there is a discontinuity in the slope of the curve. On either side of the secondary minimum there appear "spurious minima" of much the same depth as the real minimum, but of shorter duration. These irregularities look like nothing so much as a wholesale miscalculation of phases, but they must be considered in conjunction with others found between minima, especially in the latter half of the period. Here, the observations fall into two or three well-defined groups, according to phase. Not only is there an exceptionally wide scatter in the magnitude of the individual observations—as there is throughout the cycle—but the mean magnitudes of the groups are also widely scattered, and not in a way that can be explained by ellipticity and reflection effects. Since neither the author nor the editor added any explanatory remarks, it is probable that neither of them realized the full extent, or even the existence, of these anomalous observations. Under the circumstances, we have no option but to omit these recalcitrant observations from our discussion. Inevitably this gives rise to some degree of arbitrariness, particularly between minima, but the general trend of observations is not violated. Accordingly, maximum light was determined from observations 1–16, 31–48, 62–127 and 144–155. Observations 17–20, 51–61, 134–143, 176–183, 346–387, 407–481, 530–613 and 686–703 were used in the analysis of the primary eclipse, while secondary minimum, as in the other cases, was estimated directly from the light curve.

3. *The results and their comparison with previous investigations.*—The results obtained from the analysis of the light curves alone are presented in Table I. All errors quoted in this table are mean errors. The suffix a refers to the primary component: i.e. the star of greater surface intensity. The suffix b refers to the secondary component. The symbol r denotes the stars' radii expressed in units of their separation; k denotes the ratio of the two radii r_a/r_b; i is the inclination of the plane of the orbit to the line of sight; p_0 is the maximum geometrical depth of eclipse during mid-primary minimum (becoming -1 for total eclipses). The ratio J_a/J_b is that of the mean surface intensities, L is the fractional luminosity of the star, in terms of the system's maximum luminosity as unit. Spectral types in brackets have been computed. θ', θ'' are,

TABLE I

	RW Monocerotis	RW Geminorum	U Coronae Borealis	TY Pegasi
r_a	$0\cdot203\pm0\cdot010$	$0\cdot233\pm0\cdot008$	$0\cdot175\pm0\cdot014$	$0\cdot217\pm0\cdot014$
r_b	$0\cdot311\pm0\cdot007$	$0\cdot303\pm0\cdot003$	$0\cdot274\pm0\cdot012$	$0\cdot220\pm0\cdot004$
r_a+r_b	$0\cdot514\pm0\cdot007$	$0\cdot536\pm0\cdot008$	$0\cdot449\pm0\cdot008$	$0\cdot437\pm0\cdot013$
k	$0\cdot65\ \pm0\cdot05$	$0\cdot77\ \pm0\cdot025$	$0\cdot64\ \pm0\cdot096$	$0\cdot99\ \pm0\cdot06$
i	$85^\circ\cdot1\pm1^\circ$	$88^\circ\cdot7\pm1^\circ\cdot8$	$84^\circ\cdot5\pm1^\circ\cdot1$	$87^\circ\cdot9\pm0^\circ\cdot4$
p_o	-1	-1	-1	$-0\cdot841\pm0\cdot006$
J_a/J_b 1.	$17\cdot9\pm3$	$20\cdot1\pm1\cdot3$	$4\cdot4\pm1\cdot3$	$8\cdot6\pm4$
J_a/J_b 2.	$8\cdot0\pm1\cdot2$	$11\cdot4\pm2\cdot3$	$3\cdot7\pm0\cdot3$	...
Primary Spectrum	A0	B5	B5	A2
Secondary Spectrum	(gG4)	F5	(A5)	(gG1)
L_a	$0\cdot883\pm0\cdot002$	$0\cdot866\pm0\cdot001$	$0\cdot644\pm0\cdot005$	$0\cdot904\pm0\cdot016$
L_b	$0\cdot117\pm0\cdot002$	$0\cdot134\pm0\cdot001$	$0\cdot356\pm0\cdot005$	$0\cdot096\pm0\cdot016$
θ'	$31^\circ\cdot0\pm0^\circ\cdot4$	$32^\circ\cdot3\pm0^\circ\cdot5$	$26^\circ\cdot2\pm0^\circ\cdot5$	$25^\circ\cdot9\pm0^\circ.8$
D	$0^d\cdot328\pm0\cdot004$	$0^d\cdot514\pm0\cdot009$	$0^d\cdot503\pm0\cdot010$	$0^d\cdot445\pm0\cdot012$
θ''	$3^\circ\cdot8\pm0^\circ\cdot5$	$3^\circ\cdot6\pm0^\circ\cdot6$	$1^\circ\cdot5\pm0^\circ\cdot4$	...
d	$0^d\cdot040\pm0\cdot006$	$0^d\cdot057\pm0\cdot010$	$0^d\cdot028\pm0\cdot007$	...
Period (assumed)	$1^d\cdot906102$	$2^d\cdot8654970$	$3^d\cdot45220416$	$3^d\cdot0922335$

respectively, the phases of external and internal contact. D is the duration of the primary minimum, and d that of totality. P is the period of the system. The two values given for J_a/J_b are derived from the formulae

$$\frac{J_a}{J_b}=\frac{1}{k^2}\,\frac{1-\lambda_a}{\lambda_a} \tag{1}$$

and

$$\frac{J_a}{J_b}=Y(k,-1)\,\frac{1-\lambda_a}{1-\lambda_b} \tag{2}$$

where $\lambda_{a,b}$ are the depths of primary and secondary minima, respectively, and $Y(k,-1)$ is a slowly varying function of k. In each case, it has been assumed that the limb darkening coefficient of the primary component is 0·5, and of the secondary component 0·6.

The results of Table I are not widely divergent from most of the previous results cited above. The most notable exceptions to this rule are Fetlaar's elements for U Coronae Borealis and RW Monocerotis and these were derived from light curves based on visual estimates. The present analysis of the light curve of TY Pegasi did not encounter Dugan's difficulty in fitting the curve to the observations at the shoulders of primary minimum. It is true that the three (O−C) residuals in this region are of the same sign, but they are all small, and can hardly be said to represent any systematic trend.

In the analyses of the light curves of RW Monocerotis and RW Geminorum, however, an outstanding difficulty was the initial estimation of the ratio of the radii. For totally eclipsing systems, Kopal (**17**) gives two ways of determining this quantity. It may be estimated directly from the observed depths of both minima of the light curve, or determined from the shape of the light curve during partial stages of the eclipse in the course of the iterative solution for the elements. The two values so obtained are usually called the "depth k" and "shape k" respectively. For good light curves with deep minima, these two values of k should agree within the limits of observational error. For the two systems

named above, however, the depths of the two minima lead to "depth" k's greater than one—values which are ruled out by the light curve. The "shape" k's are given in Table I. For U Coronae Borealis a smaller discrepancy exists which is in the opposite sense. The relatively large error of the "shape" k for U Coronae Borealis, however, renders the significance of the discrepancy in this system rather doubtful. It is noteworthy that Miss Gordon (**18**) has recently encountered the same difficulty in her analysis of a much more accurate light curve of RT Andromedae, which is another system of this type. The present writer hopes to demonstrate, shortly, that this discrepancy in the two values of k is a consequence of the extreme distortion of, and peculiar light distribution over, the secondary components.

A particular effect of the discrepancy is the impossibility of any precise determination of the limb darkening coefficients of the primary components of the four systems, for it is known that a determination of the "shape" k depends crucially on the coefficient of limb darkening of the smaller component (which undergoes eclipse during primary minima), while the "depth" k is completely independent of it. In consequence, an equalization of the "shape" and "depth" k's for well-behaved eclipsing systems should ordinarily specify the limb-darkening of the smaller star within narrow limits. The impossibility of equalizing the two k's, therefore, eliminates this possibility of determining the limb-darkening of the primary component. These coefficients had, therefore, to be estimated on the basis of the spectral types of the respective stars for the effective wave-length of visual observations (λ 5300). The values adopted, for all four systems were $u_a = 0{\cdot}5$ and $u_b = 0{\cdot}6$ (**19**).

A further result of the discrepancy is the divergence between the values of J_a/J_b as computed from the two formulae. The first of these involves the "shape" k explicitly, and the second involves the "depth" k implicitly. For RW Geminorum, consideration of the reflection effect provided an independent determination $J_a/J_b = 10{\cdot}9 \pm 0{\cdot}8$, and this is the value used in determining L_a and L_b and the spectral type of the secondary component. For the other systems, the value (1) corresponds to the quoted values of L_a, L_b and the secondary spectrum.

The value of J_a/J_b quoted for U Coronae Borealis is of some interest. It corresponds to a difference in the visual magnitude of the two stars of about $0^m{\cdot}65$ and this is significantly less than Petrie's value of $1{\cdot}83 \pm 0{\cdot}05$ quoted earlier. If Sahade's and Struve's estimate of the secondary spectrum (**9**) is right, however, the ratio J_a/J_b should be even smaller. This light curve of Dugan's is the only one with such a deep secondary minimum, and all previous observers have found the secondary minimum to be barely noticeable. There seem to be strong arguments in favour of both hypotheses about the depth of secondary minimum, and further observations are needed to settle the question.

4. *Combination with spectroscopic observations and discussion.*—Spectroscopic observations are, at present, only available for U Coronae Borealis, RW Geminorum and TY Pegasi.* For U Coronae Borealis, the spectra of both components have been observed, three determinations of the orbit and absolute dimensions have been made, by Plaskett (**20**), Pearce (**21**), and Sahade

* According to the latest *Finding List*, RW Monocerotis has been observed spectroscopically by Millman and Hogg at David Dunlap Observatory. Dr Heard, Director of the observatory informed us in June 1956 that "the spectrum is A0 with very broad H lines, $\lambda\lambda$ 3933, 4481, and a few diffuse metal lines", and that the total velocity range is not likely to be less than 170 km/sec.

and Struve (**9**). The orbit by Struve and Sahade is characterized by an appreciable eccentricity ($e=0{\cdot}13$). The secondary minima of Dugan's light curve are quite symmetrical with respect to successive primary minima, and the system, therefore, provides yet another instance of a system with photometrically circular and spectroscopically elliptic elements. The orbit by Pearce has an eccentricity about half the value found by Sahade and Struve, and was, therefore, chosen as the most suitable with which to combine the photometric elements. The combination of the photometric and spectroscopic elements was made without taking the orbital eccentricity into account. Table II contains the absolute dimensions of the system; the symbols m, R, a and $\bar{\rho}$ denoting the masses of the stars, their radii, the semi-major axis of the relative orbit and their mean densities respectively. These quantities are all expressed in terms of the appropriate solar unit. The table also gives the absolute bolometric magnitude, M, of each star.

TABLE II

	RW Geminorum	U Coronae Borealis	TY Pegasi
Spectroscopic Mass Function	0·082	0·378 ± 0·008 (mass-ratio)	0·0038
Contact Hypothesis Mass-Ratio	0·45 ± 0·01	0·31 ± 0·05	0·15 ± 0·01
m_a	1·88	6·5	1·47
m_b	0·85	2·5	0·22
a	11·9	20·0	10·7
R_a	2·8	3·5	2·3
R_b	3·6	5·5	2·4
M_a	−1·92	−2·41	+0·57
M_b	+1·3	−0·90	+2·94
$\bar{\rho}_a$	0·092	0·14	0·12
$\bar{\rho}_b$	0·018	0·014	0·017

Notes.—The contact hypothesis mass-ratio of RW Mon is 0·50 ± 0·01.

For U Coronae Borealis the spectroscopic mass-ratio is used to derive the other quantities in the table. For the other two systems, only the contact hypothesis mass-ratio is available.

In addition to the value of the mass-ratio obtained from the spectroscopic evidence, a value may also be obtained on the assumption that the secondary component is at its Roche limit—in the sense defined in the Introduction. A table facilitating this has been published by Kopal (**2**), and the two values of the mass-ratio are given in Table II. All mass-ratios given in Table II are defined to be less than unity. Taking account of the errors involved, an inspection of the two values for U Coronae Borealis reveals that the assumption that the secondary component is at its Roche limit is quite compatible with the observational evidence.

For RW Geminorum, information is more limited. Although both spectra of the system have been identified (the observations and calculations are in agreement about the secondary spectrum of this system), measurements of radial velocities are only possible for the early-type spectrum. The only existing set of elements has been obtained by Struve (**22**). The spectroscopic observations

yield only the mass-function, but the mass-ratio, and the absolute dimensions given in Table II have been derived on the assumption that the system is a semi-detached one, with the secondary at its Roche limit. The outstanding characteristic of this system is the very low masses of the two stars, for their luminosity. The system is thus seen to be one of the R Canis Majoris type characterized by abnormally small masses and gross overluminosity of *both* components. It should be noted that if the secondary component is smaller than its Roche limit, the total mass of the system would necessarily be still less than the value quoted here. The abnormally low masses of these stars may therefore be regarded as established.

For TY Pegasi, the only available spectroscopic data are unpublished observations by Joy (**23**) which indicate that the semi-amplitude of the primary component's velocity curve is not less than 23 km/sec. According to private information from Dr Joy, this figure has been derived from only six plates on which "the lines are few and more plates would be necessary to form any definite idea of the velocity curve". This being so, the figure of $K_1 = 23$ km/sec provides only the lower limit of the mass function. The mass-ratio has again been estimated on the assumption that the system is semi-detached, with the secondary component at the Roche limit, and the absolute dimensions so obtained are consistent with a primary component which lies fairly close to, but just above, the main sequence.

The main interest in these results is the light they throw on the hypothesis that the secondary components of these systems are all at or near their Roche limits. In only one instance, that of U Coronae Borealis, is a direct and rigorous test possible, and this shows that the secondary component, though it may not yet have reached the limit, is certainly not far off. In the case of TY Pegasi, the fact that the assumption that the system is semi-detached leads to a main sequence primary component is also encouraging, but the limitations of the available spectroscopic evidence must be clearly borne in mind.

The absence of any published spectroscopic observations of RW Monocerotis preclude a definite decision in this case, but the closely similar system of RW Geminorum provides some of the most interesting, though not the most certain evidence. As has already been pointed out, the assumption that RW Geminorum is a semi-detached system gains plausibility from the resulting low masses of the component stars. This system is one in which the difficulty of reconciling the "shape" and "depth" k's was encountered. The "shape" k is determined from the primary minimum only, but the "depth" k is determined from observations of both minima. Thus, it follows that if the secondary component were distorted in such a way as not materially to alter the depth of primary minimum, but so to alter the observed depth of the secondary minimum, such a discrepancy as is observed should result. A star at its Roche limit fulfils just these conditions. The cross-section presented to the observer at both eclipses is circular to within a few per cent. The shape of the star, however, is such that the distribution of light over its surface is greatly affected by gravity darkening. The apparent disk presented at the time of primary minimum should be of fairly uniform intrinsic brightness, and should be affected only by normal limb darkening. The disk which itself undergoes eclipse at secondary minimum, on the other hand, is so affected by gravity darkening that it should appear to have a completely dark centre and to grow brighter towards the limb.

Superimposed on this, there will be the effect of a limb darkening law which is more rapid than the normal cosine law. The brightest region of such a disk should, therefore, be an annulus at some distance from the centre of the disk, and in extreme cases the disk eclipsed at secondary minimum might be almost completely dark.

This last fact provides further qualitative support for the hypothesis that the secondary component of RW Geminorum is at its Roche limit. It has already been mentioned that the light curve of this system required rectification for the reflection effect. As is well known, the effect of such a rectification is to augment the total observed light of a system, at any given phase, by the difference between the light reflected at that phase and the light that is reflected when both components are at "first quarter" with respect to each other—i.e. at quadratures. In particular, the observed depth λ_a of primary minimum, which gives the fractional luminosity of the "dark" side of the secondary component, should, when rectified give the corresponding quantity for the "bright" side. For RW Geminorum the result λ_a (unrectified) $> \lambda_a$ (rectified) was obtained. This is clearly impossible for any normal spherical, or even spheroidal star, as it implies that despite the light from the primary component reflected by the secondary component, its "bright" side is still darker than the "dark" side. It is evident, however, that such an effect is, qualitatively at least, not incompatible with the hypothesis that the secondary star is at its Roche limit.

It is possible, then, that the discrepancy between the "shape" and "depth" k's is, in itself, evidence that the systems concerned are semi-detached. In the case of U Coronae Borealis, which may not yet be at its Roche limit, the discrepancy in the two k's is much less significant.

The above discussion has been purely qualitative. It has been sufficient, however, to make it clear that a satisfactory method of determining the elements of semi-detached systems cannot be evolved until a detailed study of the distribution of luminous intensity over the surface of their highly deformed secondary components has been made. It will then be possible to predict quantitatively the effects discussed more generally here. Such a study is currently being undertaken in Manchester by the writer, and, indeed, the present investigation forms merely a preface to it.

5. *Acknowledgments.*—It is a pleasure to acknowledge the help and encouragement I have received, at every stage of the investigation, from Professor Z. Kopal. I am grateful, too, to Mrs M. M. Gorman who did the major part, both of the preliminary drawing of the light curves, and of the routine computation involved. Finally, I am indebted to the Department of Scientific and Industrial Research for the award of a maintenance grant, during the tenure of which this work was carried out.

Department of Astronomy,
University of Manchester:
1956 *June* 21.

References

(1) Z. Kopal, *Ann. d'Ap.*, **18**, 379, 1955.
(2) Z. Kopal, *Jodrell Bank Annals*, **1**, 37, 1954.
(3) J. Fetlaar, *B.A.N.*, **6**, 29, 1930.
(4) R. H. Baker, *Laws Observatory Bulletin*, No. 29, 1921.
(5) H. Shapley, *Princeton Contr.*, No. 3, 50, 1915.
(6) R. S. Dugan and F. W. Wright, *Princeton Contr.*, No. 19, 26, 1939.
(7) H. Schneller, Kl. Veröff, *Berlin-Babelsberg*, No. 22, 1940.
(8) B. V. Kukarkin and P. P. Parenago, *General Catalogue of Variable Stars*, Moscow, 1948.
(9) J. Sahade and O. Struve, *Ap. J.*, **104**, 253, 1946.
(10) R. M. Petrie, *Publ. D.A.O.*, **8**, 327, 1950.
(11) H. Shapley, *Princeton Contr.*, No. 3, 84, 1915.
(12) J. Fetlaar, *B.A.N.*, **3**, 195, 1926.
(13) E. S. Haynes, *Laws Observatory Bulletin*, No. 15, 1908.
(14) H. Shapley, *Princeton Contr.*, No. 3, 90, 1915.
(15) F. B. Wood, R. S. Dugan and N. L. Pierce, *Princeton Contr.*, No. 25, 1951.
(16) R. S. Dugan and F. W. Wright, *Princeton Contr.*, No. 19, 38, 1939.
(17) Z. Kopal, *The Computation of Elements of Eclipsing Binary Systems*, Harvard Monograph No. 8, 1950.
(18) K. C. Gordon, *A. J.*, **60**, 422, 1955.
(19) Z. Kopal, *Report of I.A.U. Commission*, 42, 1952–55, *I.A.U. Trans.* Vol. IX (in press).
(20) J. S. Plaskett, *Publ. D.A.O.*, **1**, 187, 1922.
(21) J. A. Pearce, *P. b. A.A.S.*, **8**, 219, 1935.
(22) O. Struve, *Ap. J.*, **104**, 253, 1946.
(23) A. H. Joy, private communication in a letter of 1956 May 1.

AN ASTRONOMICAL PHOTOELECTRIC SPECTROPHOTOMETER

J. E. Geake and W. L. Wilcock

(Received 1956 May 18)

Summary

An instrument is described for the direct recording of astronomical spectral profiles. It consists of a prism monochromator whose output is recorded photoelectrically as the wave-length transmitted is varied. Compensation for atmospheric seeing effects is essential when narrow slits are used, and is provided by recording, as the compensated profile, the ratio of the monochromator output to the undispersed light collected after the entrance slit. The performance of this compensation, and the limiting effects of shot noise on the accuracy of the instrument, are discussed.

The instrument has been used with a fairly high resolution (about 0·6 A) to record stellar absorption line profiles, and with a low resolution, as a slitless spectrograph, to measure the relative intensities of emission lines of planetary nebulae.

---

1. *Introduction.*—Astronomical spectra are usually investigated photographically, but there are advantages to be gained by using a photocell to measure spectral intensities directly. The reduction of the results is much simplified because the photo-emissive effect is linear, the precision of the electrical measurement involved is potentially high, and the larger intensity range over which precise measurements can be made is advantageous, particularly in the case of line emission spectra. In addition, the relatively high quantum efficiency of available photocathodes increases the speed with which a single wave-length element can be measured; and, although this is offset by the need to measure successive wave-length elements in time sequence, whereas a photographic plate records the whole spectrum at once, the photoelectric method becomes advantageous when time changes of a limited wave-length region are to be investigated.

Our instrument consists essentially of a monochromator whose output is recorded photoelectrically as the wave-length transmitted is varied. Jacquinot and Dufour (**1**) have discussed the optical properties of instruments of this kind and have pointed out their flexibility; a single instrument may be converted from slow high-resolution to fast low-resolution performance simply by increasing the monochromator slit widths, whereas similar conversion of a photographic spectrograph requires the reduction of the focal length of the camera lens. Numerous examples of such photoelectric spectrophotometers for laboratory use have been described, and examples for astronomical use have been reported by Hiltner and Code (**2**), Guérin and Laffineur (**3**), and Dobronravin and Nikinov (**4**).

The principal difficulty encountered when such an instrument is used for stellar spectrophotometry is that fluctuations in the amount of light passing the entrance slit are superimposed on the recorded spectral profile. These are due partly to changes in atmospheric transparency, but mainly to changes in the

amount of light stopped by the slit jaws as the stellar image moves about under the influence of atmospheric turbulence and imperfect guiding of the telescope. If the entrance slit is made so wide that the whole tremor disk is always included, the effect of image movement disappears, but with our instrument such a slit would yield only a low wave-length resolution. For many problems a narrow slit is necessary, and the fluctuations become so large (Fig. 4) that some method of compensation is essential. In the present instrument compensation for the fluctuations is achieved by allowing a small proportion of the undispersed light which has passed the entrance slit to fall on a second photocell. The ratio of the outputs of this photocell and the one which scans the spectrum is taken automatically; fluctuations common to both cells do not appear in the ratio, which is recorded as the compensated spectral distribution. A similar method of compensation has been described by Hiltner and Code (**2**), but for compensation purposes they used dispersed light in a small fixed wave-length range on either side of the wave-length range being scanned, whereas we have used light in which the whole spectrum is represented.

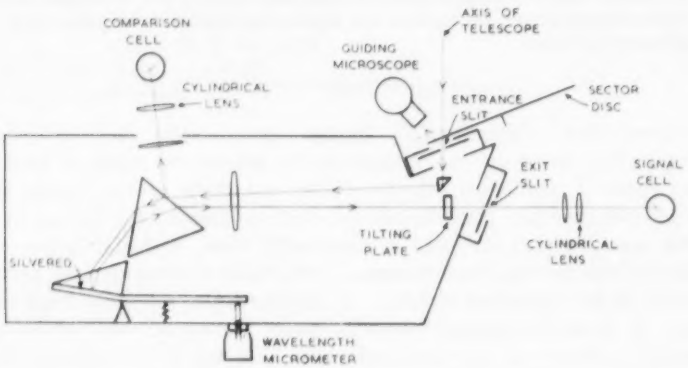

FIG. 1.

2. *Description of the instrument.* (*a*) *Optical.*—Fig. 1 is a diagram and Fig. 2 a photograph of the arrangement. The monochromator is autocollimating and of aperture *f*/6. It has two flint glass prisms, one of 51° and one of 30°, and a simple doublet lens of 25 cm focal length mounted on a micrometer-controlled slide to permit focusing. The linear dispersion is about 25 A/mm at Hγ, and the maximum resolution at this wave-length is set by optical imperfection at about 0·4 A. The entrance and exit slits are both bilaterally adjustable, and the plane of the former is inclined to the optical axis so that light reflected from a glass cover slip held in contact with the slit jaws can be used to guide the telescope.

The light passing the exit slit is focused, by means of an optical system discussed later, onto the cathode of the signal cell, which is a photomultiplier. Provision is made for cooling this cell in order to reduce its dark emission. It is enclosed in a brass tube which is surrounded by a brass jacket containing the cooling agent, either liquid air or a mixture of solid CO_2 and acetone, and the

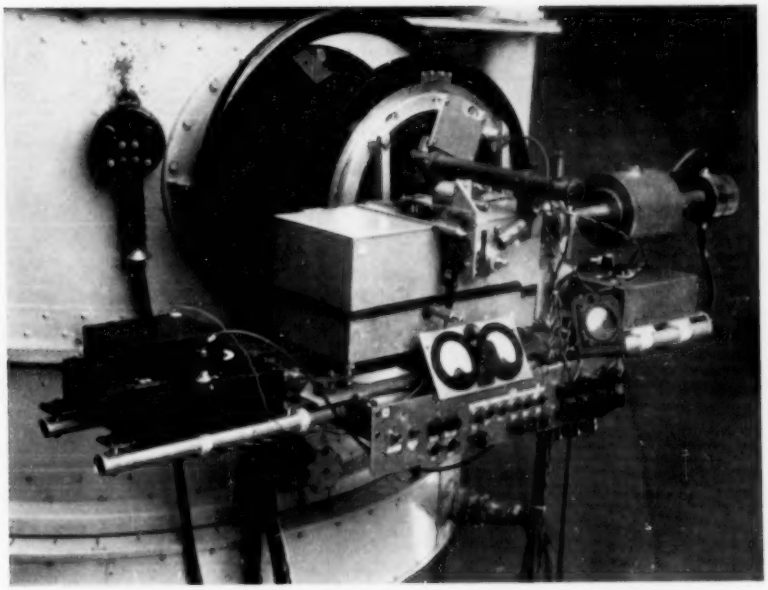

FIG. 2.—*The monochromator, with photomultiplier mountings and head amplifiers attached, mounted at the Newtonian focus of the 120 cm reflector at Asiago, Italy.*

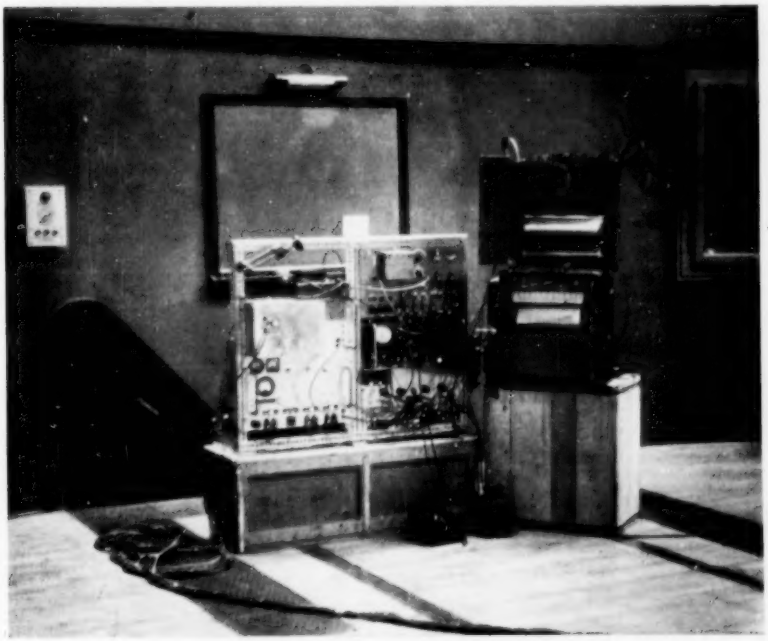

FIG. 3.

J. E. Geake and W. L. Wilcock, An astronomical photoelectric spectrophotometer.

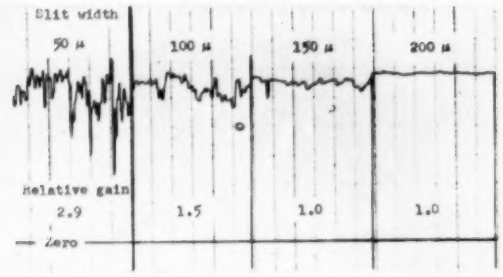

FIG. 4.—*A photoelectric recording, showing fluctuations in the light passing the monochromator entrance slit for various slit widths. The amplifier gain was adjusted to give about the same mean deflection in each case, and the relative gains are given. A slit width of 50 μ corresponds to a resolution of about 1·25 A at Hγ. The light level is such that shot noise fluctuations are negligible.*

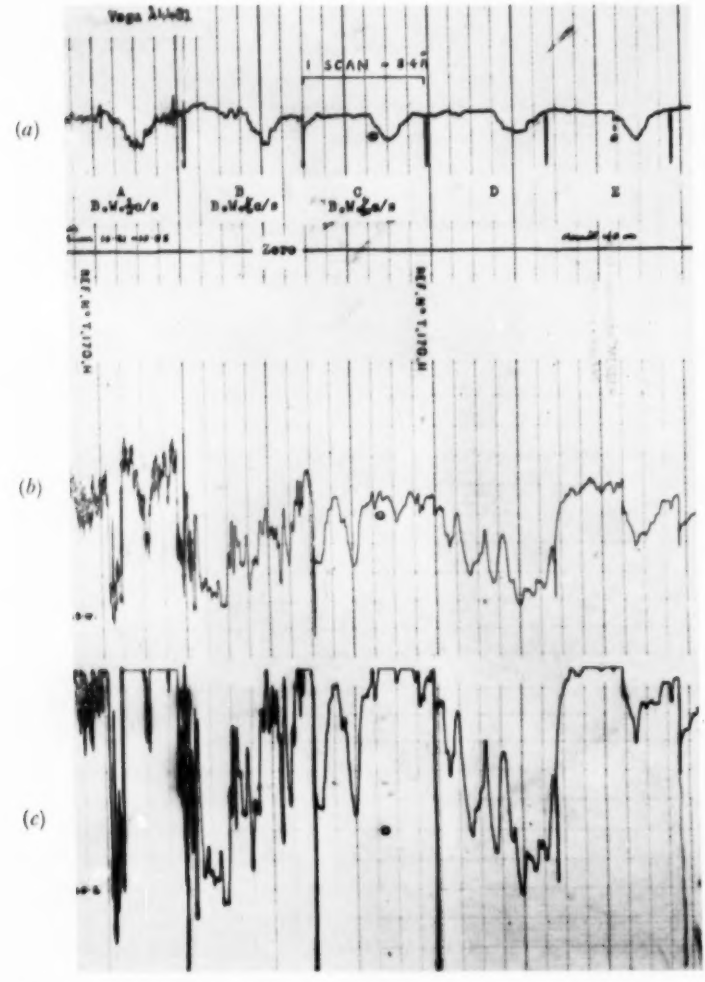

FIG. 5.—*Repeated scans of a stellar absorption line (Vega λ 4481) showing (a) the compensated record, (b) the uncompensated signal record, and (c) the comparison record. Slit width 25 μ, corresponding to a resolution of about 0·6 A. The time taken was 6 min per scan.*

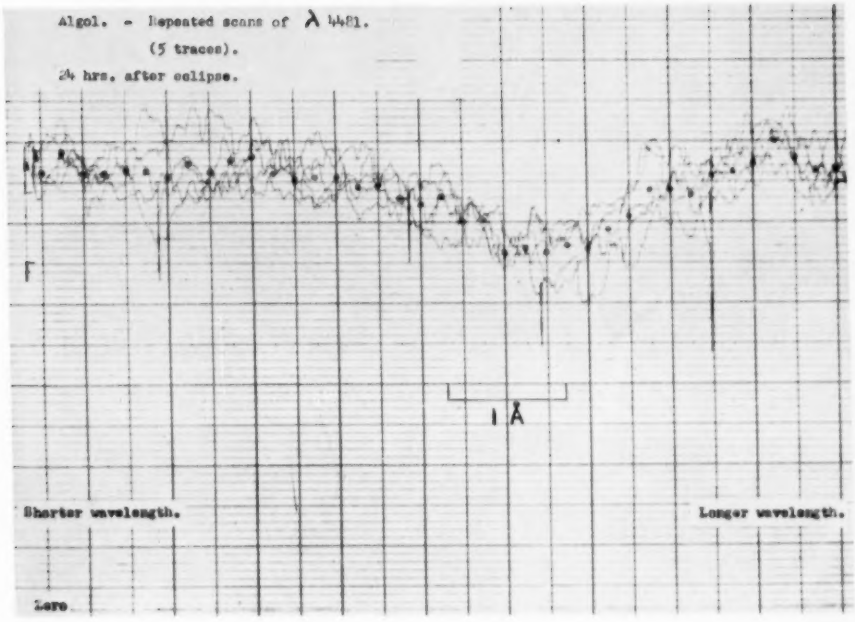

FIG. 8.—*Several superimposed scans of the MgII λ4481 line for Algol. Resolution about 0·6 A, time-constant 3 secs, time taken 5 min per scan.*

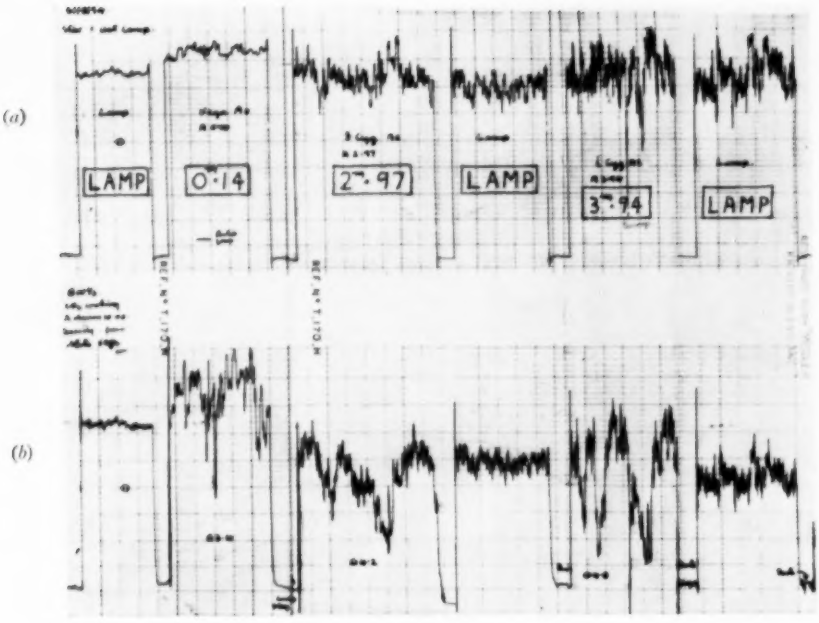

FIG. 9.—*Recordings of several class A stars of different magnitudes, with the signal cell receiving light from a fixed wavelength range of about 1 A near Hγ. The amplifier gain is different for each star. Each stellar record is accompanied by one of a test lamp producing about the same signal cell photo-current. (a) is the compensated record, and (b) the uncompensated signal record.*

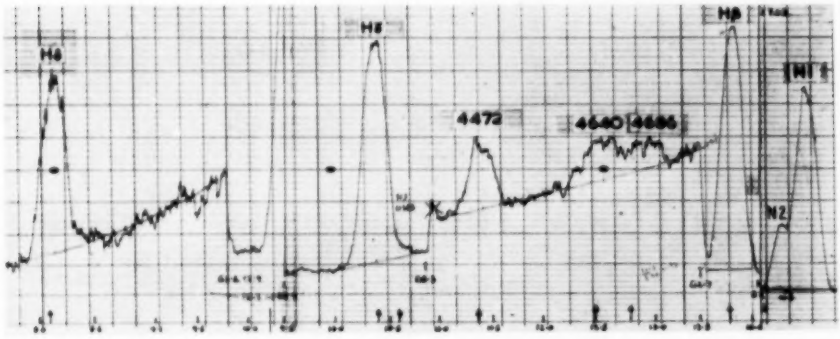

FIG. 10.—*Part of a scan showing emission lines of the planetary nebula NGC 6543. The amplifier gain was changed between lines where necessary.*

whole is lagged with expanded P.V.C. Light is admitted to the cell along a tube of Inconel, an alloy of low thermal conductivity, which also serves to attach the cell mounting mechanically to the monochromator. Another Inconel tube carries the leads from the photomultiplier base connections to a box containing the dynode resistor chain. The air surrounding the photomultiplier and its connections and resistors is dried by means of silica gel to prevent the condensation of moisture which would cause electrical leakage and misting of the cell window.

The comparison cell, also a photomultiplier, is mounted on the side of the monochromator and receives light which is inevitably reflected from the first prism face. It is not necessary to cool this cell, since it receives much more light than the signal cell.

The wave-length passed by the monochromator is set initially by means of a micrometer screw which turns the 30° prism. The spectrum is scanned by traversing it across the fixed exit slit, and two alternative methods of doing this are provided. A short scan of fixed range and rate is achieved by tilting a plane parallel glass plate in front of the exit slit, by means of a lever, cam and synchronous motor. Alternatively, the wave-length-setting micrometer screw can be turned

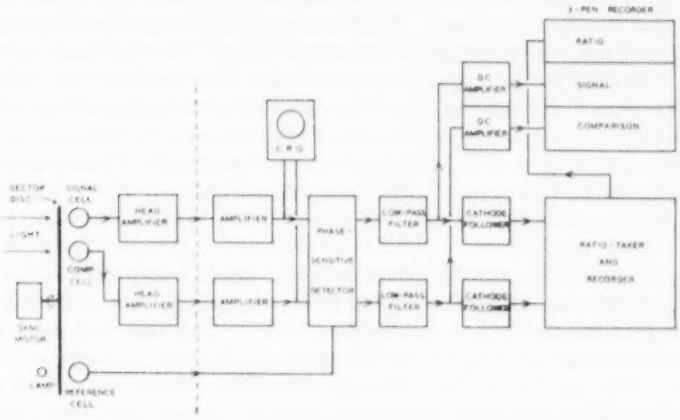

Fig. 6.—*Block diagram of the electrical system. The parts to the left of the dotted line are mounted on the telescope.*

by means of another synchronous motor; in this case a selection of pulleys and motors provides a wide choice of scanning rates, and the scan may be of any length up to the whole range of the instrument. Adjustable stops can be set at any pair of wave-lengths to provide a reproducible starting point for the scan and an automatic stop at the end.

(*b*) *Electrical.*—Fig. 6 is a block diagram of the electrical equipment. Part of this is carried with the monochromator on the telescope, while the remainder, of which Fig. 3 is a general view, is mounted on a rack on the floor of the observatory. The two parts are connected by a cable 20 m long.

The light entering the monochromator is chopped at 30 c/s by a rotating sector disk immediately in front of the entrance slit. The alternating output voltages of the two photomultipliers are amplified by separate a.c. amplifiers of conventional design, with some negative feedback in each stage to improve

the linearity of response. Each amplifier is in two parts: the first part is attached to the monochromator and the second part is with the main electrical equipment on the observatory floor. The level of signal carried by the long connecting cable is thus made so high that electrical interference picked up is negligible. A calibrated logarithmic attenuator precedes the second part of each amplifier.

The signals from the photomultipliers are accompanied by noise fluctuations, and to increase the signal-to-noise ratio it is necessary to reduce the bandwidth of the measuring system (which is equivalent to increasing its time-constant). We achieve this by using phase-sensitive detection (**5**), which involves multiplying the output waveform of each cell by a reference waveform of the same frequency and phase as the signal. The signal then emerges as a d.c. component whereas other frequencies present as noise fluctuations emerge as difference frequencies; these can be removed to any desired extent by a low-pass filter, which determines the effective bandwidth of the system.

In our instrument the output of each amplifier channel is effectively multiplied by a square reference waveform, as a high-speed relay is used to connect each amplifier output to earth for alternate half-cycles at the chopping frequency of 30 c/s. This reference waveform is locked in phase to the signal by using the chopper to control the relay. Light from a small lamp is interrupted by the chopper and falls on a low-grade photomultiplier—the reference cell—whose output is applied to the grid of a power valve in series with the relay. For simplicity we use only one relay, and this switches the two channels in anti-phase. To have the d.c. outputs of the channels of the same sign it is therefore necessary to have the a.c. outputs of the amplifiers also in anti-phase. This is achieved by having one valve stage fewer in the comparison amplifier, which is permissible since the comparison cell normally receives much more light than the signal cell.

Simple resistance–capacity filters are used in each channel with a choice of values giving time-constants ranging from 1 to 45 sec; it may be shown that the corresponding equivalent bandwidths, from which the total noise may be calculated, are from $\frac{1}{2}$ to 1/90 c/s. The filters in the two channels are carefully matched. The use of a square reference waveform, which contains all the odd harmonics of its fundamental frequency, gives the output stage additional pass-bands centred on these frequencies, and it can be shown that in these bands the signal-to-noise ratio is lower than in the fundamental; the amplifiers are therefore designed to have a low response to these higher frequencies.

The ratio of the d.c. outputs of the two channels is taken automatically and recorded by means of a modified Leeds and Northrup "Speedomax" recorder (**2**) which is essentially a self-balancing potentiometer. The signal channel output is connected to the normal input terminals, and the battery which originally supplied a constant potential to the potentiometer wire is replaced by the output of the comparison channel. The pen then records the ratio. For convenience in testing the equipment a separate 3-pen recorder is used to record the outputs of the two channels separately alongside a duplicate of their ratio. A cathode-ray oscilloscope monitors the a.c. output of either amplifier and can also be used to test the contacts of the high-speed relay.

The high voltage required by the signal and comparison photomultipliers is supplied by a stabilized r.f. power pack. The h.t. supply for the amplifiers

is stabilized, and the heaters of the amplifiers and output stages are supplied from a rectifier stabilized by a large accumulator.

To facilitate the use of the equipment by a single observer, meters showing the positions of the pens on the 3-pen recorder are attached to the monochromator, and several of the important electrical controls can be operated remotely. A push-button which stops the wave-length traverse and recorder charts simultaneously is also provided; this enables the scan to be stopped should an interruption occur, and subsequently re-started without showing a break in the record.

3. *Compensation technique.*—The first tests were carried out with the instrument installed at the Newtonian focus of the Smith–Clarke 18 in reflector at the Jodrell Bank Experimental Station of Manchester University. The signal and comparison photomultipliers were R.C.A. 1P21 tubes, and following the usual astronomical practice the optical system was arranged to image the telescope objective on the cell cathodes. The compensation with this arrangement was unsatisfactory, for reasons which will now be discussed.

When the telescope objective is viewed through the slit, dark regions with their edges parallel to the slit jaws encroach from time to time on the edges of the image of the objective. This effect, which we observed visually when the telescope was guided on a bright star, is due to the slit jaws acting as Foucault knife-edges. The compensation will be imperfect if identical views of the objective are not presented to the two cells, or if the distributions of sensitivity over the two photocathodes are different. The first effect was removed by ensuring that any obstructions which were necessary in one optical path were copied exactly in the other. The second effect, which is particularly important for 1P21 photomultipliers whose photocathodes are obscured by a closely-spaced wire grid, was made much less harmful by placing cylindrical lenses just in front of the photocells. These served to compress the illuminated region on each cathode to a narrow strip parallel to the slits. With this arrangement the compensation was found to be satisfactory. Fig. 5 shows an example, taken from the 3-pen recorder, of the uncompensated signal cell output and the compensated result, when narrow slits were used.

Recently the instrument has been transferred to Asiago, Italy, where it is being used at the Newtonian focus of the 120 cm reflector of the University of Padua. Various mechanical modifications were necessary and we took the opportunity to try a different kind of photomultiplier. With R.C.A. cells, used as described above, the effectiveness of the compensation was found to be critically dependent on the positions of the photocathodes. Laboratory tests on E.M.I. Type 6094 photomultipliers, which have unobstructed photocathodes, showed that although there were appreciable local variations of sensitivity over the cathode surface there were small areas of substantially constant sensitivity which were large enough to include displacements of the star image under average seeing conditions. We therefore redesigned the optical systems to image the entrance slit on the photocathodes. The compensation was as good as before, but no better, and the positioning of the photocathodes was found to be just as critical. The E.M.I. cells were, however, retained for other reasons: the ratio of dark current to sensitivity for our best E.M.I. cell at room temperature was found to be as low as that for our best R.C.A. cell at the temperature of solid CO_2.

As explained in the next section this means that whereas it was desirable to cool the R.C.A. cell when used on all but the brightest stars, cooling the E.M.I. cell is not profitable and some inconvenience is avoided. A further advantage of the E.M.I. cells is that they are much less microphonic.

4. *Performance of the instrument.* (i) *Noise tests.*—The recorded output of a photomultiplier which is exposed to a constant light flux shows noise fluctuations. These are due mainly to the shot effect of the photocurrent and the dark current, and the ratio of signal to r.m.s. noise is given approximately by

$$S/N \propto \frac{i_p}{[(i_p+i_d)\Delta f]^{1/2}}$$

where i_p = photocurrent at cathode, i_d = equivalent dark current at cathode*, and Δf = equivalent noise bandwidth of the recording system. In our instrument the comparison cell receives much more light than the signal cell, so that S/N for the comparison channel is always much higher than S/N for the signal channel. The above proportionality may therefore be expected to hold for the compensated record if i_p and i_d refer to the signal cell.

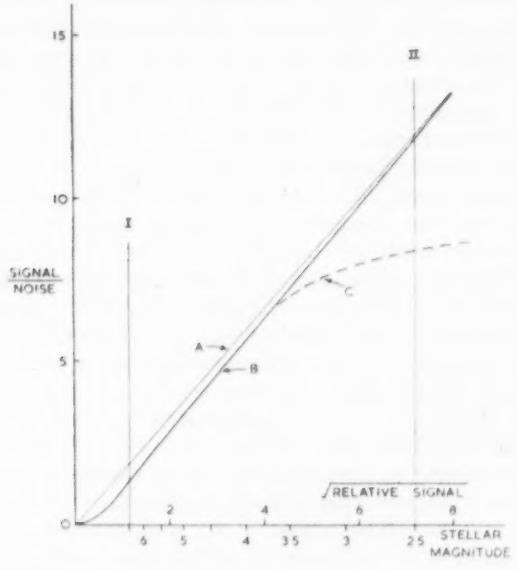

FIG. 7.

By laboratory tests with a lamp of variable brightness we have measured S/N as a function of i_p for our instrument with an E.M.I. photomultiplier, which was selected for its unusually low dark current, as the signal cell. The relation between S/N and $\sqrt{i_p}$ is shown as line B in Fig. 7 for a bandwidth of $\frac{1}{2}$ c/s, which corresponds to a time constant of 1 sec. Our tests have also verified that $S/N \propto 1/\sqrt{\Delta f}$. Comparison with stellar records has enabled the $\sqrt{i_p}$ scale

* The actual dark current may not all originate in cathode emission: by i_d we mean that fictitious cathode dark current which would produce the observed dark noise.

to be calibrated in terms of stellar magnitude: the calibration refers to Ao stars, at a wave-length near Hγ, using 50μ slits (giving a resolution of 1·25 A), and on a night of average seeing with the 120 cm telescope.

The dark current of a photomultiplier may be reduced considerably by cooling (**6**), and line A in Fig. 7 shows the ideal performance which the instrument would have if the dark current of the E.M.I. cell were removed completely. The vertical separation of lines A and B thus represents the maximum improvement that could be produced by cooling. The effect of dark current becomes increasingly important as the amount of light, and therefore the photocurrent, is reduced: at the point where $i_p = i_d$, the improvement produced by removing the dark current would be $\sqrt{2}$, and this photocurrent is represented by limit I in Fig. 7. Roughly speaking cooling produces a worthwhile improvement to the left of limit I. If i_d at room temperature is very small, i_p at limit I is also very small, and it may not be profitable to use the instrument at all in the region where cooling would produce an improvement, because an unreasonably long time constant would be required to produce a useful accuracy. This we found to be the case for our instrument using the E.M.I. cell: limit I occurs at about magnitude 6·5 for an Ao star, using the 120 cm telescope, and a resolution of 1·25 A near Hγ. With a bandwidth of $\frac{1}{2}$ c/s, corresponding to a time-constant of 1 sec, S/N is then about 1·2, so that to make $S/N = 15$, say, it would be necessary to use a time-constant of about 1 minute. For fainter stars or greater accuracy a still longer time-constant would be needed, and the time to record a spectral profile would be inconveniently long.

(ii) *Linearity*. The photometric linearity of the system was tested in the laboratory, using the inverse square law. A diffusing screen illuminated by a small lamp was placed in front of the slit, and the output of each channel was measured with the lamp at various measured distances from the screen. No departures from linearity were revealed by this test, which was accurate to about 1 per cent.

(iii) *Seeing compensation*.—The fluctuations in the cathode current of the signal cell due to seeing are proportional to i_p, whereas the shot noise is proportional to $\sqrt{i_p}$. Any seeing fluctuations which remain in the compensated record will therefore be larger in relation to shot noise fluctuations for brighter stars. The relative contributions of these two sources of fluctuations have been investigated by comparing compensated records from stars with records from a steady light source. Part of such a test, made with the 18 in telescope on an average night, is shown in Fig. 9. This shows recordings of several stars of different magnitudes, taken without scanning in wave-length, and with a slit corresponding to a resolution of about 1 A at Hγ. The amplifier gain was adjusted to give a convenient deflection in each case. Beside each stellar record is the record of a test lamp whose brightness was adjusted to give about the same deflection at the same amplifier gain, so that the amount of light reaching the signal cell from the lamp was the same as that from the star. The lamp records show only noise fluctuations inherent in the signal cell photocurrent (the dark current noise is insignificant), while the stellar records contain additional fluctuations due to imperfect seeing compensation. Only for the brightest stars are the fluctuations in the stellar record appreciably greater than those in the corresponding lamp record.

From similar tests with the 120 cm telescope it is found that on an average night with resolution 1·25 A at Hγ the residual seeing fluctuations are equal to the photocurrent shot noise fluctuations for an A0 star of magnitude 2·5. This condition of equality is shown in Fig. 7 as limit II, and curve C represents the actual performance of the instrument with this imperfection of compensation taken into account. Some of the imperfection may be due to scintillation in colour, but we are not satisfied that the effects of non-uniformity of the cell cathodes have been completely eliminated.

(iv) *Variation of sensitivity with wave-length.*—The variation of the sensitivity of the instrument with wave-length is usually unimportant when single absorption lines are scanned, but it must be determined when intensities are to be compared over a large wave-length range. The instrument in this context includes the telescope and the atmosphere. In the case of the nebular work described below the wave-length response was calibrated by scanning the continuum of a star of known colour temperature at the same altitude as the nebula.

The useful wave-length range of the instrument is roughly 3950 A to 6000 A. The fall-off in sensitivity at the long wave-length end is due to the photocathode, and at the short wave-length end to absorption by the glass of the prisms.

5. *Some applications of the instrument.* (i) *Observations of profiles of stellar absorption lines.*—A programme of observations of time changes in absorption line profiles of variable stars was begun at Manchester and is being continued at Asiago. Fig. 8 shows a typical record of the Mg II λ4481 line in the spectrum of Algol, taken at Manchester with a resolution of 0·6 A, which is near the maximum resolution of the instrument. The record is on the large chart of the Speedomax recorder, and several successive scans of the line were superimposed by turning the chart back to the same point at the beginning of each scan. The noise is predominantly that inherent in the photocurrent. In this respect it is interesting to compare this record with Fig. 5 (*a*), which shows the same line at the same resolution in the spectrum of a much brighter star, Vega. There the fluctuations are predominantly due to imperfections of compensation.

It is worth noting that for stars which are so faint that it would take too long to record satisfactory line profiles, records suitable for the precise determination of equivalent widths may be obtained with wider slits.

(ii) *Measurement of relative line intensities in the spectra of planetary nebulae.*—The instrument is particularly suited to the determination of relative intensities of emission lines in the integrated light of planetary nebulae, and a programme of such measurements is also in progress at Asiago. For this purpose the entrance slit is made wide enough to pass the whole of the image of the nebula, and an equal or slightly larger exit slit passes each monochromatic image in turn as the wave-length drum is turned. The resolution of the instrument used in this way depends on the size of the nebula.

Part of a record from the planetary nebula NGC 6543 is shown in Fig. 10. A complete analysis of observations of this nebula will be given elsewhere, but it is interesting to note the large intensity range conveniently covered by the instrument. The intensity of Nl, for example, is more than 300 times that of He II λ4686; to accommodate such differences the calibrated attenuator in the amplifier was adjusted between lines to give convenient deflections on the recorder.

6. *Acknowledgments.*—The authors are grateful to Professor L. Rosino and to the authorities of the University of Padua for permission to use the 120-cm telescope at Asiago, and for generous help given; also to Dr H. J. J. Braddick for his help and advice, and to several other colleagues who have assisted with the observational work.

One of us (J. E. G.) is grateful to the Department of Scientific and Industrial Research for a grant during the tenure of which the first part of the work described in this paper was carried out.

The Physical Laboratories,
University of Manchester:
1956 *May* 17.

References

(1) P. Jacquinot and C. Dufour, *J. rech. cent. nat. rech. sci.*, Labs. Bellevue (Paris), **6**, 91, 1948.
(2) W. A. Hiltner and A. D. Code, *J. Opt. Soc. Am.*, **40**, 149, 1950.
(3) P. Guérin and M. Laffineur, *C. R. Acad. Sci (Paris)*, **17**, 1692, **1954**.
(4) P. P. Dobronravin and V. B. Nikinov, *Publ. Crimean Astr. Obs.*, **13**, 32, 1955.
(5) See, for example, H. J. J. Braddick, *The Physics of Experimental Method*, p. 342, London, 1954.
(6) R. W. Engstrom, *J. Opt. Soc. Am.*, **37**, 420, 1947.

SURFACE PHOTOMETRY OF THE GLOBULAR CLUSTERS 47 TUCANAE AND OMEGA CENTAURI

S. C. B. Gascoigne and E. J. Burr

(Communicated by the Commonwealth Astronomer)

(Received 1956 March 16)

Summary

Photoelectric measurements of surface brightness, colour and integrated magnitude have been made for the globular clusters ω Cen and 47 Tuc. For ω Cen the integrated photographic magnitude is 4·25, mean colour 0·68 and absolute magnitude −10·45, or $2{\cdot}0 \times 10^6$ suns. For 47 Tuc the corresponding figures are: P, 4·7; $P-V$, 0·67; absolute magnitude −10·0, or $1{\cdot}3 \times 10^6$ suns. The two clusters do not follow the same law of luminosity distribution, and the light profile of 47 Tuc resembles quite closely that found by de Vaucouleurs for elliptical galaxies. 47 Tuc is redder at the centre than in the wings.

1. In recent years there has been a marked revival of interest in the dynamical theory of globular clusters and the closely related one of elliptical galaxies, papers on the subject having appeared from Camm (**1**), Kurth (**2**), Belzer, Gamow and Keller (**3**), de Vaucouleurs (**4**), Woolley (**5**) and others. A primary requirement of such theories is that they account satisfactorily for the observed variation of surface brightness across a cluster. It is therefore important that data be available against which they can be tested. All previous work in this field has been photographic, the most recent having been published in 1936 (**6**). Since that time the superiority of photoelectric methods has become clearly established, and there can be no doubt of the advantages to be gained by their application to this type of problem in particular. A second of the factors which has led to the present programme is that 47 Tuc and ω Cen, the two brightest and largest globular clusters, and hence the most suitable for this kind of investigation, are accessible only to southern observers. Finally these objects are of considerable intrinsic importance, and are badly in need of better colours and magnitudes.

Two difficulties are inherent in this kind of work. First, because a cluster consists of a finite number of stellar sources its light distribution is highly discontinuous, and to admit any sort of interpretation must be smoothed. While the smoothing may be achieved easily enough—photographically, by using extra-focal plates, or photoelectrically, by scanning through a hole of finite aperture—it is difficult in practice to decide on just what degree of smoothing to adopt, and each cluster tends to become a particular case. Secondly, the cluster is seen against a background, or more accurately through a foreground, of field stars, night sky emission and general diffuse radiation. The fluctuations in this foreground are difficult to take into account, and set a limit to the faintness of the outer regions which can be detected, and to the accuracy of the photometry as a whole.

The observations described in this paper were made with a 1P21 multiplier and photometer, on loan to one of us from the Lick Observatory. The multiplier current was amplified in a d.c. amplifier, made by Mr D. G. Thomas to a design of Dr G. E. Kron, and recorded on a Brown recording potentiometer (except for Fig. 1 (*c*), which was recorded on an Esterline–Angus). Blue and yellow filters were used to transmit spectral ranges corresponding closely to the International *P* and *V* systems. The yellow filter was 2 mm of Schott GG 11, and the blue 1 mm of Schott BG 12 together with 1 mm of Chance OY 10, the function of the latter being to exclude the ultraviolet. The photometer was used either at the Cassegrain focus of the 30-inch Reynolds reflector, or with the 9-inch Oddie refractor. The clusters were measured through holes of different diameters, and were also scanned along a diameter from west to east, by stopping the telescope drive or altering its rate. North–south scanning was not practicable.

It is convenient to collect here some of the principal data relating to 47 Tuc and ω Cen, and also to summarize some of the main results of this paper. The distances and moduli are from a compilation of Shapley's (**7**); both are uncertain, especially for 47 Tuc. The distance to the galactic centre has been taken as 8·4 kpc. The distance moduli are apparent (i.e. not corrected for absorption).

TABLE I

	47 Tuc	ω Cen
Right ascension (1900)	$00^h\ 22^m$	$13^h\ 24^m$
Declination (1900)	$-72°\ 21'$	$-47°\ 03'$
Longitude (*l*)	272°	277°
Latitude (*b*)	−45°	+15°
Distance from sun	7·6 : kpc	6·8 kpc
Distance from galactic centre	8·6 : kpc	6·4 kpc
Distance from galactic plane	5·4 kpc	1·7 kpc
Concentration class	III	VIII
Apparent distance modulus ($m-M$)	14·7	14·7
Total magnitude (*P*)	4·7	4·25
Absolute magnitude (*P*)	−10·0	−10·45
Luminosity	$1·3\times10^6$	$2·0\times10^6$
Mean colour (*P*–*V*)	0·67	0·68
Central brightness (*P* mag/sq. sec)	15·2	17·6
Effective radius	2′·7 = 6·0 pc	5′·05 = 10·0 pc
Maximum radius	22′ = 48 pc	40′ = 79 pc

2. *Observations of 47 Tuc.*—The following observations were made of 47 Tuc:

(i) measurements in blue and yellow of the light received through apertures of various diameters, from 41″ upwards. These are detailed in Table II. The observations on the 9-inch were made on three nights.

(ii) two-colour measurements on the 30-inch reflector through a 58′ hole at about a dozen points, distant up to 12′ from the centre. These observations were also made on three nights.

(iii) scans in blue and yellow through a 58″ hole on the Reynolds at diurnal speed (4′·55 per minute of time).

(iv) scans in yellow at 0·2745 diurnal speed (1′·25 per minute of time), made on the Reynolds through 16″, 26″ and 58″ apertures. Two of these are reproduced in Fig. 1.

(v) a scan in yellow at diurnal speed through an aperture of 9′ diameter on the 9-inch refractor,

The measurements were reduced to zero air-mass and referred to the P, V system by observations on the same night of stars in one of the Harvard Standard Regions C 12, D 2, E 9 (**8**). (In this paper P and V mean IPg and IPv as defined by the Cape Observers). The connection between IPv and IPg and Johnson and Morgan's V and B is :

$$V = \text{IPv}; \quad B = 0{\cdot}91\ \text{IPg} + 0{\cdot}09\ \text{IPv} + 0{\cdot}16.$$

On a few occasions the star β Oct was used as intermediary, although because of the wide difference between its colour and that of the cluster it was not very suitable for this purpose. Our magnitude and colour for this star agree to within 0·01 mag with those found at the Cape (**9**).

To combine the above data into a light profile for the cluster we have to take into account field stars, irregularities and lack of circular symmetry in the cluster itself, and distortions introduced by the finite size of the scanning aperture and by the response time of the amplifier and recorder. The nature of some of these difficulties is illustrated by Fig. 1, which shows scans at 1′·24 per minute through

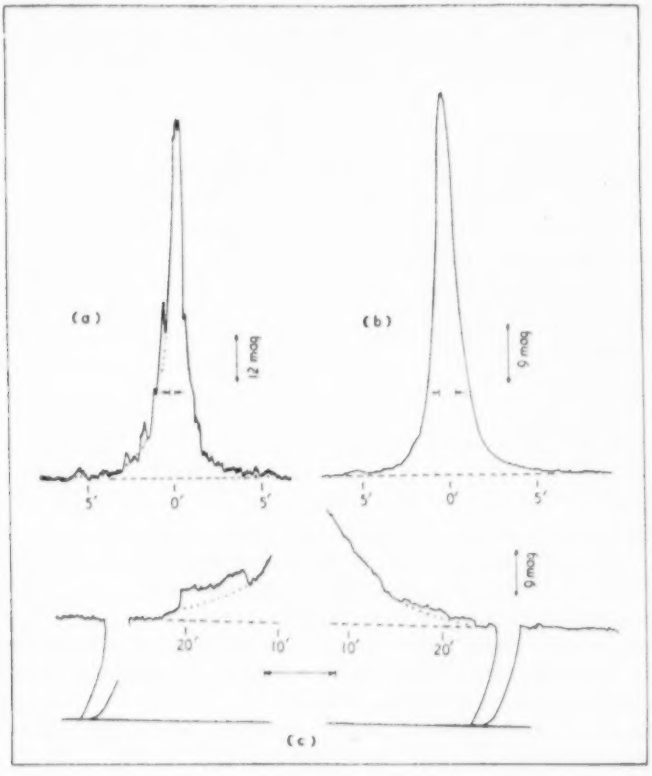

FIG. 1.—*(a) Scan of 47 Tuc made in yellow with a 16″ diameter hole at 0·2745 diurnal speed (1′·25 arc per minute); (b), as (a), with a 58″ diameter hole, and (c), a scan in yellow at diurnal speed through a 9′ diameter hole : (c) was made with an Esterline–Angus recorder. In each record the broken horizontal line indicates the sky background, the full line zero illumination. The magnitude scales, hole diameters and distances from the centre are also indicated.*

holes of 16″ and 58″ diameter, and at 4′·55 per minute through a 9′ hole. The smoothing introduced by the larger holes is very noticeable. The distortion which arises from the finite response time of the recorder is less obvious. Particularly in the central region where the brightness is changing rapidly, the recorder pen is unable to keep up with the light signal at the scanning speeds available. It was decided in consequence to derive the brightness within a radius of about 60″ from the data in Table II. If the surface brightness in units of a tenth magnitude star per square minute of area is denoted by f, and the light emitted within a radius r by $l(r)$, we have

$$l(r) = 2\pi \int_0^r rf(r) \, . \, dr.$$

Table II gives the $l(r)$ for various values of r. These values were plotted against r^2, as shown in Fig. 2, and a smooth curve drawn through them and differentiated graphically to give f. In particular the brightness at the centre corresponds to the slope of the curve at the origin.

TABLE II

Light received from 47 Tuc and ω Cen through circular apertures of various diameters, expressed in terms of that of a tenth magnitude star. Sky corrections have been applied

Telescope	Diameter	V	P	$P-V$
		47 Tuc		
9-inch refractor	41″ arc	16·2	8·0	$0·76_5$
	63	29·6	14·8	75
	100	47·7	25·2	69
	154	72·6	38·9	68
	223	95·1	51·0	67_8
	543	155·6	84·1	67
sky	543	6·0	3·5	
30-inch reflector	58	28·8	14·4	0·75
	116	54·5	28·1	72
		ω Cen		
9-inch refractor	100″ arc	13·3	6·6	0·76
	154	28·8	15·5	67
	223	54·0	28·4	70
	543	180·3	97·5	67
30-inch reflector	26	1·00	0·495	76

The 47 Tuc observations with the 9-inch are the means of three nights. Other observations refer to one night only. The observations on the 30-inch through the 116″ hole was made at the Newtonian focus, the others at the Cassegrain focus.

Unpublished star-counts of 47 Tuc to 16 mag, kindly made available by Dr de Vaucouleurs, indicate that the cluster is elliptical, the ratio of the axes being $0·92 \pm 0·02$, and the position angle of the major axis $37° \pm 1°$. As this is also the angle between the minor axis and the diameter along which our scans were made, it seemed unnecessary to make corrections for ellipticity when deriving the integrated magnitude of the cluster. No evidence was found for E–W asymmetry.

In the outer regions the values for the surface brightness were combined from the various scans. It is clear that no one scan can cover more than a limited region of the cluster. The irregularities must be almost entirely inherent in the cluster. In Fig. 1 (*a*) for example there is only a ten per cent chance of a field star

brighter than 14 mag occurring in the strip measured (16″ wide by 15′ long). The profile actually adopted is shown by the dotted lines. The arbitrary nature of these lines seems unavoidable. In the case of Fig. 1 (*c*) a correction for the finite size of the scanning aperture shows the true curve to lie slightly within the

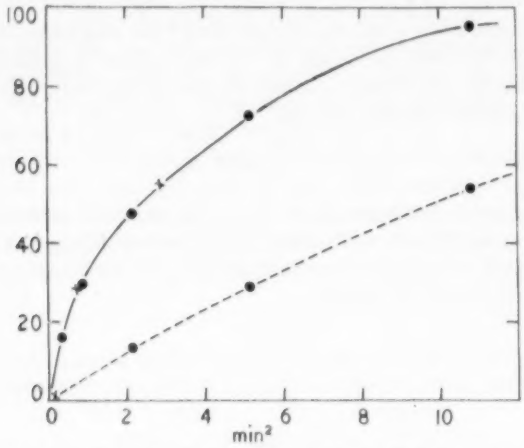

FIG. 2.—*The light received from 47 Tuc (full line) and ω Cen (broken line) through circular apertures of various diameters. The light, expressed in terms of that of a tenth visual magnitude star, is plotted against the area of the hole in square minutes.*

observed curve (**10**). According to this scan the brightness of the cluster drops off very rapidly at the edge, and it cannot be traced photoelectrically beyond a radius of 22′, when its brightness is about five per cent of that of the sky. This radius is almost certainly an underestimate. Shapley's value, derived from microphotometer tracings, is 27′, and de Vaucouleurs' star counts indicate a radius of at least 40′ and possibly 60′. The sky brightness was found to be 13·2 mag/sq min, or 22·1 mag/sq sec (pg); this is reasonable for a latitude of −45°.

Information on the colour of the cluster and on its variation with radius can be extracted from (i), (ii), and (iii) above. Thus from the data in Table II, we find the colours in successive annuli to be:

Annulus :	0″–20½″	20″–31½″	31½″–50″	50″–77″	77″–111½″	111½″–271½″
Colour :	0·77	0·74	0·60	0·65	0·67	0·65$_5$

These results are plotted in Fig. 3, together with the colours derived from measurements at various points (ii), and from two-colour scans (iii). Some of the plotted points therefore refer to whole zones, and others only to small regions. Even so the agreement is not good. The annular measurements are the means of three nights and should be reasonably free from observational error. The effect of field stars should be negligible.

The major effect here is probably that the hole used (area 0·72 sq min) was too small to take a good sample of the cluster. Sandage (**11**) found that 0·20 of the light of M3 came from stars with M_v brighter that −1·8. If this is true for 47 Tuc, a fifth of the light will come from stars of apparent magnitude brighter than 12·5. 5′ from the centre the surface brightness is equivalent to 4·1 stars of mag 12·5 per square minute (Table III). Thus there is about a sixty per cent

chance of a star brighter than 12·5 mag appearing in the hole used here, while the total light measured through the hole is only that from about three such stars. The corresponding fluctuation in colour could easily be a tenth of a magnitude. A corollary to this is that unless holes of large angular size can be used, star counts will give a more satisfactory picture than will a photometer of the outer structure of globular clusters.

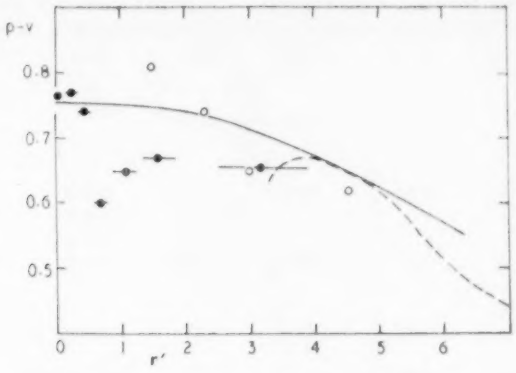

FIG. 3.—*Variation of colour with radius in 47 Tuc. Filled circles, means of annuli; open circles, measurements at points along the diameter of position angle 90°. The horizontal lines indicate the widths of the annuli. The broken line was derived from two-colour scans, and the full line is that adopted.*

But in spite of the large scatter there seems little doubt that 47 Tuc is bluer in the wings than in the centre. This effect had been foreshadowed by Stebbins, who in the course of a description of some photoelectric measurements of globular clusters said: "Probably most of these clusters have varying integrated colour from centre to outside. We have found as much as 0·17 difference on the V–I scale, (0·06 on the P–V scale) inner redder than the outer region, but a study of this difference will involve a check upon the possible instrumental effects" (**12**). In the present work the unexpected feature is therefore not so much the existence of the effect as its magnitude.

Colour differences of this sort may be significant. An immediate interpretation is that the blue stars in globular clusters are to be found farther from the centre, and hence are less massive than the red stars; this is at variance with current ideas, which suppose that almost all the light of globular clusters comes from stars of substantially the same mass.

Final results are collected in Table III. Columns 4 and 5 show $l(r)$, the amount of light within a radius r. It will be shown later in the paper that, except near the centre of the cluster, the logarithm of the surface brightness decreases very nearly as $r^{1/4}$. If we assume that this law continues to hold, the contribution to the integrated magnitude beyond the observable region (22′) is 0·05 mag; this figure is probably an upper limit. The integrated visual magnitude of 47 Tuc is then 4·01 ± 0·05 say, and the mean colour is 0·67. This gives a mean photographic magnitude of 4·68: Shapley's estimate was 4·5 (**7**). Half the light of the cluster is found within a radius of 2′·7, or 6·0 parsecs at the distance assumed in Table I.

TABLE III

Photometric measurements of 47 Tucanae

(1)	(2)	(3)	(4)	(5)	(6)	(7)	(8)
″							
0	60·2	0·75	0·0		82·3	445	0·00
10	49·6				63·2	341	0·37
20	31·1				28·6	154	0·73
30	21·1		26·1	6·46	14·5	78·1	1·10
40	15·4				8·63	46·6	1·47
50	11·7				5·67	30·6	1·83
60	8·9	0·75	57·3	5·61	3·93	21·2	2·20
70	6·8						2·6
80	5·5				1·87	10·1	2·9
90	4·5		81·4	5·23			3·3
100	3·7				1·03	5·6	3·7
110	3·13						4·0
120	2·65	0·74	100·5	5·00	0·621	3·35	4·4
140	1·98				0·416	2·25	5·1
160	1·62				0·274	1·48	5·9
180	1·19	0·71	127·9	4·74	0·198	1·07	6·6
200	0·96						7·3
220	0·79						8·1
240	0·66	0·67	147·1	4·58	0·0834	0·45	8·8
′							
5	0·41	0·62			0·0417	0·225	11·0
6	0·280				0·0243	0·130	13·2
7	0·202		183·1	4·35			15·4
8	0·150				0·0099	0·054	17·6
9	0·114						19·8
10	0·090		203·3	4·23	0·0050	0·027	22·0
12	0·058				0·00297	0·016	26·4
14	0·038				0·00181	0·0098	30·8
16	0·025		227·1	4·11	0·00112	0·0061	35·2
18	0·017				0·00071	0·0039	39·6
20	0·010				0·00044	0·0024	44·0
22	0·007 :		237·6	4·06	0·0003 :	0·0015 :	48·4
sky	0·09						

Columns (1) *and* (8) *are distances in angular measure and in parsecs. Column* (2) *is the surface brightness in tenth visual magnitude stars per min*^{2}. *Column* (3) *is the P–V colour, and the total light inside a radius r is shown in column* (4) *as a number of tenth magnitude stars, and in column* (5) *in stellar magnitudes (both visual). Column* (6) *is the space density in tenth magnitude stars per cubic minute and column* (7) *the space density in stars of zero absolute magnitude per cubic parsec.*

3. *Observations of ω Cen.*—The following observations were made of ω Cen:

(i) measurements in blue and yellow of the light received through apertures of various diameters. These are detailed in Table II.

(ii) scans in yellow through a 140″ diameter hole on the 30-inch reflector at a speed of 10′·2 arc per minute of time

(iii) scans in yellow through a 26″ diameter hole on the 30-inch reflector at a speed of 2′·81 arc per minute of time (one of these is reproduced in Fig. 4).

The measurements were reduced to zero air-mass as before and related to the *P*, *V* system by observations of stars in E6 (**8**).

The reductions proceeded much as before. The surface brightness of ω Cen varies less rapidly but is rather more irregular than that of 47 Tuc. As

with 47 Tuc the bumps on the wings are almost certainly inherent, and the profile was drawn through them, as shown in Fig. 4. The dip in the centre is real, and must be due either to a deficiency of cluster stars or to a highly localized patch of absorbing matter (cf. Plate 2 of reference (**13**)). Such irregularities are not uncommon in globular clusters. In default of a better procedure it was decided to draw a smooth curve through the dip, and to determine the brightness in the central regions as before, by graphical differentiation of the data in Table II. In this computation it was necessary to take into account the well-known departure

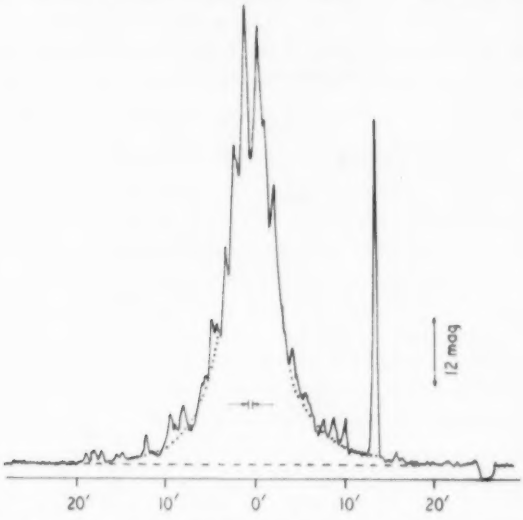

FIG. 4.—*A scan of ω Cen in yellow through a 26″ diameter hole at 0·2745 diurnal speed (2′·81 arc per minute of time). The full horizontal line indicates zero illumination, the broken line the sky background. The dotted line is the adopted curve.*

from circular symmetry of ω Cen. From a study of Schilt's photographic measures (**14**) and Shapley's star counts (**15**), it was decided that the isophotes could be represented well enough by a series of concentric ellipses with major axes all directed east and west. Combining as much data as possible to smooth out local irregularities, the ratio of the axes b/a was estimated as a function of the semi-major axis a from Schilt's Fig. 1 ($a<9'$) and from Shapley's star counts ($4'{\cdot}5<a<14'$). The resulting points and the adopted curve are shown in Fig. 5. The curve has been extrapolated on the assumption that the isophotes are circular when a is very small or very large.

The results are collected in Table IV. As has been pointed out, the figures for the innermost minute represent a considerable degree of smoothing. The colours of the annuli, derived from Table II, are as follows:—

Annulus :	0–100″	100″–154″	154″–223″	223″–543″
Colour :	0·76	0·60	0·73	0·66, all ±0·03.

These figures are again much more irregular than would be expected, but as they stand hardly suggest any systematic colour variation in ω Cen. More observations are needed to clear up this point.

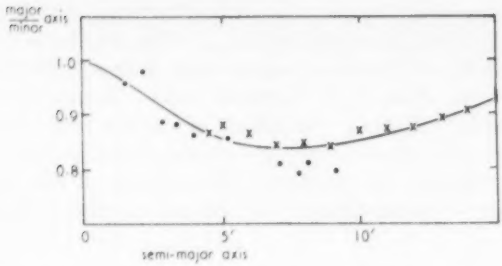

FIG. 5.—*Ellipticity of ω Cen. The filled circles are from Schilt's surface photometry, the crosses from Shapley's star counts.*

TABLE IV

Photometric measurements of ω Centauri

(1)	(2)	(3)	(4)	(5)	(6)	(7)	(8)
′							
0	6·65			1·00	1·37	12·9	0·0
½	6·4						1·0
1	5·7	18·7	6·82	0·98	1·09	10·3	2·0
1½	4·8						
2	4·1	59·6	5·56	0·94	0·67	6·3	4·0
2½	3·4						
3	2·8	105·9	4·94	0·91	0·38	3·6	5·9
4	1·75	148·0	4·58	0·87	0·218	2·16	7·9
5	1·14			0·85	0·125	1·18	9·9
6	0·73	205·5	4·22	0·84	0·072	0·68	11·8
7	0·51			0·84	0·0427	0·40	13·8
8	0·38	244	4·06	0·84	0·0266	0·25	15·8
9	0·29			0·85			17·8
10	0·221	272	3·91	0·85	0·0145	0·137	19·8
11	0·160			0·86			21·7
12	0·116	292	3·84	0·87	0·0070	0·067	23·7
14	0·065	303	3·80	0·90	0·0030	0·028	27·6
16	0·044	312	3·77	(0·92)	0·00154	0·0145	31·6
18	0·034	319	3·74	(0·94)			35·6
20	0·0265			(0·96)	0·00074	0·0070	39·5
24	0·0167				0·00043	0·0040	47·4
28	0·011			(1·00)	0·00029	0·0027	55·3
32	0·0071				0·00016	0·0015	63·2
36	0·0041			1·00	0·00010	0·0009	71·1
40	0·002 :	363	3·60				
sky	0·20						

Columns (1) *and* (8) *are radii in angular measure and in parsecs. Column* (2) *is the surface brightness in tenth visual magnitude stars per min*^{2}. *The light inside a radius r is shown in column* (3) *as the equivalent number of tenth magnitude stars, and in column* (4) *in stellar magnitudes. Column* (5) *is the ratio of the axes, column* (6) *the space density in tenth magnitude stars per cubic minute, and column* (7) *the space density in zero absolute magnitude stars per cubic parsec.*

40′ from the centre the brightness of the cluster has fallen to about one per cent of that of the sky. The resulting diameter of 80′ is rather larger than the 65′·4 found by Shapley (7). The sky was found to be about 0·8 mag brighter than in the vicinity of 47 Tuc. It is to be emphasized that all our sky measures are the

means of a number of areas, chosen to avoid either abnormally dark patches or conspicuously bright field stars. Out to 40′ the integrated visual magnitude is 3·60. To extrapolate beyond this point we assume that the logarithm of the surface brightness continues to decrease as $r^{1.4}$ (cf. Section 4). The contribution from the unobserved part is then 0·03 mag and the total 3·57. The mean colour is 0·68. This gives a mean photographic magnitude of 4·25, appreciably brighter than Shapley's 4·7 (:). Half the light is concentrated within a radius of 5′·05, or 10 parsecs.

We note here that half the variables are contained within a radius of 6′·7 arc. From the open nature of this cluster it seems unlikely that many can have been missed, even in the centre. This may be an indication that the variables are less massive than the stars which produce most of the light of the cluster.

Schilt's measurements have been referred to above. After an adjustment has been made to the zero of his calibrating stars, his figures agree with ours to about 0·05 mag in the mean. In view of the unsatisfactory magnitudes Schilt had to use for these stars, this agreement is as close as could be expected.

4. *Discussion.*—It has been supposed for many years that globular clusters obey a common law of luminosity distribution, although the only real evidence for this statement seems to be a photographic investigation by Lohmann (**6**), who, after allowing for scale factors, found substantially identical distributions for the light in the clusters, M5, M15 and M92. Star counts have also been used as basis for this comparison, and recently a very good series has been published for M92 by Tayler (**16**). Our results are compared with Lohmann's and Tayler's in Fig. 6, where we plot log f/f_c against r/r_c, f_c being the brightness (or star count)

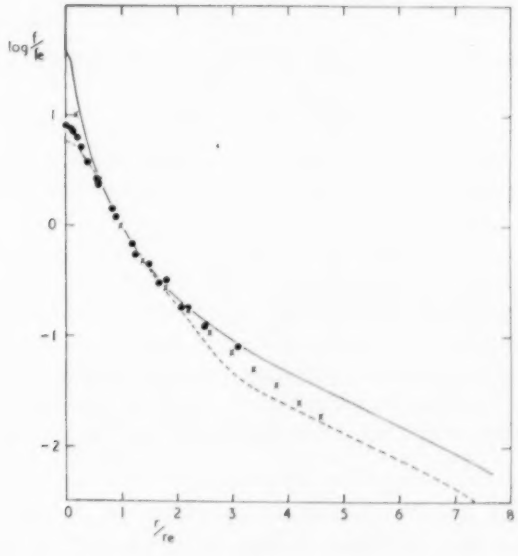

FIG. 6.—*Relative brightness as a function of relative radius for a number of globular clusters. The full line is 47 Tuc, the broken line ω Cen. The circles are Lohmann's photographic results from M5, M15, and M92, the crosses Tayler's star counts for M92.*

at the effective radius r_e, i.e. that which contains half the light of the cluster. From Lohmann's work the effective radii for M5, M15 and M92 were found to be 100″, 58″ and 75″ respectively.

In the figure the full line is 47 Tuc, the broken line ω Cen, the points Lohmann's (from three clusters) and the crosses Tayler's. It is clear that 47 Tuc and ω Cen differ significantly both from each other and from Lohmann's and Tayler's clusters. On the other hand Lohmann's and Tayler's data confirm each other well, as they should, for the stars Tayler counted supply almost all the light of the cluster, and he found their radial distribution to be largely independent of magnitude.

Three comments may be made. First both 47 Tuc and ω Cen are abnormal in being at least four times brighter intrinsically than any other globular cluster. Secondly, there is a steady gradation in concentration class from III for 47 Tuc through IV and V for Lohmann's clusters, to VIII for ω Cen: as will be shown shortly the reality of this gradation is supported by measurements of absolute surface brightness. Finally our method of smoothing the centre of ω Cen may not be free from objection. However, the differences in Fig. 6 seem well in excess of any observational error.

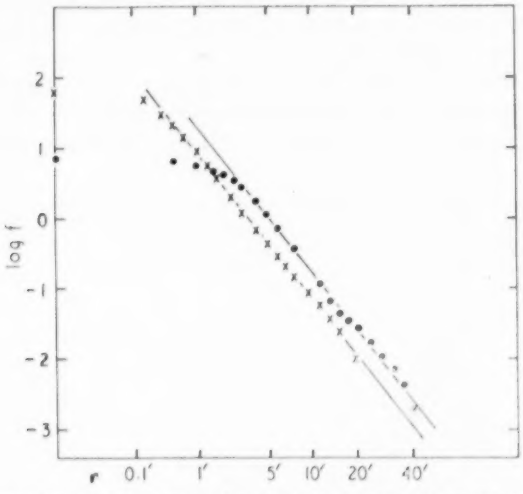

FIG. 7.—*Log surface brightness against the fourth root of the radius for 47 Tuc (crosses) and ω Cen (dots).*

An interesting comparison can be made between the brightness distributions in 47 Tuc, ω Cen and the elliptical galaxies. Of the various empirical laws which have been proposed for the latter we select that of de Vaucouleurs (**4**). This is

$$\log f/f_e = -3{\cdot}33\{(r/r_e)^{1/4} - 1\}$$

f_e and r_e defined as above.* In Fig. 7 we plot log f for the two clusters against $r^{1/4}$, r in minutes. Over a brightness range of 3000 the 47 Tuc points lie within $\pm$ 0·03 of a straight line, and the deviations from the line are in the same sense as

* de Vaucouleurs (private communication) considers the figure 3·33 preferable to the 3·25 which he originally suggested.

those of elliptical galaxies (cf. Fig. 2 of (**4**)). But according to de Vaucouleurs the central brightnesses of elliptical galaxies is about 160 times the brightness at the effective radius, whereas the corresponding figure for 47 Tuc is only about 40.

The ω Cen observations also fit a straight line, over a brightness range of about 1000, though the deviations are greater than with 47 Tuc. For distances from the centre greater than about 3′ the two clusters follow the same brightness law to within better than 20 per cent, and differ only in that ω Cen is relatively much fainter in the centre. That the two lines have the same slope is of course only a coincidence. With an elliptical galaxy this slope would correspond to an effective radius of 2′·61; with the clusters the true effective radius is larger, because of the lower central intensity.

The absolute central brightness of 47 Tuc is considerably in excess of that of other globular clusters. The following table, which includes some figures for elliptical galaxies, illustrates the point:

TABLE V

Central brightnesses of some globular clusters and galaxies, in numbers of tenth photographic magnitude stars per square minute

	Globular Clusters				
Cluster	47 Tuc	M 15	M 92	M 5	ω Cen
Concentration class:	III	IV	IV	V	VIII
Central brightness:	30	8·5	6·55	4·4	3·4
	Elliptical Galaxies				
NGC numbers:	221	3115	3379	4494	4649
Type:	E2	E7	E0	E0	E2
Central brightness:	100	12	21	10	7

Note, *inter alia*, the tendency in the globular clusters for central brightness to vary regularly with concentration class.

We derived ϕ, the light emitted per unit volume, from the equation

$$\phi(r) = -\frac{1}{\pi}\int_r^R \frac{f'(x)}{(x^2-r^2)^{1/2}}\,dx,$$

where f is the surface brightness and R the cluster boundary (**17**). To avoid the infinity in the integrand we replaced x^2 by r^2+z^2; the integral then becomes

$$\phi(r) = -\frac{1}{\pi}\int_0^Z g\,(\sqrt{r^2+z^2})\,dz.$$

We have written $g(r)$ for $f'(r)/r$, and the upper limit $(R^2-r^2)^{1/2}$ is denoted by Z. The function g, which is always finite, was found by numerical differentiation of $\log f$, and plotted on semi-log paper, the requisite interpolations being made graphically. This scheme, which worked well, seems simpler and more convenient than others which have been proposed (**18, 19**). The contributions to ϕ for z larger than about $2r$ were small, and for practical purposes the upper limit could be taken as infinite. For points near the observed boundary it was necessary to extrapolate. For 47 Tuc we did this by assuming that the surface brightness continued to fall according to de Vaucouleurs' law; with ω Cen the experimental law $\log f = -0{\cdot}62-0{\cdot}048r$ was better for large r. The values of ϕ for these points may therefore be rather uncertain.

The space densities are shown in column 6 of Table III for 47 Tuc, and in the same column in Table IV for ω Cen, in units of a tenth visual magnitude

star per cubic minute. In column 7 in each table we have converted these to zero absolute visual magnitude stars per cubic parsec. This step requires a knowledge of the cluster distances, but this is not critical, a half-magnitude error in the modulus producing a change of only twenty per cent in the conversion factor. Averaging over stars within ten parsecs we find that in the region of the Sun the light emission is equivalent to that from 0·0005 stars of zero absolute magnitude per cubic parsec. That at the centre of ω Cen is about 30000 times, and at the centre of 47 Tuc about a million times this figure. To an observer at the centre of 47 Tuc the light of the stars would be equivalent to that from several thousand full moons, and the resulting illumination quite comparable with terrestrial twilight.

Acknowledgments.—The writers would like to thank Professor R. v. d. R. Woolley for the continued interest he has shown in this work, Dr de Vaucouleurs for the use of his star counts of 47 Tuc and for some valuable criticism, and Mr D. G. Thomas for constructing and maintaining the amplifier. Our principal obligation is, however, to the Director of the Lick Observatory, Dr C. D. Shane. Without his very generous loan of a multiplier and photometer it would not have been possible to undertake the programme described here.

Commonwealth Observatory,
Mount Stromlo,
Canberra, Australia
1956 *March* 8.

References

(1) G. L. Camm, *M.N.*, **112,** 155, 1952.
(2) R. Kurth, *A.N.*, **282,** 97, 1955.
(3) J. Belzer, G. Gamow and G. Keller, *Ap. J.*, **113,** 166, 1951.
(4) G. de Vaucouleurs, *M.N.*, **113,** 134, 1953.
(5) R. v. d. R. Woolley, *M.N.*, **114,** 620, 1954.
(6) W. Lohmann, *Zeit. f. Ap.*, **12,** 1, 1936.
(7) H. Shapley, *Pop. Astr.*, **57,** No. 5, 1949 (=H. R. 320).
(8) C 12 and D 2 from Kron, *Ap. J.*, **118,** 502, 1953 and unpublished work; E 6 and E 9 from Cape Mimeogram No. 3, 1953.
(9) Cape Mimeogram No. 1, 1953.
(10) E. J. Burr, *Aust. J. Physics*, **8,** 30, 1955.
(11) A. R. Sandage, *A. J.*, **59,** 162, 1954.
(12) J. Stebbins, *M.N.*, **110,** 420, 1950.
(13) W. Chr. Martin, *Leid. Ann.*, **17,** pt. 2, 1938.
(14) J. Schilt, *A.J.*, **38,** 109, 1928.
(15) H. Shapley, *Star Clusters*, McGraw-Hill, 1930, p. 93.
(16) R. J. Tayler, *A.J.*, **59,** 413, 1954.
(17) W. Smart, *Stellar Dynamics*, C.U.P., 1938, p. 301.
(18) H. G. van Bueren, *B.A.N.*, **11,** 403, 1952.
(19) I. King, *P.N.A.S.*, **31,** 684, 1950 (=H.R. 340).

A NOTE ON THE SPECTRA OF SOME VARIABLE STARS IN THE MAGELLANIC CLOUDS

M. W. Feast

(Communicated by the Radcliffe Observer)

(Received 1956 June 7)

Summary

Spectra (86 A/mm at $H\gamma$) have been obtained of a number of variables in both Magellanic Clouds. Four long period cepheids in the Small Cloud and six in the Large Cloud show normal supergiant spectra of late F and early G type near maximum. There appears to be no spectroscopic evidence for their being other than normal Population I cepheids. HV 2882 is a foreground Me variable. The R CrB variable W Men is a member of the Large Cloud and has an absolute magnitude at maximum of $-5^{m}\cdot4$.

The long period cepheids.—This note gives the results of a spectroscopic study of some variable stars in the two Magellanic Clouds. The majority of stars considered are long period cepheids. These stars are of interest since it has been suggested that they may differ significantly from galactic Population I (classical) cepheids. Such a conclusion would be of far-reaching significance both for the interpretation of the Magellanic Clouds and also for all determinations of extragalactic distances based on the cepheids. The position has been summarized by Gascoigne (**1**). The discussion of the problem has up till now rested mainly on the results of photoelectric observations of Magellanic Cloud and galactic cepheids. The results given in Gascoigne's Fig. 15 show the cloud variables to be apparently bluer than the galactic ones. This led Gascoigne and Kron (**2**) to suggest that the cloud variables were in fact Population II (W Virginis) cepheids. Such a suggestion appears to be ruled out by the change in the distance of the Clouds (**3**) which indicates that the cloud variables have about the same luminosity as galactic Population I cepheids of similar periods. The discrepancy in the colours remains however and its interpretation as due to the underestimation of the reddening of galactic cepheids is not entirely favoured by Gascoigne (**1**). It is clear that spectroscopic work on the cloud variables might help to clarify the position.

The results on some Harvard variables classified as cepheids are given in Table I. There are four variables in the Small Cloud and six in the Large Cloud as well as one star which turns out to be a foreground object. The variables are arranged in order of increasing period and an approximate phase of the observation is given if available. The latter depend mainly on unpublished epochs kindly supplied by Dr Shapley and Mrs Nail. The possibility that some of these calculated phases may be in error must be borne in mind in discussing the observations, especially in view of Gaposchkin's work on HV 2447 (**4**) which indicates that the long period cepheids may be somewhat less regular in their behaviour than those of shorter period. The spectra from which the

types were estimated were all obtained with the *f*/2 camera (86 A/mm at Hγ) of the 2-prism spectrograph at the Cassegrain focus of the 74-inch Radcliffe reflector. In view of the faintness of the stars the spectra were not widened as much as is the usual practice in using the MK system and a few spectra were less well exposed than might have been desirable. However the spectral types should not be in error to any appreciable extent. The average exposure time for the spectra listed was about 270 minutes. The spectra were classified on the MK system by comparison with standard stars drawn from the list of Johnson and Morgan (**5**)

TABLE I

Cepheid Variables in the Magellanic Clouds

HV	Small or Large Cloud	Period	Date	Phase	Spectrum	Magnitude P	Colour (*P*–*V*)	
873	LMC	34·34	1956 Jan. 5	0·03	F8 I	[12·6–15·0]		
2294	LMC	36·53	1955 Dec. 1	0·13	F7 I(a)	12·6–15·3	0·3–1·6	
2195	SMC	41·78	1955 Dec. 1	0·94	Go I :	[12·6–14·2]		
2369	LMC	48·27	1956 Jan. 12	0·35	late F–early G	[12·0–14·2]		
834	SMC	73·5	1955 Sept. 9 1955 Oct. 8		F8 Ia F8 Ia	12·3–13·4	0·4–0·9	
829	SMC	88·5	1955 Aug. 16		Go I :	12·0:–13·4	0·35:–0·95	
5497	LMC	98·86	1956 Jan. 19	0·52	G2 I	[12·3–13·6]		(1)
2447	LMC	118·6	1956 Mar. 9	0·34	Go I	12·8–14·3	0·9–1·6	(3)
821	SMC	127	1953 Dec. 12 1955 Oct. 3	0·91 0·10	Go I G1 I	12·4–13·5	0·7–1·3	
883	LMC	134	1956 Jan. 12	0·22	G2 I :	12·5–14·3	0·8–1·5	
2882	Foreground	171·82	1956 Jan. 5	0·64	Me	[12·3–15·1]		(2)

(1) It appears doubtful if the variable was as faint as would be indicated by the calculated phase.
(2) K7e (HA100), Mb (HB 754) = HDE 270419.
(3) K5 (HA100) = HDE 269362.

Photoelectric magnitudes and colours from Gascoigne (**1**). Those in brackets are Harvard photographic.

The radial velocities of the stars were measured in a Hartmann spectrocomparator against the supergiant Go star β Aqr and were all found to agree well with the expected velocities for cloud members. In cases where more than one spectrum was available the agreement of the velocities is good. It is not considered desirable to publish the individual velocities at this stage since further work is contemplated on these and other variables. The velocities average +133 km/sec for the Small Cloud and +274 km/sec for the Large Cloud. HV 2882 has a low velocity indicating that it is a galactic, foreground, object. This is confirmed by the spectrum which shows TiO absorption and Hγ emission. It seems to be a normal Me variable.

The Magellanic Cloud variables appear to be normal late F and early G type supergiants. No abnormalities were noticed and in particular no emission lines were found which would have indicated them as possibly Population II

(W Virginis) cepheids. It is instructive to compare the present results with those found by Code (**6**) for galactic cepheids. He found that over the range of periods studied by him there was no change in spectral type at maximum with the period. Code's results and those of this note are shown in Fig. 1.

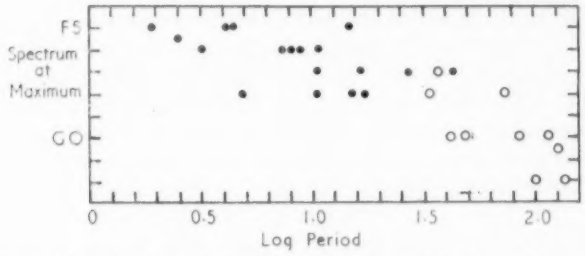

FIG. 1.—*Relationship between spectral type at maximum and log period for galactic cepheids, Code* (**6**) *(filled circles) and Magellanic Cloud cepheids (open circles).*

It should of course be borne in mind that a spurious dependence of type on period could result from the types used not referring exactly to maximum light, there being a strong dependence of type at minimum on period. However, the dependence of type on period which appears when the longer period stars are considered is borne out by the colours of the cloud variables (**1**) which also show a slight dependence on period.

It would appear that, although the Magellanic Cloud variables studied here have exceptionally high luminosities for obvious reasons of observational selection, there is no spectroscopic suggestion that they are other than normal Population I cepheids. In considering the problem of the difference in colour of the cloud and galactic cepheids Code's spectroscopic observations deserve to be given some weight for they indicate that for the range of periods studied by him the intrinsic colours should show little dependence on the period whereas Eggen's colours of Code's stars (**7**) show a marked increase of reddening with period, a phenomenon shown by galactic cepheids in general—see Gascoigne (**1**), Fig. 15. The constant spectral types make a good case for attributing the changes in colour to an underestimation of interstellar reddening, the effect being dependent on the period since the long period stars are brighter and on the average more distant. In fact a very recent paper by Stibbs (**8**) does indicate that galactic cepheids suffer much greater space reddening than hitherto supposed. It appears that the case for considering the Magellanic Cloud cepheids as normal Population I cepheids is now sufficiently strong for the intrinsic colours of the cepheids to be obtained from observations of these stars. This would probably lead to a somewhat greater space reddening of galactic cepheids than is found by Stibbs who used the space absorption deduced by Oort, van Rhijn and Parenago from B star colours, but this conclusion does not seem out of the question.

The R CrB variable W Men.—The variable W Men [$05^h\,27{\cdot}1-71°14$ (1950) $13^m{\cdot}8-16^m$ pg] was discovered by Luyten (**9**). As will be seen from its coordinates it lies in the direction of the Large Magellanic Cloud. Its importance lies in the fact that it is an R CrB type variable and if it is actually a member of the Large Cloud it is the only star of the class known in an extragalactic system and the only one with a known distance and absolute magnitude. The only other means

available at present for determining the absolute magnitude of this class of variable are spectroscopic criteria. The stars show supergiant spectral characteristics but, in view of the considerable abnormalities also found (particularly strong C, weak H), little reliance has in the past been placed on the spectroscopic parallaxes.

In view of the faintness of the star it was necessary to use a short trail to obtain a spectrum with the *f*/2 camera, and the spectra are necessarily not of the best quality. They are however good enough for certain definite conclusions to be reached. The best spectrum was obtained on 1953 December 1 and another spectrum (in all respects similar) on 1954 February 10. It had been intended to obtain more spectra in 1956 but examination of the field on January 18 and March 8 showed that the star had faded out of reach of the spectrograph. On both occasions it was probably fainter than 16^{m} visual. This circumstance at least has the advantage that one can be certain of the identification of the star observed with the variable, a matter of some concern with so faint a star in such a rich field. The radial velocity of the star is about +260 km/sec in good agreement with the expected velocity for a cloud member in this position. The spectral type is necessarily somewhat uncertain; it appears, however, to be a supergiant of type F5–G0, most probably F8 with Hγ weak for the class. The observations therefore suggest that W Men has a typical R CrB type spectrum though the spectra are not suitable for determining whether or not C and C_2 are present. We may conclude that the supergiant characteristics shown by the R CrB variables are real indicators of high luminosity in these stars. Using a distance modulus of $19^{m}{\cdot}2$ for the clouds (**3**) we find an absolute magnitude at maximum for W Men of $-5^{m}{\cdot}4$.

Acknowledgments.—I am much indebted to Dr H. Shapley and Mrs V. McKibben Nail for kindly supplying unpublished Harvard data and maps on some of the variables discussed in this note. I should also like to thank Dr A. D. Thackeray for his encouragement and for many helpful suggestions.

Radcliffe Observatory,
Pretoria :
1956 *May* 31.

References

(1) S. C. B. Gascoigne, *Aust. J. Sci. Suppl.*, **17**, 23, 1954.
(2) S. C. B. Gascoigne and G. E. Kron, *P.A.S.P.*, **65**, 32, 1953.
(3) A. D. Thackeray and A. J. Wesselink, *Obs.*, **75**, 33, 1955.
(4) S. Gaposchkin, *A.J.*, **60**, 455, 1955.
(5) H. L. Johnson and W. W. Morgan, *Ap. J.*, **117**, 313, 1953.
(6) A. D. Code, *Ap. J.*, **106**, 309, 1947.
(7) O. J. Eggen, *Ap. J.*, **113**, 367, 1951.
(8) D. W. N. Stibbs, *M.N.*, **115**, 323, 1955.
(9) W. J. Luyten, *H.B.*, 846, 1927.

RED SUPER-SUPERGIANTS IN THE LARGE MAGELLANIC CLOUD

M. W. Feast and A. D. Thackeray

(Received 1956 December 7)

Summary

Five members of the Large Cloud have been discovered with absolute visual magnitudes about −9·0, spectral types from F8 to G5 : and with colours between +0·37 and +1·45. Four of these stars are among the 30 brightest known members of the Cloud. The census of the brightest blue stars must be regarded as complete, but owing to the difficulty of distinction of foreground stars more red super-supergiants probably remain to be discovered.

The Magellanic Clouds offer a unique opportunity to study individually the brightest stars in an external system. The high degree of resolution guarantees in most cases that the slit of a spectrograph will isolate the light from single stars. In apparent magnitude there is a gain of 5 magnitudes over corresponding objects in M31. Consequently the number of objects which can be reached spectroscopically with existing equipment is very large. If one adopts 13·6 mag. as a practical working limit for spectra at 86 A/mm with the Radcliffe reflector, Shapley's luminosity function for the Large Cloud suggests that there are between 2000 and 3000 members within range of this equipment.

The Henry Draper Extension covering the region of the Large Cloud contains some 200 objects classified as O, B or Con, mostly brighter than 12·0 mag. From a sample of 25 such objects observed spectroscopically with the Radcliffe reflector (**1**) we can be sure that the great majority, if not all, are members of the Cloud. The HDE "B" or "Con" stars prove to be mostly late B or early A types with very narrow hydrogen lines. The presence of a true absorption O star still remains to be established. It is probable that the HDE "O" objects (some of which are as faint as 15 mag.) are mostly Wolf–Rayet type.

The HDE Catalogue also contains over 3000 stars classified as A or later. Most of these are foreground stars. But it is of the utmost importance to disentangle the minority of true members of type later than A. One such star was included in the previous tabulation (**1**), and as a result of further investigations the following bright stars have been found to be Cloud members from velocity shifts and supergiant characteristics.

Red Super-supergiants in the Large Cloud

Star	HDE Sp	HDE m	MK Type	SP_g	SP_V	SCI	M_V	Remarks
268757	Mo	10·5	G5: Ia	11·8	10·3	+1·45	−8·9	near NGC 1743
269723	K5	11·4	Go Ia	10·8	9·9	+0·92	−9·3	near NGC 2014
269953	Ko	12·0	F8 Ia	10·7	10·0	+0·74	−9·2	near NGC 2085
271182	Ko	9·7	F8 Ia	10·2	9·8	+0·37	−9·4	
30 Dor No. 50	...	...	F8-Go Ia	...	...	...	...	

The magnitudes and colours in the fifth to seventh columns have been determined photoelectrically by Dr A. J. Wesselink on the Cape system using the Radcliffe 74-inch reflector and Cassegrain photometer. These results are to be regarded as provisional and in any case, in view of the large discrepancies from the HDE (photographic) magnitudes given in the third column, it appears likely that these objects of exceptionally high luminosity are variable in light.

The absolute visual magnitudes listed in the eighth column are based on an assumed distance modulus of 19·2 for the Large Cloud (**2**). It seems to be undesirable to apply the term "supergiant" to objects covering a range of some 7 magnitudes, and we would suggest the term "super-supergiant" to be appropriate to objects with M_V brighter than $-7{\cdot}0$.

With the exception of 271 182, which is in a loose grouping of stars containing some known Cloud members, all the above stars are near nebulae and clusters. 30 Dor No. 50 is not in the HDE and its precise position will be defined in a later paper devoted to the 30 Dor complex. Its magnitude has not been measured but it is estimated as between $10^{m}{\cdot}5$ and $11^{m}{\cdot}0$ pg so that its absolute magnitude is of the same order as that of the other stars.

Spectral classification.—The MK types in the fourth column have been obtained from Radcliffe spectra with dispersions of 86 and 49 A/mm at Hγ. The MK standards δ C Ma (F8 Ia) and HR 2974 (G0 Ia) match well the last four stars, except that in 30 Dor No. 50 the H lines cannot be used owing to the superposition of strong nebular H emission; also in this star all lines appear to be somewhat weakened, perhaps due to their being partly filled in by a nebular continuum.

Judging by the strength of the G band and the weakness of H, 268757 is clearly somewhat later in type than HR 2974 (G0 Ia), but certainly not as late as M (HDE). It is understood that the star has been classified as K from an ADH objective prism spectrum (**3**). Accurate classification is difficult on account of the fact that there are no MK Ia standards between G0 and M1. No good match is found with G0 Ib, G5 Ib, K2 Ib or K3 Iab. A fairly good match is provided by α Aqr (G2 Ib), but Sr II 4215 and some other lines are stronger in 268757. The classification as G5: Ia is subject to considerable doubt.

Radcliffe spectra of long period cepheids in the Clouds taken at 86 A/mm have been classified at F7 Ia to G2 I (**4**). At this dispersion, the super-supergiants reported in this paper show no certain differences spectroscopically from the cepheids which are about 2 magnitudes fainter. We must conclude that the MK criteria are insensitive to luminosity among the very brightest stars.

Colours.—Detailed discussion of the colours and magnitudes of these stars is postponed to a later communication when it may be hoped that further instances of such red super-supergiants will have been discovered. But it will be noticed that the colours, for the first three stars at least, do appear to be redder than for normal F to G giants, although they accord well with the colours of the cepheids (**4**). This fact probably accounts for the HDE classifications as K or M.

A comparison of the colours and spectral types suggests a rather abrupt increase in the colour index setting in at about F8 to G0. A similar effect is also shown by the cepheids as will be seen by comparing the colour-period (**5**) and spectrum-period (**4**) relations.

As is well known, G to K dwarfs are bluer than giants of the same spectral type, the same degree of ionization being produced by the lower pressures and lower surface temperatures of giant atmospheres. In the super-supergiants of

this paper one may expect even lower surface temperatures to be required to reproduce a G0 spectral type.

Owing to doubts concerning the temperatures and bolometric corrections appropriate to these objects calculations of radii are most unreliable, but for 268757 a radius of the same order as that of the red component of VV Cep (2400 ⊙) is suggested.

The possibility of interstellar reddening has to be borne in mind particularly for stars involved in nebulosity, but the absorption cannot be put high without having to assign unacceptably high intrinsic luminosities. Moreover, in the case of 271 182 near the northern border of the Cloud, there is no associated nebulosity and no appreciable absorption can be expected in this region.

Frequency of red super-supergiants in the Large Cloud.—Mrs Nail and Shapley (**6**) have found that star counts in the Large Cloud indicate the presence of red supergiants brighter than 14 mag. The five member stars reported here indicate that even in the brightest range of magnitudes ($M = -9$ and brighter) red super-supergiants can exist in appreciable numbers. Among stars of apparent magnitude 10·4 or brighter, there are some 18 known blue Cloud members (excluding a few cases of clusters formerly regarded as individual stars) and *at least* 4 red Cloud members with types F8 or later. We can be reasonably sure that the census of the brightest blue members is complete, but we are very far from being able to claim the same for red members; in fact the probability of finding more instances seems to be fairly high. We can conclude that among the 30 brightest members of the Large Cloud not less than 20 per cent are likely to be red F8 and later types, few are earlier than B 5 and none earlier than B0. The conclusion is rather surprising since the brightest Population I stars are normally regarded as blue.

A detailed list of proved members and foreground stars will be published at a later stage. But as a guide to the extent of the search for bright members of types later than B we give below the frequency distribution of HDE magnitudes of stars that to date have proved to be foreground objects.

Number of proved foreground stars (LMC)

Range of m.	8·0 8·4	8·5 8·9	9·0 9·4	9·5 9·9	10·0 10·4	10·5 10·9	11·0 11·4	11·5 11·9	⩾ 12·0
Number	2	6	8	4	12	5	3	3	4

The investigated stars brighter than 10·0 mag. included many type A stars from the HD catalogue because it was hoped that objects like HD 33579 (**1**) might be found. But it now seems reasonably certain that any such object would have been marked out by the peculiarity of exceptionally narrow lines and that no cases have been missed.

Radcliffe Observatory,
Pretoria:
1956 *November* 30.

Note added 1957 *February* 8.—A star (HDE 269810, $12^{m}\cdot1$, Sp. G0) near the nebula NGC 2032 has been proved to be the first instance of a true absorption O member of the Cloud. It is more than 1 mag fainter than the limit for inclusion among the 30 brightest members.

References

(1) M. W. Feast, A. D. Thackeray and A. J. Wesselink, *Obs.*, **75**, 216, 1955.
(2) A. D. Thackeray and A. J. Wesselink, *Obs.*, **75**, 33, 1955.
(3) Bart J. Bok and D. Hoffleit, private communication.
(4) M. W. Feast, *M.N.*, **116**, 583, 1956.
(5) W. Buscombe, G. de Vaucouleurs and S. C. B. Gascoigne, *Austr. Journ. Sci.*, **17**, 30, 1954 (Fig. 15).
(6) V. McK. Nail and H. Shapley, *P.N.A.S.*, **39**, 358, 1953 (Harv. Repr. 373).

NOTICE TO AUTHORS

1. *Communications.*—Papers must be communicated to the Society by a Fellow. They should be accompanied by a summary at the *beginning* of the paper conveying briefly the content of the paper, and drawing attention to important new information and to the main conclusions. The summary should be intelligible in itself, without reference to the paper, to a reader with some knowledge of the subject; it should not normally exceed 200 words in length. **Authors are requested to submit MSS. in duplicate. These should be typed using double spacing and leaving a margin of not less than one inch on the left-hand side. Corrections to the MSS. should be made in the text and not in the margin.** Unless a paper reaches the Secretaries more than seven days before a Council meeting it will not normally be considered at that meeting. By Council decision, MSS. of accepted papers are retained by the Society for one year after publication; unless their return is then requested by the author, they are destroyed.

2. *Presentation.*—Authors are allowed considerable latitude, but they are requested to follow the general style and arrangement of *Monthly Notices*. References to literature should be given in the standard form, including a date, for printing either as footnotes or in a numbered list at the end of the paper. Each reference should give the **name and initials** of the author cited, irrespective of the occurrence of the name in the text (some latitude being permissible, however, in the case of an author referring to his own work). The following examples indicate the style of reference appropriate for a paper and a book, respectively :—

A. Corlin, *Zs. f. Astrophys.*, 15, 239, 1938.

H. Jeffreys, *Theory of Probability*, 2nd edn., section 5.45, p. 258, Oxford, 1948.

Alternatively, the Harvard reference system may be used.

3. *Notation.*—For technical astronomical terms, authors should conform closely to the recommendations of Commission 3 of the International Astronomical Union (*Trans. I.A.U.*, Vol. VI, p. 345, 1938). Council has decided to adopt the I.A.U. 3-letter abbreviations for constellations where contraction is desirable (Vol. IV, p. 221, 1932). In general matters, authors should follow the recommendations in *Symbols, Signs and Abbreviations* (London : Royal Society, 1951) except where these conflict with I.A.U. practice.

4. *Diagrams.*—**These should be designed to appear upright on the page, drawn about twice the size required in print and prepared for direct photographic reproduction except for the lettering, which should be inserted in pencil. Legends should be given in the manuscript indicating where in the text the figure should appear.** Blocks are retained by the Society for 10 years; unless the author requires them before the end of this period they are then destroyed.

5. *Tables.*—**These should be arranged so that they can be printed upright on the page.**

6. *Proofs.*—Costs of alteration exceeding 5 per cent of composition must be borne by the author. Fellows are warned that such costs have risen sharply in recent years, and it is in their own and the Society's interests to seek the maximum conciseness and simplification of symbols and equations consistent with clarity.

7. *Revised Manuscripts.*—When papers are submitted in revised form it is especially requested that they be accompanied by the original MSS.

Reading of Papers at Meetings

8. When submitting papers authors are requested to indicate whether they will be willing and able to read the paper at the next or some subsequent meeting, and approximately how long they would like to be allotted for speaking.

9. Postcards giving the programme of each meeting are issued some days before the meeting concerned. Fellows wishing to receive such cards whether for Ordinary Meetings or for the Geophysical Discussions or both should notify the Assistant Secretary.

CONTENTS

Printed in London by Taylor & Francis, Ltd., 1957 April